LONDON METROPOLITAN UNIVERSITY

# DEVELOPMENT OF BLOCKING ANTIBODIES TO THE VOLTAGE-GATED CALCIUM CHANNEL Cav3.2


Presented by

**Marta Kaleta**


Thesis submitted in partial fulfilment of the requirement for the degree of Doctor of Philosophy (PhD)


Director or Studies: Professor Christopher Palmer

Second Supervisor: Professor Christopher Branford-White

School of Human Sciences

Faculty of Life Sciences and Computing

London Metropolitan University


March 2018

# Abstract

T-type voltage-dependent calcium channel Cav3.2 is a four-domain channel participating in various physiological and pathological processes principally in the nervous system but also in non-excitable cells. Upregulation of Cav3.2 or mutations in this channel are found in pain syndromes, certain cancers and epilepsy.

This thesis describes the experiments aimed at generating antibodies directed to Cav3.2 that could alter the gating of these channels.

A structural analysis of Cav3.2 channel was performed *in silico* on the basis of the published protein sequence using bioinformatics tools. The analysis identified several putative extracellular loops of Cav3.2. Three of these loops were chosen as targets for antibodies due to their proximity to the channel's pore.

Antibodies were chosen to target these loops due to the relative ease of their production, and were generated against synthetic peptides with the corresponding sequence attached to a carrier protein and injected into rabbits. The antibodies obtained were purified from the sera and analysed for their affinity to the corresponding peptides *in vitro* using ELISA and flow cytometry.

A stable cell line HEK/Cav3.2 was analysed to confirm the localisation and accurate expression of functional Cav3.2 in these cells. This cell line was used to assess the binding of the generated antibodies and their influence on Cav3.2 current.

In order that the influence of the antibodies on the gating of Cav3.2 channel could be measured, a calcium sensitive fluorescent dye-based assay was developed and validated. The generated antibodies proved to be partial inhibitors of Cav3.2 channel conductance, confirming that extracellular loops of Cav3.2 are a promising drug target which may pave the way to designing selective anti-Cav3.2 inhibitors.

# Acknowledgements

*I thank Christ Jesus our Lord, who has given me strength.*

1Tim 1:12

I would like to thank my supervisor Professor Chris Palmer for allowing me to work on this project under his supervision. I am grateful for his erudite guidance, valuable advice and patience. I have learnt so much from him throughout my research degree and this will remain with me forever.

I am also very grateful to my second supervisor, Professor Chris Branford-White.

I am grateful to my parents, Aniela and Adam, who have always supported me throughout my endeavours in fulfilling my dreams and funded my education in Poland and later in the UK.

To my brother, Zbyszek, I would like to say thanks that in growing up together we have always remained great friends. Good luck with your PhD research – but I've beaten you to it!

I am grateful to my Granny Zosia and Auntie Lidzia for their care and loving support for me and for their weekly phone calls to enquire about my well-being and whether I'd eaten well.

I am also very grateful to all staff, friends and colleagues at the School of Human Sciences, the Faculty, the SuperLab and the Research Office at London Metropolitan University who have always been very friendly to me and helped with my research wherever possible. I am very grateful for the London Metropolitan University Vice-Chancellor Scholarship that enabled me to pursue this degree.

Special thanks to my fiancée Colin for all his love and patient support, especially when I needed that extra boost to finish this work. He proof-read the copy and made an infinite number of cups of tea when I needed them so badly – you make me so happy and I am so grateful we are together!

# Contents

# Index of Figures

# Index of tables

# Part I

# 1. Introduction

‘The human brain has 100 billion neurons, each neuron connected to 10 thousand other neurons. Sitting on your shoulders is the most complicated object in the known universe.’ (Michio Kaku).

The 20$^{th}$ century has brought enormous progress in medicine and technology that still continues into the 21$^{st}$ century. Generations of scientists work tirelessly to gain more and more insight into the human physiology and pathology of various diseases. Human genome mapping was declared complete in 2003. Treatment for various diseases is at hand. It would seem that the human body holds no more secrets. But the functioning of the human brain still remains a mystery and the whole nervous system is the least understood part of the body. Billions of interconnected neurons form a structure that governs all life functions, thoughts and feelings. The communication of neurons occurs continuously at a very high rate and requires complex neurotransmitter and ion movements. One of the ions that play an important role in the nervous system and in other body systems is calcium ion ($Ca^{2+}$).

Calcium has played a very important role in the physiology of all living organisms since the very origin of life. The primordial ocean contained sodium, chloride, magnesium, calcium and potassium ions and only a small amount of other ions (Case *et al.,* 2007). For this reason these five ions have the greatest importance in the metabolism of all living organisms. Calcium was present at a lesser level (0.04 %) than the other ions but gained more significance due to its unique chemical properties. One of these important properties is a high coordination number of Ca2+ meaning that this ion can form coordination complexes with ligands such as carboxylate groups of amino acids through interaction with oxygen in this group (Nara, Morii and Tanokura, 2013). Calcium ions have irregular coordination geometry which results in their ability to interact with a wide variety of biological molecules including proteins, lipids and carbohydrates (Case et al., 2007). Calcium ions can bind to carboxylate oxygen with a higher affinity than other ions

and also display faster protein binding kinetics than other ions. Moreover, these interactions are highly reversible unlike e.g. disulfide bond formation (Case et al., 2007). However, high concentration of $Ca^{2+}$ causes the aggregation of proteins and nucleic acids and precipitation of phosphates needed for energetic purposes (Carafoli and Klee, 1999).

Calcium is the most abundant metal in the human body. It is predominantly present in bones and cartilage where its salts (*e.g.* calcium phosphate and calcium sulphate) are an important structural component. Calcium ions ($Ca^{2+}$) also take part in the metabolism as a second messenger in signal transduction pathways, muscle contraction, neurotransmitter release, fertilisation and as a cofactor of many enzymes including protein kinase C and prothrombinase which is involved in the coagulation cascade (Carafoli and Klee, 1999).

Calcium metabolism must be tightly regulated to maintain homeostasis. Since the origins of life, the level of $Ca^{2+}$ inside the primitive cell was significantly lower than in the extracellular environment. This led to the evolution of pumps and ion channels responsible for maintenance of the calcium gradient across the cell membrane. In modern eukaryotic cells cytosolic Calcium concentration is about 100 nM while extracellular (serum) concentration is 2 mM (Case *et al.,* 2007). Calcium influx from the outside of the cell to the cytoplasm triggers a range of cellular responses that include increased proliferation, survival and apoptosis. These responses are brought on by $Ca^{2+}$ complexes with proteins *e.g.* calmodulin, calpeptin, troponin C and various kinases (Carafoli and Klee, 1999). Moreover, the endoplasmic reticulum (ER) serves as an intracellular storage pool with micromolar $Ca^{2+}$ concentration being more close to the extracellular $Ca^{2+}$ level. An increase in cytosolic $Ca^{2+}$ level may be due to extracellular $Ca^{2+}$ influx (via calcium channels) or release from the ER. Upon relevant stimulation (*e.g.* Growth Factor Receptor activation) cytoplasmic $Ca^{2+}$ level increases due to release from the ER. The efflux of calcium ions from this internal pool is sensed by yet an unidentified

secondary messenger, which in turn causes the entry of extracellular $Ca^{2+}$ via opened calcium channels (Petersen, Michalak and Verkhratsky, 2005).

## 1.1. Calcium channels

The cell membrane is impermeable to ions, thus ion exchange between the cell and the environment depends on ion channels and pumps. Primitive ion channels probably consisted of poly-hydroxybutyrate polymers and were simple aqueous pores in the cell membrane (Hille, 1992). Later in evolution these polyesters were replaced by protein – two transmembrane (TM) domains surrounding the pore, connected via a pore loop. The next step was the development of additional membrane spanning domains and sometimes dimerization or tetramerization of the resulting subunits (Hille, 1992). The pore allows the ions to pass through the open channel. The pore defines the selectivity of the channel, *i.e.* which type of ion can be conducted. Many channels are selective for one type of ions only but some are less specific, *e.g.* permeable to monovalent cations ($Na^+$, $K^+$). The pore also defines the conductance of a channel – the amount of ions passing through the channel and thus the electrical current generated. The additional domains, aside from the pore structure, are usually responsible for the gating properties of a given channel. Ion channels are divided into groups according to their selectivity (*e.g.* $K^+$ channels) or according to the stimuli that evoke the channel response. Ion channels can be ligand-gated, voltage-gated or can respond to sensory stimuli, *e.g.* heat, cold, mechanical stress, osmolarity changes (Aidley and Stanfield, 1996).

Ligand-gated channels are found in a wide variety of cells and are operated by the binding of specific ligands – mainly small organic molecules such as hormones and neurotransmitters. The binding of ligands usually occurs away from the pore and causes conformational changes in the structure of the channel resulting in the channel opening and ion influx or efflux for a defined time. Ligands activating the channels may bind at the extracellular side of the channel protein and directly gate the channel (ionotropic receptors activated by ligand such as gamma-aminobutyric acid, glycine, serotonin). Other channels are gated by intracellular ligands *i.e.* secondary messengers such as

cyclic AMP or G-protein. Ligand-gated calcium channels *e.g.* inositol triphosphate receptors and ryanodine receptors are localised in the ER where they participate in calcium release to the cytoplasm (Aidley and Stanfield, 1996).

Voltage-gated channels are sensitive to changes in membrane electrical potential. Most of the voltage-gated channels are composed of four domains, each of which has six transmembrane segments. The pore loop is between the fifth and sixth domain (S5-S6), and the segment adjacent to them (S4) acts as a voltage sensor. S4 is highly conserved and contains several positively charged amino acids (lysine and arginine) making it sensitive to changes in membrane potential. These changes cause the transition of the channel between resting, activated and inactivated states membrane (Hille, 1992). In the resting cell the membrane potential is hyperpolarized to about -60 to -80 mV depending on the type of cell. At this potential all voltage-gated channels are in a resting state, this means they are closed and no ion passage occurs. In this state the channel is available for activation. When the membrane potential increases (depolarizes) and reaches the activation threshold for the given type of channel, the channel changes conformation and the pore opens, allowing the ions to flow through. This conformational change has not yet been described in detail but it has been proposed that the opening of the channel pore starts with the outward movement of the adjacent transmembrane domains. Open (active) channels remain open for a defined time specific for a particular type of channel. After that time the channel spontaneously inactivates, even in the presence of an activating stimulus. The inactivated channel is closed and no ion conductance occurs. In order for a channel to reactivate, the activating stimulus must be withdrawn. In the case of voltage-gated channels, the membrane potential must return to the hyperpolarized state. The channel then returns to the resting state and is available for subsequent activation (Purves *et al.,* 2001).

The voltage-gated channels serve as transducers of electrical signals on the cell membrane into localized changes in ion concentration which in turn triggers further cellular responses. Voltage-gated channels are usually found in excitable cells *e.g.* in

the nervous system, where they are crucial for nerve impulse propagation along the axons and for neurotransmitter release at nerve terminals (Purves *et al.,* 2001). Voltage-gated calcium channels (VGCC) are more abundant and diverse than ligand-gated calcium channels. To date ten members of the VGCC family have been cloned and described. These channels have various physiological properties and are further divided into High-Voltage Activated (HVA) and Low-Voltage Activated (LVA) calcium channels (Zamponi, 2005). The main difference between these subfamilies is the voltage dependence of the channels. HVA are activated by a relatively large depolarisation of the cell membrane – a rise from resting potential -90 mV to -30 mV is required. HVA can be further divided into L-, N-, P-/Q- and R-type depending on the type of current they display. Cav1.1 – Cav1.4 display L-type currents 'long-lasting' in terms of opening time. Cav2.1, Cav2.2 and Cav2.3 are responsible for P-/Q-, N- and R-types of current, respectively (Zamponi, 2005). The main pore-forming unit of calcium channels ($\alpha_1$) consists of 24 transmembrane segments arranged into four domains around the central pore loop. Auxiliary subunits $\alpha_2$, β, γ and δ of HVA channels have been described (Dolphin, 2012). Subunits $\alpha_2$ and δ form a dimer anchored in the cell membrane by the δ subunit and the $\alpha_2$ subunit is located on the surface of the cell. Subunit β is located intracellularly while subunit γ is a transmembrane protein. The $\alpha_1$ subunit itself is sufficient to create the functional calcium channel; the auxiliary subunits regulate gating properties and the surface expression of HVA channels. L-type channels (Cav1.x) have been found in skeletal and cardiac muscle, endocrine cells, adrenal gland and mast cells. These channels are sensitive to dihydropyridine, phenylalkylamine and benzothiazepine antagonists. Cav2.x channels are predominantly found in nerve terminals and dendrites and are responsible for neurotransmitter and hormone release and dendritic calcium currents. Cav2.x channels are insensitive to the blockers used for for L-type channels but are specifically blocked by peptide toxins isolated from snake and spider venoms (ω-agatoxin and ω-conotoxin). The HVA channels are highly homologous within classes

(above 80 % sequence identity) and share 52 % identity between classes (Catterall *et al*. 2005).

By contrast, LVA channels are activated by a low voltage (approximately -60 mV) and inactivate quickly thus displaying a 'transient' current (T-type). To date three LVA channels have been identified: Cav3.1, Cav3.2 and Cav3.3. The Cav3.x channels are phylogenetically the most distant from the other classes and share only 28 % sequence identity with Cav1.x and Cav2.x Catterall *et al*. 2005).

Cav3.1 has been found in the brain (especially in the hippocampus, thalamus, hypothalamus), ovary, placenta and heart (sinoatrial node). It has been proposed that it participates in thalamic oscillations. Cav3.2 has also been found in the brain and heart coexpressed with Cav3.1. Moreover Cav3.2 is present in the kidney, smooth muscle, liver and adrenal cortex (Perez-Reyes *et al.,* 2008). These LVA channels have been implicated in various metabolic processes and pathological states and are thus potential therapeutic targets for many diseases; yet research on these channels is hampered by a lack of specific inhibitors, and difficulties in separating these currents from the more abundant L-type currents. The overlapping expression of Cav3.1 and Cav3.2 in the same cell types further complicates the research on these channels.

Cav3.x calcium channels are voltage gated but their activity is further modulated by other metabolic processes and ligands such as phosphokinase C and neurotransmitters (Perez-Reyes *et al.,* 2008).

## 1.2. The structure of Cav3.2

The T-type calcium currents were described in 1985 in cells of dorsal root ganglion and cardiac myocytes (Tsien and Wheeler, 1999). These currents have been reported to be insensitive to the classic calcium channel blockers such as dihydropyridines, suggesting the presence of a new family of calcium channels. However, the T-type channels for a long time escaped identification due to the high diversity in sequences between HVA and LVA channels. Cav3.2 was identified in 1998 by screening the cDNA libraries for short sequences similar to any of the previously described calcium channels sequences (Cribbs *et al*., 1998). A clone structurally similar to one transmembrane spanning region of carp Cav1.1 was identified. This cDNA has been sequenced, found to encode for a putative ion channel and named Cav3.2. Expression of the cloned Cav3.2 and electrophysiological recordings confirmed its T-type channel properties. Cav3.2 is encoded by the *CACNA1H* gene located on the human chromosome 16 and the mouse chromosome 17 (Cribbs *et al*., 1998). The size of the human protein is 2353aa and the mouse – 2365aa.

The sequence of Cav3.2 is shown in annex 1. The structural studies using Kyte-Doolittle hydropathy prediction tool have revealed the presence of four homologous internal repeats (domains). This is a characteristic structure for all voltage-gated calcium channels and sodium channels. Each of the Cav3.2 domains (named D1-D4) has six transmembrane segments and a pore loop between the fifth and sixth transmembrane segments (Fig. 1). These pore loops together contribute to the formation of the pore barrel (Fig. 2) and the ionic selectivity of the channel. In LVA calcium channels each of the four pore loops contain a glutamate residue preceded by a threonine residue (T-X-E). In Cav3.2 the glutamates in pore loops in domains 3 and 4 have been replaced by aspartate residues in a conformation D-X-W, leading to the abbreviation EEDD. The fourth segment of each domain is thought to act as a voltage sensor due to its positive

charge. Every third amino acid residue in the S4 segment is positively charged (arginine or lysine). These voltage sensors are supposed to move outwards during the depolarization of the cell membrane, yet the exact mechanism of their role in channel gating remains unclear. Large parts of Cav3.2 molecule are located intracellularly and within the cell membrane with the exception of short extracellular loops linking the segments. The N-terminus is 101 amino acids long and the C-terminus contains 490 amino acids. Both N- and C- terminal peptides have a potential to interact with other subunits (as in the case of HVA calcium channels), but none of such interactions has yet been confirmed (Williams *et al*. 1999; Catterall *et al*. 2005). The extracellular loops connecting segments S1/S2 and S3/S4 are relatively short (8-22 amino acids). Three pore loops that are also partially located on the external side of the cell membrane are 52-77 amino acids long, only the pore loop in domain 1 is bigger – 141 amino acids. The first two intracellular loops connecting the domains are 374 and 275 amino acids long, respectively, and possibly contain a structure acting as a gating brake (Arias-Olguín *et al.* 2008), while the third region linking domains is much shorter (61 amino acids) and has not yet been reported to play any role in the channel function.

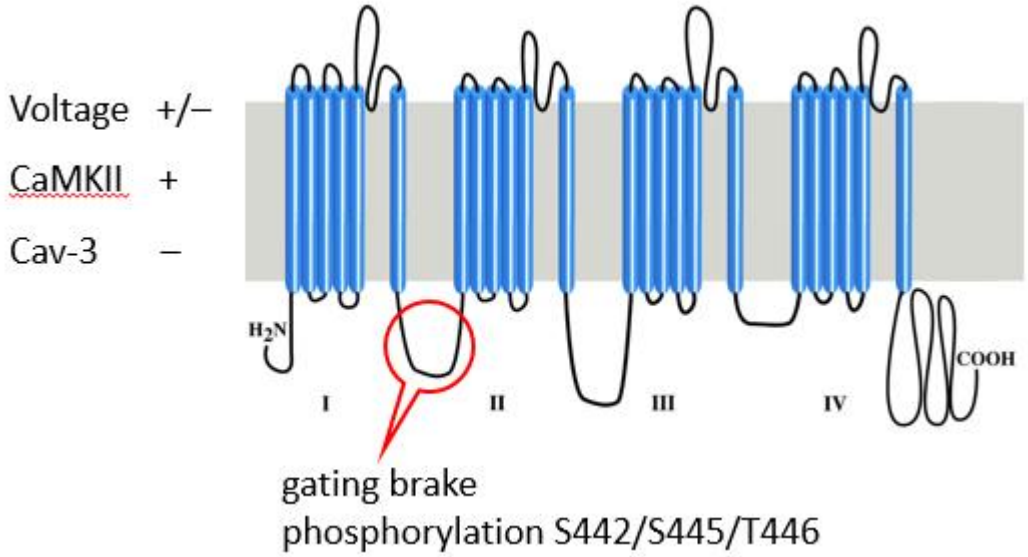


Figure 1. **Structure of Cav3.2 – membrane arrangement of the polypeptide chain**

Schematic diagram showing the predicted structure of Cav3.2: one polypeptide chain is arranged into four domains. Each domain contains six transmembrane segments. N- and C- termini and loops connecting domains are localised on the inner side of the plasma membrane. Short loops linking the transmembrane segments are on the surface of the cell. Each domain has a pore loop between segments 5 and 6 contributing to the pore barrel. The channel can be either simulated or inhibited by membrane potential changes (Perez-Reyes *et al.,* 2008). Calmodulin-dependent protein kinase II (CaMKII) stimulates calcium currents (Wolfe *et al.,* 2002). Caveolin-3 (Cav-3) decreases current density of Cav3.2 (Markandeya *et al.,* 2011). Intracellular loop between domains I and II has been proposed to act as a gating brake (Arias-Olguín *et al.,* 2008). Phosphorylation of serine (S442, S445) and threonine (T446) residues causes a shift of activation and inactivation curves towards more negative potentials (Blesneac *et al.,* 2015). This list of regulatory mechanisms is not exhaustive. Image generated using GIMP 2.8.16 software.

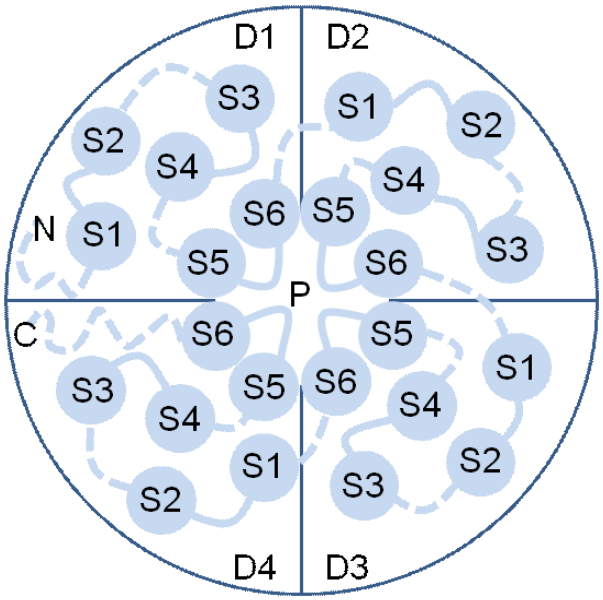


Figure 2. **Structure of Cav3.2 – top view**

Schematic diagram showing the top view of the Cav3.2: the four domains (D1-D4) are arranged around the pore loop (P). Each domain consists of six transmembrane segments (S1-S6). Extracellular loops linking the TM segments are shown as solid lines. Intracellular peptides linking the segments and domains are indicated by broken lines. N and C indicate the N- and C-termini of the protein. Image generated using GIMP 2.8.16 software.

## 1.3. Cav3.2 localisation and physiological function

Cav3.2 has initially been found in human kidney, liver and heart with the highest level detected in kidney (Cribbs *et al.,* 1998). Further studies on other species revealed that this protein is also present in rat cardiac myocytes – the level of expression of Cav3.2 was reported to be high in embryonic and neonatal hearts and declined in adulthood, remaining mostly in sinoatrial node (Ono and Iijima, 2010). Cav3.2 is implicated in hypertension in rats, as the level of Cav3.2 expression was increased in rats with spontaneous hypertension (David *et al.,* 2010). Histoblot analysis of Cav3.2 expression in murine brain showed highest level of Cav3.2 in the hippocampus and the molecular layer of the cerebellum (Aguado *et al.,* 2016). Immunoelectron microscopy analysis further pinpointed the Cav3.2 to somato-dendritic domains of CA1 pyramidal cells, Purkinje cells and hippocampal interneurons (Aguado *et al.,* 2016). To date this channel has been implicated in the following physiological and pathological phenomena:

1. Childhood Absence Epilepsy (CAE) is a disease characterized by short seizures of sudden onset involving the impairment of consciousness, disruption of activity and blank stare. Electroencephalogram recordings have indicated the presence of spike-wave discharges suggesting the involvement of a thalamic burst firing in the disorder. Chen *et al.* (2003) analysed a link between CAE in the Chinese Han population and Single Nucleotide Polymorphisms (SNPs) in CACNA1H gene. There were 12 missense mutations found only in CAE patients. Seven of those mutations were confined to an intracellular loop linking domains 1 and 2 of Cav3.2 (I-II loop), indicating a possible contribution of this loop to the development of CAE. Most of these SNPs occur in the region encoding amino acids 640-780. Further studies by Vitko *et al.* (2005) revealed that three of these mutations increase Cav3.2 excitability, two of them have little or no effect and one

decreases the firing of Cav3.2. Subsequent deletions of large regions of I-II loop have revealed the involvement of this loop in channel gating. Deletions in the proximal region of I-II loop (first 62 amino acids following the S6 segment of domain 1) altered activation and inactivation kinetics. Deletion of amino acids 429-539 rendered the channel more voltage-sensitive, lowering the activation threshold and increasing inactivation time. Deletions in the middle of the I-II loop did not alter the gating properties of the channel expressed in HEK293 cells, yet increased the T-type currents in analysed cells. This was due to the increased surface expression of mutated Cav3.2 on the cell membrane. The deletion of amino acids 540-618 increased the surface expression of Cav3.2 almost fourfold compared to wild type Cav3.2.

Moreover, Cav3.2 has been found to be inhibited by ethosuximide at pharmacologically relevant concentration ($IC_{50}$ = 3mM), a drug commonly used in the treatment of generalized absence epilepsies such as CAE. This suggests that the therapeutic effect of ethosuximide in epilepsies may partially result from the inhibition of Cav3.2.

2. Autism Spectrum Disorder (ASD) is an early onset, lifelong developmental disorder of the brain. People affected by this syndrome have problems with communication and an altered perception of their surrounding environment. Some of them may demonstrate sensory hyper- or hyposensitivity and repetitive behaviour (Schmunk and Gargus, 2013). The origin and pathophysiology of ASD is unclear. Most likely it is a polygenic disorder that may possibly be aggravated by environmental causes such as pollution, infections or pregnancy complications. Calcium signalling disturbances have been proposed to participate in the development of ASD (Schmunk and Gargus, 2013). Timothy syndrome is a disorder of multiple organs, which involves congenital heart disease and arrhythmia, immune deficiency, webbing of toes and fingers and

autism (Splawski *et al.,* 2004). *De novo* mutation in CACNA1C gene coding for Cav1.2 calcium channel has been found in all 16 tested individuals with Timothy Syndrome (Splawski *et al.*, 2004). Splawski *et al.* (2006) also investigated mutations in the CACNA1H gene as possibly contributing to ASD. Four mutations in highly conserved regions of CACNA1H were found in ASD patients but not in healthy controls, suggesting the participation of Cav3.2 channelopathy in the pathogenesis of ASD. The mutated Cav3.2 genes were then expressed in HEK293 cells and electrophysiological recordings revealed decreased excitability of the mutant channels. Two of these mutations were localised in the voltage sensor segment (S4): R212C in domain 1 and R902W in domain 2. This replacement of positively charged arginine residues with cysteine and tryptophan caused a decrease in the voltage sensitivity of the channel (rise in voltage activation threshold) and decrease in current density. These changes also have slowed the inactivation rate, resulting in prolonged $Ca^{2+}$ entry to affected cells. The A1874V mutation is located at the intracellular C-terminus of Cav3.2 and also increased the voltage activation threshold and prolonged the activation and inactivation rates. The W962C mutation in the pore loop region of domain 2 did not alter the voltage sensitivity of the mutant Cav3.2 but resulted in decreased current, suggesting that the level of membrane expression of this protein may be lower than in WT Cav3.2 (Splawski *et al.,* 2006). The exact role of Cav3.2 in ASD has not yet been elucidated and other calcium channelopathies were suggested to contribute to the development of ASD (Schmunk and Gargus, 2013).

3. Aldosterone secretion from zona glomerulosa cells: known T-type channel blockers such as mibefradil and nickel ions inhibited aldosterone release from acutely isolated rat adrenal zona glomerulosa cells (Uebele *et al*. 2004). Stimulation of adrenal zona glomerulosa cells with high $K^+$ concentration causes a synthesis of aldosterone through the $Ca^{2+}$-dependent mechanism. Mibefradil

and nickel ions inhibited this process, suggesting a possible involvement of Cav3.2. However, it is currently unclear what the exact mechanism of this phenomenon is. A lack of selective inhibitors of Cav3.2 and other LVA channels hindered further investigation of $K^+$-evoked aldosterone secretion (Uebele *et al*. 2004).

4. Coronary circulation: coronary arterioles from mice lacking Cav3.2 showed normal contractile responses but attenuated relaxation resulting in permanently constricted arterioles and focal myocardial fibrosis (Cribbs *et al*. 1998). Further experiments reported by Chen *et al.* (2003) clarified that muscle contraction is triggered by activation of L-type channels. A lack of function of Cav3.2 in knockout mice results in reduced relaxation of muscle and reduced response to nitroprusside and acetylcholine (relaxants). The involvement of Cav3.2 was confirmed by the finding that coronary arteries in wild type mice showed reduced relaxation when Cav3.2 was inhibited by nickel ions (Chen *et al.,* 2003).

5. Peripheral processing of noxious signals: mice lacking Cav3.2 channels exhibit attenuated pain responses to various noxious stimuli. Choi *et al*. (2007) produced knockout $Cav3.2^{-/-}$ mice and tested their response to various noxious stimuli. Visceral pain was evoked by the intraperitoneal injection of irritant agents: acetic acid normally triggering inflammatory reaction and magnesium sulphate triggering immediate non-inflammatory pain sensation. Cav3.2 deficient mice showed a reduced number of writhing movements following these procedures. $Cav3.2^{-/-}$ mice also had prolonged latency to mechanical (tail clip) and thermal (hot plate) stimuli. Intradermal formalin injections into the hind paw normally evokes biphasic pain response. The first phase depends on the direct stimulation of peripheral nociceptive neurons and was shortened in mice lacking Cav3.2. The second phase is the inflammatory pain caused by the injected chemical. Cav3.2

deficient mice also had a reduced duration of the paw licking phase, suggesting that Cav3.2 plays a significant role in the processing of all peripheral pain stimuli (Choi *et al*., 2007). The authors also tested Cav3.2 involvement in neuropathic pain and found no significant link between Cav3.2 deletion and neuropathic pain responses following spinal nerve ligation (SNL) procedure. SNL of lumbar nerve 5 is used as a model of neuropathic pain in mice. Cav3.2$^{-/-}$ mice showed normal pain response to L5 SNL. This finding suggests that Cav3.2 is not involved in neuropathic pain, which is in contrast with some earlier findings, *e.g.* Bourinet *et al.* (2005), who reported that silencing of Cav3.2 expression caused reduction in hyperalgesia caused by chronic constriction injury (CCI). These seemingly contrasting findings can probably be explained by the differences in the neuropathic pain processing following CCI and SNL procedures. It is not fully understood how both procedures induce neuropathic pain behaviour, therefore it is possible that two distinct mechanisms are involved in these syndromes and only one of them involves signal processing through Cav3.2.

## 1.4. Role of Cav3.2 in non-excitable cells

The electrophysiological properties of Cav3.2 have been well described as has the mechanism of action of this channel in excitable cells. Nevertheless, as mentioned previously, Cav3.2 has been found in a variety of non-excitable cells. The mechanism of action in these cells, however, remains unclear. The Resting Membrane Potential (RMP) of non-excitable cells is constant at about -50 mV, although this value fluctuates depending on the cell cycle stage and other factors such as ion channel activity (Yang and Brackenbury, 2013). Accurate measurement of RMP *in vitro* and *in vivo* can be achieved with the use of voltage sensitive dyes that change fluorescence depending on the membrane potential (Adams and Levin, 2012).

Cav3.2 should remain inactivated at RMP, thus raising the question about its role in the cell membrane. Theoretically Cav3.2 should remain inactive and closed in a cell membrane with RMP -50 mV. However, if a channel can be voltage gated this does not necessarily mean that it must be gated by voltage changes. It is theoretically possible that the Cav3.2 channel is gated by another mechanism in addition to its ability to sense voltage changes. There is a possibility that Cav3.2 may be regulated by calmodulin kinase II (CAMKII) in response to calcium depletion (Wolfe *et al.* 2002). Moreover as mentioned earlier, activation and inactivation curves of Cav3.2 overlap at about -60 mV creating the window current. It has been suggested that this window current may be involved in $Ca^{2+}$ entry in non-excitable cells.

This $Ca^{2+}$ entry may be physiological or may play a role in the pathogenesis of several diseases including cancer. Chemin *et al.* (2000) reported that the overexpression of Cav3.2 does not affect the proliferation rate of HEK293 cells. In their experiment a stable cell line expressing Cav3.2 has been generated. The level of intracellular $Ca^{2+}$ was measured using Fura-2 AM, a calcium-sensitive dye reported to increase fluorescence

in response to elevated Cav3.2 activity. Bromodeoxyuridine labelling and flow cytometry was used to assess cell cycle kinetics; however, cell cycle activity and proliferation rate remained unaffected. These findings suggest that the expression of Cav3.2 alone is not sufficient to confer an advantage to cell proliferation. In contrast, several studies have reported the increased expression of Cav3.2 in several cancer lines including:

1. Prostate cancer – Mariot *et al.* (2002) demonstrated that prostate adenocarcinoma cells LNCaP increase Cav3.2 expression during neuroendocrine (NE) differentiation. This differentiation has been associated with increased tumour malignancy and poor prognosis. A surge in T-type currents in LNCaP cells correlates with neurite extension and over-expression of neuronal markers such as chromogranin A and neuron-specific enolase. The NE differentiation is not triggered by Cav3.2 over-expression because the morphological changes in cells were observed before the increase in T-type currents (Mariot *et al.,* 2002). Nevertheless, blocking Cav3.2 with nickel ions for a prolonged time (5 days) resulted in a 30 % reduction in neurite elongation. The proposed explanation of this phenomenon is that the over-expression of Cav3.2 channels leads to increased cytosolic $Ca^{2+}$ level through window current influx and this in turn stimulates neurite expansion, either directly or by stimulation of secretion of growth factors. Moreover, $Ca^{2+}$ is involved in the control of exocytosis, hence the secretion of mitogenic factors (*e.g.* neurotensin and PTH-related peptides) by differentiated LNCaP cells is indirectly dependent on Cav3.2 over-expression (Mariot *et al.,* 2002). Gackière *et al.* (2008) confirmed the over-expression of Cav3.2 channels in prostate cancer tissues obtained from patients after surgical removal of tumours. Moreover, Cav3.2 channels are more abundant in cancerous tissue (significant immunostaining and T-type currents) compared to benign prostate hyperplasia, where the anti-Cav3.2 antibodies only gave weak

staining and T-type currents were not detectable, possibly due to very low current density.

2. LNCaP cells increase Cav3.2 expression after neuroendocrine differentiation associated with higher aggressiveness of tumours. Gackiere *et al*. (2008) report that no T-type currents or action potentials were detected in LNCaP cells suggesting that Cav3.2 expression participates in prostate cancer progression by promoting a steady influx of $Ca^{2+}$ ions into the cell. Moreover, the blockade of $Ca^{2+}$ entry by TH-1177 slowed down the progression of prostate cancer in mice. TH-1177 was later confirmed to block Cav3.2 and its splice variant δ25B (Haverstick *et al*. 2000) in mice.

   Prostate cancer: malignant neuroendocrine differentiation of prostate cancer cells is associated with an increased expression of Cav3.2 and could promote the progress of the disease by enhancing the secretion of potential mitogenic factors (Gackiere *et al*. 2008).

3. Fibroblast transformation by oncogene *ras* abolishes the T-type current. Strobeck *et al.* (1999) reports that fibroblasts undergo morphological changes after transformation with various oncogenes such as *ras*, *mos* and *src*. Flat fibroblasts become rounded or spindle-shaped. This change is associated with malignant transformation and metastatic cancer progression. Cell shape and rearrangement of cytoskeleton is mediated by $Ca^{2+}$. Calcium influx into cells with relatively low RMP relies on LVA channels such as Cav3.2. Strobeck *et al.* (1999) proved that GDP/GTP-binding protein Ras and its downstream pathway are associated with silencing the T-type currents. Mutant Ras is consitutively active. Ras has three major effector pathways, one of them being the mitogen-activated protein kinase (MAPK) pathway. The authors used various mutants deficient in subsequent elements of MAPK pathway and found that MAPK kinases (MEK)

are the elements that influence the T-type channel activity. Constitutively active MEK abolished the T-type currents and allowed for morphological transformation. The introduction of MEK inhibitor restored T-type currents and prevented morphological changes. Moreover, Cav3.2 inhibitor, mibefradil was shown to promote morphological changes in fibroblasts transformed by oncogenes, but mibefradil alone was not sufficient to trigger morphological changes in non-transformed cells (Strobeck *et al.* 1999).

4. Breast cancer – MDA-MB-231 and MCF-7 express Cav3.2 when grown below confluency. NNC-55-0396 (a novel anti-Cav3.2 compound) and si-RNA against Cav3.1 and Cav3.2 decreases the proliferation rate of the cell lines mentioned above (Taylor *et al*., 2008). Moreover, the membrane potential of MCF-7 varies between -58 and -2.7mV and it is especially hyperpolarized during $G_0/G_1$ and S phases of the cell cycle, *i.e.* where an increased level of intracellular $Ca^{2+}$ is required. This hyperpolarisation may increase entry of $Ca^{2+}$ due to window current (Taylor *et al*., 2008). Restriction Landmark Genomic Scanning showed that Cav3.2 was overexpressed in breast cancer samples from Japanese women compared to normal breast tissue (Asaga *et al.* 2006).

## 1.5. Electrophysiology of Cav3.2

Cav3.2 was cloned in 1998 (Cribbs *et al.,* 1998) and its electrophysiological properties have since been measured using patch-clamp studies. The electrophysiology studies were conducted on the channel heterologously expressed in HEK293 cells (Vitko *et al.,* 2005 and Zhong *et al.,* 2006) and in *Xenopus laevis* oocytes (Park *et al.,* 2007).

Cav3.2 produces a characteristic T-type transient current similar to Cav3.1 and Cav3.3. This current is 'transient' due to the fast inactivation of these channels. The original current traces obtained by Cribbs *et al.* (1998) are shown in Fig. 3. Cav3.2 channel is selective for $Ba^{2+}$ and $Ca^{2+}$ and its conductance is 9pS. There is a small difference in the channel currents depending on the ion used as a charge carrier: $Ba^{2+}$ or $Ca^{2+}$ (Fig. 3; Klöckner *et al.,* 1999).

The potential for half-activation has been reported in at least two publications: −44 ± 0.3 mV (Cribbs *et al.,* 1998) and -45.8 ± 0.7 mV (Klöckner *et al.,* 1999). The inward current reaches maximum at -29.4 ± 0.6 mA (Klöckner *et al.,* 1999). The half-activation times ($\tau_a$) and half-inactivation times ($\tau_h$) range from depend on the voltage and are shown in Fig. 4.

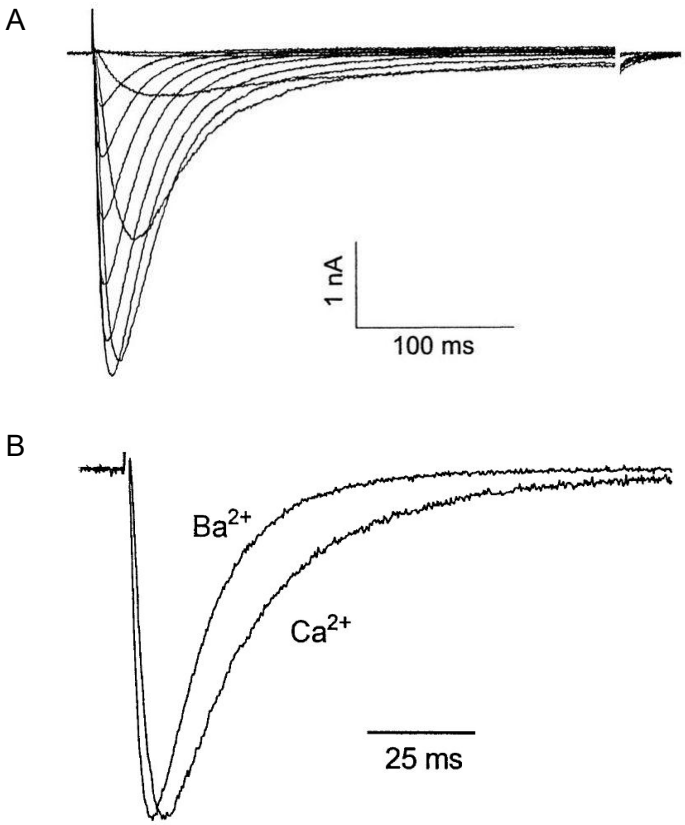


Figure 3. **Currents in HEK293 cells expressing Cav3.2**

A) Whole-cell inward currents were obtained using the patch clamp method and produced by 10 mmol/L $Ba^{2+}$ depolarising pulses. Barium ions were used in this experiment as they have smaller ionic radii than calcium ions and therefore produce larger current. Adapted from Cribbs *et al.* (1998).

B) Current traces were obtained in the same cell and slightly differ depending on charge carrier ion. $Ca^{2+}$ elicited currents have slower activation and deactivation compared to $Ba^{2+}$ currents. Adapted from Klöckner *et al.* (1999).

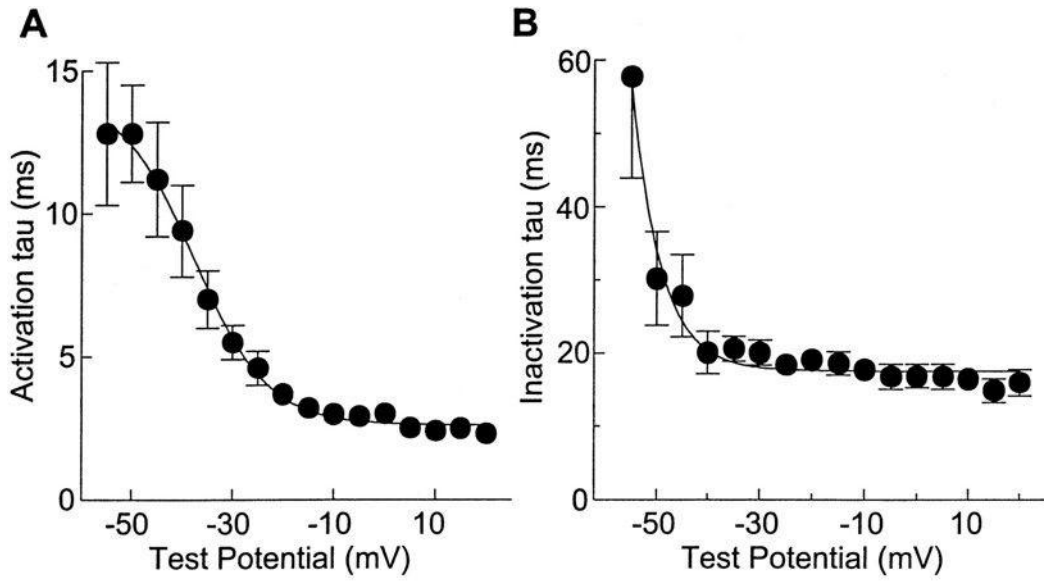


Figure 4. **Activation and inactivation time constants for Cav3.2**

A) Half-activation time ($\tau_a$) for Cav3.2 ranges from 13 ms at -50 mV to 3 ms at -10 mV. At positive voltages the $\tau_a$ remains stable at 3 ms.

B) Half-inactivation time ($\tau_h$) for Cav3.2 rapidly decreases from 60 ms at -50mV to 20 ms at -30 mV. After that the decrease in $\tau_h$ reaches plateau. At positive voltages the $\tau_h$ remains stable at 18 ms. Adapted from Cribbs *et al.* (1998).

Steady-state inactivation of Cav3.2 is voltage dependent. The channel inactivates at increasing voltages and the potential for half-inactivation is −75.3 ± 0.3 mV (Cribbs *et al.,* 1998). At depolarized potentials lower than -90 mV Cav3.2 inactivation is completely removed (channel active) while at potentials -50 mV and higher the channel is completely inactivated (Klöckner *et al.,* 1999).

The activation and inactivation curves overlap creating the so-called 'window current' peaking at -65 mV (Fig. 5) (Catterall *et al*. 2005). As mentioned earlier, the inactivation of Cav3.2 is rapid, thus creating the transient current. The low-voltage threshold of activation allows this channel to participate in pacemaking *e.g.* in heart and thalamus relay neurons.

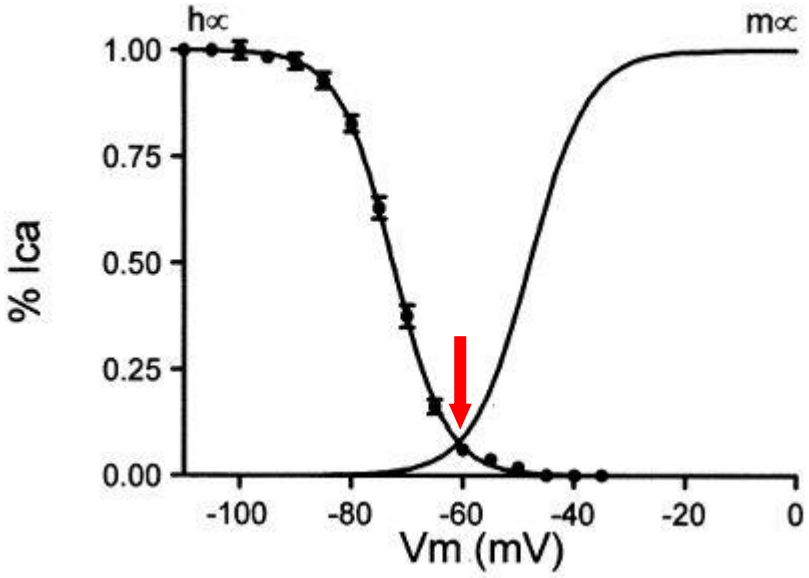


Figure 5. **Window current of Cav3.2**

Voltage dependence of the activation (mα) and inactivation (hα) of Cav3.2 overlap with a maximum at about -65 mV. This causes influx of $Ca^{2+}$ into cells with more depolarized RMP through the so-called window current. The arrow indicates the potential of maximal window current. Vm – depolarising membrane voltage; % Ica – normalised $Ca^{2+}$ current. Adapted from Chemin *et al*. (2000).

## 1.6. Molecular pharmacology of Cav3.2

To date no highly selective inhibitors of T-type calcium channels are known. All of the known inhibitors exhibit some degree of blocking other channels. One of the first developed drugs able to block T-type channels is mibefradil, which blocks T-type with 10- to 15-fold higher affinity than to L-type channels. This drug had been marketed as an anti-hypertensive, but subsequently withdrawn due to its influence on major cytochrome P450 enzymes leading to serious interactions with other drugs (Michels *et al*. 2002, Heady *et al*. 2001). Another class of drugs which inhibit both T-type and L-type calcium channels is dihydropyridines *i.e*. efonidipine, niguldipine, nicardipine and Bay K8644. These agents generally block both L-type and T-type channels although it depends on whether one of the enantiomers or a racemic mixture has been used. Bay K8644 is particularly interesting because its (+)-(R)-enantiomer acts as an antagonist for L-type channels whilst the (–)-(S)-enantiomer is an agonist of these channels. Both enantiomers are antagonists of T-type channels thus enabling differentiation between these two channel types (Heady *et al*. 2001).

Lipoic acid used to treat pain disorders exerts its effects by influencing Cav3.2 channels. It oxidises thiol residues on the cytoplasmic side of the channel causing its inactivation (Lee *et al*. 2009).

The only known inhibitor of LVA channels selective for Cav3.2 is $Ni^{2+}$ (nickel ion). The other two members of the LVA group are insensitive to nickel. Kang *et al.* (2006) reported that the crucial residue responsible for blocking Cav3.2, is His-191 in the extracellular loop between the third and fourth segments of domain I (D1:S3/S4). In addition, they showed that the substitution of His-191 with Glutamine or Alanine rendered the channel insensitive to nickel. Similarly, Q172H mutation in D1:S3/S4 of Cav3.1 channel increased its sensitivity to nickel almost to the level of Cav3.2. Other drugs able to block T-type

calcium channels are phenylalkylamines, benzothiazepines and some peptides isolated from snake, spider or scorpion venom *e.g.* agatoxin, kurtoxin, conotoxin and ProTx-I. ProTx-I inhibits Cav3.1 with a higher affinity than Cav3.2 and exchange of D4:S3/S4 fragment between these channels changed their responsiveness to ProTx-I accordingly (Ohkubo *et al*. 2010).

Hitherto, little research has been done to elucidate the mechanism of the action of the above inhibitors except for nickel, lipoic acid and ProTx-I. It is not known whether these agents block the channel by pore occlusion or modification of its gating properties. Pore occlusion is generally an 'all-or-nothing' mechanism whilst gating modifiers can render the channel more or less sensitive to voltage or change its activation/inactivation times. The latter mechanism is more interesting from a therapeutic point of view as this would allow for the fine tuning of calcium channel activity.

## 2. Aims of this study

The main aim of this study was to investigate the mechanism of the action of Cav3.2 and attempt to develop new inhibitors for this channel.

Antibodies have been postulated as potential blockers of Cav3.2. To date several ion channels have been successfully blocked using antibodies and this method seems to be a promising development in design of highly specific ion channel inhibitors. However, no such antibody for a calcium channel has been described.

This study was designed to bridge this gap in knowledge and attempt to develop antibodies against Cav3.2. The key question addressed in this thesis is whether specific antibodies against Cav3.2 can be generated and used for altering Cav3.2 kinetics. Several antibodies against specific regions of Cav3.2 have been generated and the effect of these antibodies on Cav3.2 was thoroughly investigated.

A fluorescence-based assay for measuring Cav3.2 activity was implemented and validated. This assay was then used as the main tool for assessing the effects of the antibodies generated in this project on Cav3.2 gating properties.

# 3. Research design

## Research hypothesis: Cav3.2 channel gating is affected by polyclonal antibodies generated against Cav3.2 peptide sequences.

The research described in this thesis is divided into four main stages which together provide the answer to the initial hypothesis. Each of these stages consists of several tasks which are described in detail in their respective chapters. A general overview of the research, the initial set up and the modifications that have been made during the study are summarised below.

Antibodies are gaining increasing significance as therapeutic agents due to their high selectivity, specificity and relative ease of production. The development of antibodies has several advantages over developing new chemical entities targeted at particular proteins. Antibodies are easier to direct to specific sequences within a given protein and only require the provision of a target peptide, while the development of chemical blockers is often based on modifications of a known inhibitor and it is usually difficult to target a particular site within the protein. For these reasons antibodies appear to be good allies in the pursuit for new Cav3.2 channel blockers. The generation of antibodies using the whole protein as an immunogen would yield a diverse population of antibodies binding to regions over the entire protein sequence. In this case the antibodies generated might have a good affinity to the protein but most likely they would not bind to the regions that are crucial for Cav3.2 gating. Therefore these antibodies may not possess the ability to alter the kinetics of the channel. Moreover, using the whole protein as an immunogen would require prior expression and purification of Cav3.2 which may prove difficult due to the protein being membrane- embedded. Therefore the generation of antibodies against a set of selected peptide sequences was chosen for this research project.

**The first step of my research** comprised of a detailed analysis of Cav3.2 structure in order to identify the target sequences to which the antibodies could bind. The structural analysis was performed on the basis of the published Cav3.2 sequence. The identification of transmembrane domains and the intracellular and extracellular regions of Cav3.2 has been performed using the Kyte-Doolittle hydropathy prediction tool and other bioinformatics tools and the results are described in Chapter 1.

There were several requirements for the anti-Cav3.2 antibodies that would increase the likelihood of generating a good Cav3.2 inhibitor. Firstly, the antibodies should be suitable for use on living cells. Antibodies cannot diffuse through cell membrane due to their size and low lipid solubility. There is a possibility of an antibody being internalized via endocytosis, but this pathway requires antibody receptors on the cell surface, does not guarantee the activity of the internalized antibody and therefore has not been considered for this project. For this reason the project focused on the generation of antibodies that bind to predicted extracellular domains of Cav3.2. Only these antibodies have a potential for use on living cells and do not require transport across the cell membrane to access the epitope. Moreover, hydrophilic peptide sequences are more immunogenic than the hydrophobic ones. These hydrophilic sequences are exposed to the hydrophilic environment, either on the cytoplasmic side of the cell membrane or on the cell surface. Secondly, although the exact gating mechanism of voltage-sensitive ion channels has not been elucidated, several regions have been proposed as being crucial for the channel gating, namely segments S4 and the regions surrounding the channel mouth (Catterall, 2011). Generating antibodies that bind to or close to these regions would increase the chances of influencing Cav3.2 kinetics. These changes in ion channel kinetics could be caused by the restriction of the movement of ion channel domains upon the binding of antibodies. Another possibility is that the binding of antibodies would affect the local electric field that triggers the opening of the channel and therefore would also either inhibit or promote the channel activation.

Three Cav3.2 peptide sequences have been finally chosen as immunogens to generate the antibodies. The choice of target epitopes is further explained in Chapter 1 alongside other requirements that were taken into account for the design of the antibodies.

**The second main stage** of this project was the production of the antibodies against the target peptide sequences and the testing of the affinity of these antibodies to Cav3.2. This stage is described in detail in Chapter 2 and Chapter 3. Briefly, the selected peptides were synthesised and coupled to a carrier protein (Keyhole Limpet Haemocyanin) in order to elicit an immune response in host organisms. The immunisation of rabbits was chosen for this purpose due to their relative phylogenetic distance from humans and the amount of serum that can be obtained from one animal. The resulting antibodies were isolated from the rabbit serum by affinity purification using the target peptides coupled to sepharose beads. This procedure guarantees extraction only of the antibodies that bind specifically to the selected epitope and removal of all non-specific immunoglobulins. The development of the immune response was monitored during the immunisation procedure and after the completed protocol using ELISA. This assay provided information on the immunogenicity of a given peptide and the affinity of the generated antibodies to the target sequence. Further tests were conducted to assess the affinity of the generated antibodies to their respective target sequences. Western Blotting was utilized to confirm the affinity of the antibodies to the peptides within the whole protein. Lysates of cells expressing Cav3.2 were used as a positive control to assess whether the generated antibodies bind to denatured Cav3.2. The Western Blot procedure with commercial anti-Cav3.2 antibodies also served to confirm expression of Cav3.2 in the cell lines used in the experiments. Flow cytometry analysis and immunocytostaining were employed to assess the affinity of the generated antibodies to the native protein embedded in the cell membrane. Peptides used for immunisation were in linear form that may differ from the arrangement of the native protein, hence the antibodies may be only able to bind to denaturated protein, *e.g.* in Western Blotting. These two experiments also provided information on the specificity of the generated antibodies, *i.e.* whether the antibodies bind

only to cells expressing Cav3.2 and not to wild type cells. Immunocytostaining procedure also served to verify the localisation of Cav3.2 in cells heterologously expressing Cav3.2. No cell lines available for laboratory use endogenously express Cav3.2; hence this project relied on cells transfected with Cav3.2. Transiently transfected cells were initially used in the research, although due to variations in transfection efficiency these cells were deemed unsuitable and were replaced by stably transfected cells. Heterologous expression of proteins is widely used but can produce misleading results that may be due to aberrant localisation of the protein such as retention in the endoplasmic reticulum, or abnormal protein folding resulting in non-functional molecules. In this experiment the localisation of Cav3.2 to the cell membrane was confirmed by immunocytostaining.

**The third part of the project** required the implementation and validation of an assay that would allow for testing of the effect that the generated antibodies exert on the Cav3.2 gating properties. There are various methods of investigating Cav3.2 kinetics, described in detail in Chapter 4. The fluorescence based assays measuring calcium influx through Cav3.2 channel were particularly well suited for this project. These assays allow for a relatively high-throughput assessment of inhibitory properties of the tested compounds. Moreover, one of them – the window current assay does not require manipulation with the cell membrane potential. This assay exploits the steady influx of $Ca^{2+}$ ions through a tiny fraction of Cav3.2 channels that are open at resting membrane potential. Therefore this assay probably most closely mimics the behaviour of Cav3.2 channel in non-excitable cells such as breast and prostate cancer that express Cav3.2. The attempt to validate this method was first performed using transiently transfected cells. However, as mentioned earlier, the results obtained on those cells depended on the transfection efficiency that varied between experiments. The use of the stable cell line expressing Cav3.2 rectified the problem and allowed for the successful implementation of the assay. The assay was validated with known Cav3.2 inhibitors such as mibefradil and nickel ions and has been confirmed to give results consistent with the published information on

Cav3.2 pharmacology. A detailed description of the window current assay and the results obtained during validation procedure are presented in Chapter 4.

**The final stage of the research** involved *in vitro* assessment of the changes in Cav3.2 kinetics accomplished by the generated antibodies. There is no published data on the use of antibodies in a fluorescence based assay. For this reason it was necessary to test and evaluate a wide range of conditions such as the concentration of the antibodies, the incubation times and conditions (*e.g.* shaking). The window current assay has some limitations that had to be taken into account, especially the incubation time. A long incubation time (over 1 hour) caused signal decay and therefore it was not possible to measure the long-term effect of the presence of antibodies on the Cav3.2 activation. Nevertheless, data available on the use of antibodies in other assays performed on viable cells (*e.g.* patch-clamp) state the incubation time as 20 min and it is probable that this incubation time should suffice also in the fluorescence-based assay.

The binding of antibodies depends also on the ionic strength of the solution. However, the window current assay requires the use of defined buffers in order to elicit the fluorescence response; therefore it was not possible to alter the buffer composition.

Furthermore, the antibodies have been tested simultaneously with other Cav3.2 modulators to assess their competitiveness in binding to Cav3.2. This experiment was also intended to provide information on which regions bind other Cav3.2 inhibitors – binding of antibodies themselves may not directly affect the channel kinetics but may work by displacing other Cav3.2 modulators.

The co-application of antibodies and drugs was also intended to test whether there is a cumulative effect of drugs and antibodies on Cav3.2 kinetics. The results obtained are described in detail in Chapter 5.

# 4. Materials

### Chemicals

| | |
|---|---|
| Accutase | Sigma-Aldrich |
| Acrylamide/Bisacrylamide | Sigma-Aldrich |
| Agar resin | Agar Scientific |
| BCA protein assay kit | Pierce Biosciences |
| BSA (Bovine serum albumin) | Sigma-Aldrich |
| Calcium chloride | Sigma-Aldrich |
| Coomassie Brilliant Blue R-250 | ThermoFisher |
| Choline chloride | Sigma-Aldrich |
| DAPI-Fluoroshield Mounting Medium | Abcam |
| DMSO (Dimethyl sulfoxide) | Sigma-Aldrich |
| DTT (Dithiothreitol) | ThermoFisher |
| EDTA | Sigma-Aldrich |
| Ethanol | Sigma-Aldrich |
| FBS (Foetal Bovine Serum) | Biosera |
| Fluo-4-AM | Invitrogen |
| Glucose | Sigma-Aldrich |
| G-418S (Geneticin sulphate) | Formedium |
| Gramicidin | Invitrogen |
| Guava ViaCount reagent | Guava Technologies, UK |
| HEPES | Sigma-Aldrich |
| Hydrochloric acid (HCl) | Sigma-Aldrich |
| Magnesium chloride | Sigma-Aldrich |
| Magnesium sulfate | Sigma-Aldrich |
| Mibefradil hydrochloride | Tocris |

| | |
|---|---|
| Nickel chloride | Sigma-Aldrich |
| Paraformaldehyde | Ambion |
| PBS (Phosphate Buffered Saline) | Gibco |
| Penicillin / Streptomycin | Sigma-Aldrich |
| Poly-L-lysine | Sigma-Aldrich |
| Potassium chloride | Sigma-Aldrich |
| Potassium dihydrogen phosphate | Sigma-Aldrich |
| Protease Inhibitor Cocktail for use with Mammalian Tissue | Sigma-Aldrich |
| Protein molecular weight marker | ThermoFisher |
| Puromycin | Sigma-Aldrich |
| RIPA buffer | Sigma-Aldrich |
| SDS (sodium dodecyl sulphate) | Sigma-Aldrich |
| Sodium azide | Sigma-Aldrich |
| Sodium bicarbonate | Sigma-Aldrich |
| Sodium chloride | Sigma-Aldrich |
| Sodium hydroxide | Sigma-Aldrich |
| Sodium pyruvate | Sigma-Aldrich |
| Sucrose | Sigma-Aldrich |
| Tris-EDTA | Sigma-Aldrich |
| Triton X-100 | Sigma-Aldrich |
| Trypsin/EDTA solution | ThermoFisher |
| Tunicamycin | Sigma-Aldrich |
| Tween 20 | Sigma-Aldrich |
| Zinc chloride | Sigma-Aldrich |

**Eukaryotic cell lines**

1. HEK293 – Human Embryonic Kidney

This cell line has been obtained from ATCC-LGC Standards UK. This cell line is easy in propagation and is often used in experiments involving the expression of transgenic protein. This cell line was generated by the adenovirus transformation of human foetal kidney cells (ATCC, 2016). The cells are of epithelial origin and are non-excitable, *i.e.* are unable to propagate and spread action potential to surrounding cells.

2. HEK/Cav3.2

This cell line was a kind gift of Professor Edward Perez-Reyes of the University of Virginia, School of Medicine. It has been obtained by the stable transfection of HEK293 cells with a linearized pcDNA3.1 plasmid carrying full-length Cav3.2 cDNA under the control of cytomegalovirus (CMV) promoter (information obtained from Prof. Perez-Reyes; Gomora *et al.,* 2002). The plasmid (map shown in Fig. 6) also contains a neomycin resistance gene. This allows for the selection of cells expressing Cav3.2 by the addition of geneticin (G-418) to the growth medium (Gomora *et al.,* 2002).

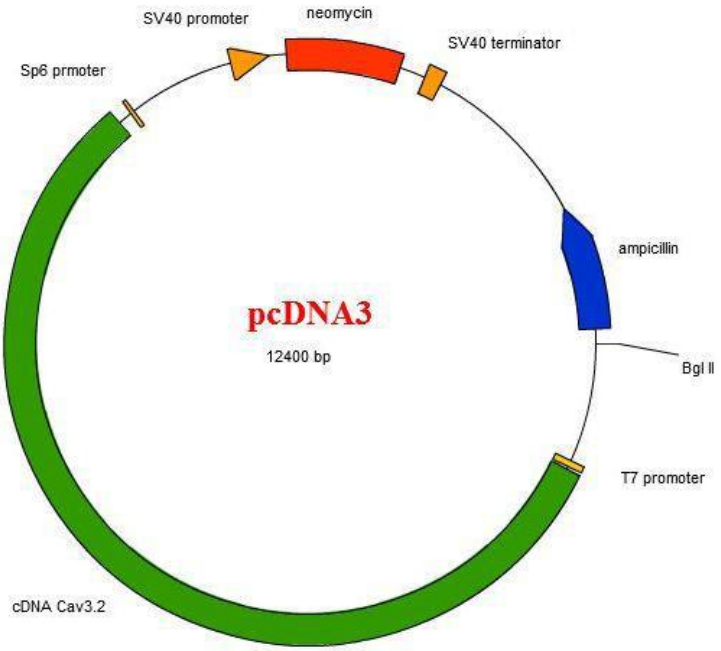


Figure 6. **Map of the plasmid used to express the Cav3.2 gene in HEK293 cells**

The plasmid contains a full length cDNA copy of the Cav3.2 gene under the control of a CMV promoter. The plasmid also contains a neomycin resistance gene which facilitates the selection of cells expressing the plasmid.

# 5. Methods

## 5.1. Growth conditions

HEK293 and HEK/Cav3.2 cells were grown in 100 mm cell culture dishes. The growth medium was DMEM/F-12 (Gibco) supplemented with 10 % FBS, 100 U/ml penicillin, 100 mg/ml streptomycin and 0.5 mM sodium pyruvate. The volume of medium used was 10 ml per 100 mm dish. HEK/Cav3.2 cells were cultivated with the addition of 1 mg/ml G418S (geneticin; final concentration) to maintain the expression of Cav3.2. Cells were incubated in a Heraeus HeraCell 150 incubator at 37°C and 5 % $CO_2$ until they reached the desired level of confluency. Following cell growth the cells were either used for experiments or passaged.

## 5.2. Passaging cells

Cells at 80-90 % confluency were split every three to five days. Cells were washed once with growth medium, and trypsin/EDTA solution was added to the cells. After 1 min incubation at room temperature the trypsin/EDTA solution was removed and the cells were incubated at 37 °C for 5 min. Growth medium was then added to the dishes and the resulting cell suspension was transferred to a 50 ml centrifuge tube and spun at 100 *g* for 5 min. The supernatant was discarded; cells were resuspended in fresh growth medium, split at ratio 1:3 and transferred to new cell culture dishes.

## 5.3. Freezing cells/ banking

Low passage number cells were used for the preparation of frozen stock. Cells were grown to confluency, detached with trypsin/EDTA as described above and washed in growth medium. Cells were then resuspended in ice-cold freezing medium containing 10 % DMSO at density 1 x $10^7$ cells/ml. Cell suspension was transferred to cryo-vials (1 ml/vial) and the individual tubes were sealed with parafilm to prevent cross-contamination in liquid nitrogen. The cryo-vials were placed in a Styrofoam container and cooled in a -80°C freezer at a rate of approximately -1 °C/min. After overnight storage at

-80 °C, the frozen stock cells were transferred to a liquid nitrogen tank (-183 °C) for long-term storage.

## 5.4. Thawing of cells

To reconstitute cell cultures from frozen stock, the cryo-vial was removed from the liquid nitrogen and immediately thawed in a water bath at 37 °C. The vial was disinfected with Bioguard and the content was transferred to 10 ml of pre-warmed complete growth medium in a culture dish. The cells were incubated at 37 °C in 5 % $CO_2$ overnight to re-attach to the dish surface; then the medium was replaced with fresh growth medium to remove traces of DMSO.

## 5.5. Cell treatment prior to window current assay

Cells used for window current assay were grown in 96 well plates. The plates were coated with poly-L-lysine to enhance the cells' adherence to the bottom of the wells. 50 µl of poly-L-lysine (0.01 % w/v) was added to each well and the plate was incubated at room temperature for 20 min. The coating solution was then removed and the plate was sterilized under a UV lamp for 30 min.

Cells used for the window current assay were harvested by trypsinization from dishes at approximately 80 % confluency. The cells were then resuspended at a density 5 x $10^5$ cells/ml and 100 µl of cell suspension was added to each well. The plate was then incubated at 37 °C and 5 % $CO_2$ for at least 24 hours to allow the cells to reach confluency. In some experiments the cells were pre-treated with tunicamycin to remove potential sugar residues at the predicted N-glycosylation site in the D1:S3/S4 region. The cells on the plate were grown with 2 µg/ml tunicamycin added to the growth medium 20 hours prior to window current assay.

## 5.6. Window current assay

Once cells grown in the 96 well plate reached 100 % confluency, they were used for a window current assay. The growth medium was removed and the cells were carefully washed once with HBSS-HEPES so as not to dislodge the cells. The cells in each well were then overlaid with 50 µl of 2 µM Fluo-4 AM in HBSS-HEPES and the plate was incubated for 20 min at 37°C to load cells with Fluo-4 AM. After the incubation the loading solution was removed and cells were washed once with HBSS-HEPES. In order to assess the inhibitory effect of test compounds, 100 µl of HBSS-HEPES containing the test compounds was added to the wells and the plate was incubated for 20 min at room temperature in the dark on a rotary shaker. After incubation the plate was transferred to an Omega FluoStar plate reader and the assay was performed. The Fluo-4 dye was excited at 485 nm and the resulting fluorescence was recorded at 520 nm. The fluorescence in each well was recorded for 60 s at 0.2 s intervals. Each interval measurement consisted of 5 flashes per well. The baseline fluorescence level was measured for 5 s, then 100 µl of high $Ca^{2+}$ solution was automatically injected and the fluorescence reading continued for 55 s. High $Ca^{2+}$ solution was HBSS-HEPES with 20 mM $CaCl_2$; the addition of this solution raised the $Ca^{2+}$ concentration in wells to 10 mM.

## 5.7. Transient transfection

Human Embryonic Kidney 293 (HEK293) cells were grown in Dulbecco's Modified Eagle's Medium (DMEM) supplemented with 10 % Newborn Calf Serum and 1 % penicillin-streptomycin. The cells were transfected using FuGENE 6 transfection reagent (Roche). The day prior to transfection the cells were trypsinized and seeded at density 2 x $10^4$ cells per well in a 96-well plate coated with poly-L-lysine. The cells were then incubated overnight at 37 °C, 5 % $CO_2$ to achieve a level of confluency of 70-80 %. The transfection mix was prepared by the addition of 2.6 µg plasmid DNA (3.5 µl of the plasmid solution) and 7.8 µl FuGENE 6 reagent (ratio 3:1) to 120.5 µl of OPTIMEM

medium. Transfection mix (5 µl) was added to each well and the cells were incubated at 37 °C, 5 % $CO_2$ for 72 hours prior to performing the window current assay.

## 5.8. Preparation of cell lysate

Cells were grown in DMEM/F-12 medium supplemented with 10 % FBS and 1 % penicillin-streptomycin in 100 mm cell culture dishes until 90 % confluency was achieved. The growth medium was removed and the cells were washed twice with Phosphate Buffered Saline (PBS). The cells were treated with 800 µl of RIPA buffer with Protease Inhibitor Cocktail. The dishes were incubated on ice for 5 min. The cell lysate was then collected with a cell scraper and transferred to a microcentrifuge tube. The aggregate of denatured nucleic acids was removed and the lysate was clarified by centrifugation at 8000 g for 10 min at 4 °C to remove cell debris. The supernatant was transferred to a fresh microcentrifuge tube and stored at -20 °C.

## 5.9. Determination of protein concentration

A BCA Protein Assay Reagent Kit was used to quantify protein concentration in cell lysates. Eight standard samples were prepared using Bovine Serum Albumin (BSA) in range 25 – 2000 µg/ml. The Working Reagent (WR) was prepared by mixing 50 parts of reagent A with 1 part of reagent B. Reagent A contains sodium carbonate, sodium bicarbonate, bicinchoninic acid and sodium tartrate in 0.1 M sodium hydroxide, reagent B contains containing 4 % cupric sulfate. This method combines the Biuret reaction (reduction of $Cu^{2+}$ cation in presence of protein in alkaline medium) with bicinchoninic acid detection of $Cu^{1+}$ cation. Each standard sample and the analysed sample (0.1 ml of each one) was pipetted into labelled tubes and 2.0 ml of WR was added to each tube. The samples were incubated at 37 °C for 30 min. The colour development was proportional to the amount of protein in the sample and was read spectrophotometrically at 562 nm. The BSA samples were used to create a standard curve (linear regression) which allowed for the calculation of protein concentration in the analysed samples. The

standard curves were prepared alongside the measured samples for every assay and a typical standard curve is shown in Fig. 7.

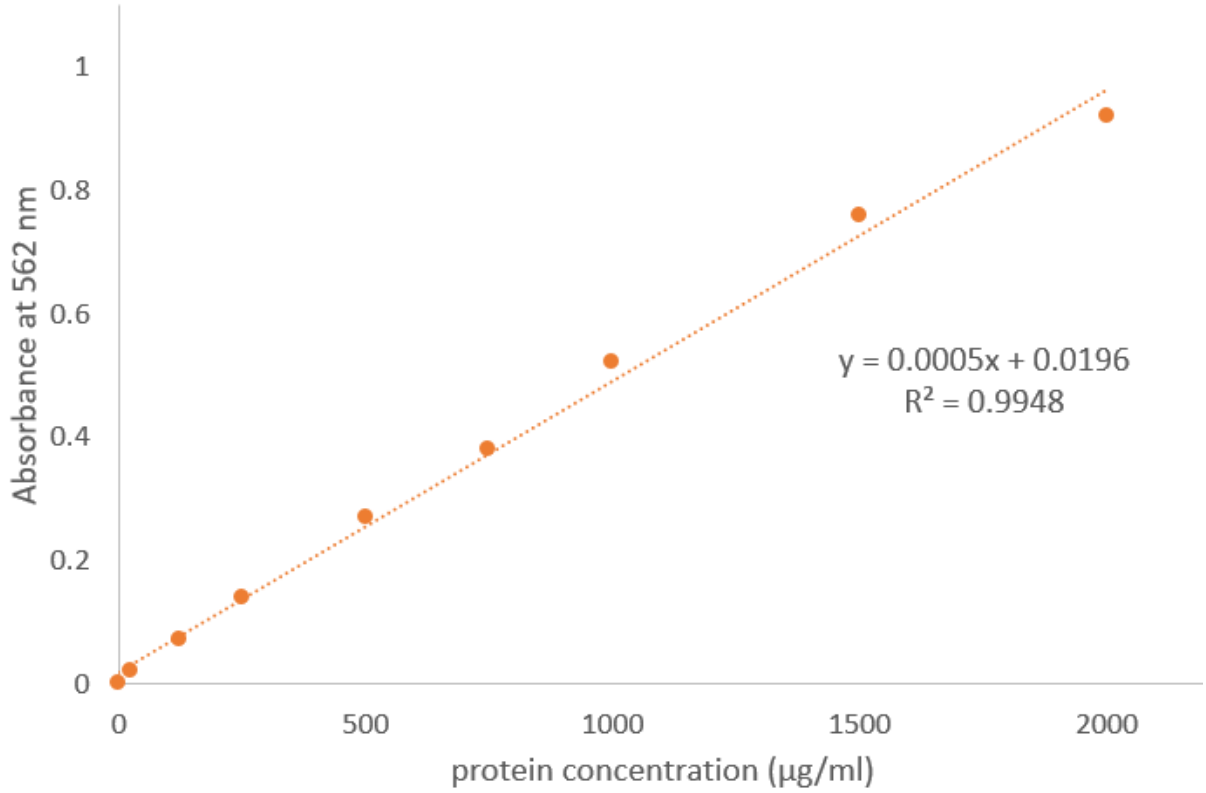


Figure 7. **Example standard curve of protein concentration.**

Absorbance of eight standard samples of Bovine Serum Albumin was measured to create a standard curve. Microsoft Excel software was used to create a linear regression curve (dotted line) and to calculate the curve equation and $R^2$ value. The equation was used to calculate the protein concentration in the cell lysate samples.

## 5.10. Western Blotting

10 µl of 2x Tris-Glycine SDS Sample Buffer (Thermo Fisher Scientific) was added to 10 µl of cell lysate. The proteins were denatured by heating at 95 °C for 5 min. 15 µl of cell lysates with sample buffer was then loaded into the wells of 10 % polyacrylamide gel (Novex® 10 % Tris-Glycine Mini Gel – Thermo Fisher Scientific) and analysed by SDS-PAGE using X-Cell *SureLock* Mini-Cell apparatus and Tris-Glycine SDS Running Buffer (Thermo Fisher Scientific). Novex® Sharp Protein Standard was used as a protein molecular weight standard. Electrophoresis was conducted at 125 V for approximately 90 min until the dye had reached the bottom of the gel. The proteins were then transferred onto a PVDF membrane. The transfer of proteins from the gel to the membrane was performed using X-Cell *SureLock* Mini-Cell. Stock solution of 25x Tris-Glycine Transfer Buffer (Thermo Fisher Scientific) was diluted to required concentration and methanol was added to final concentration of 20%. The transfer was performed overnight at a constant current of 16 mA. After the transfer procedure, the membrane was transiently stained to check for an even transfer of proteins using Pierce Reversible Protein Stain Kit for PVDF Membranes (Thermo Fisher Scientific) and following the instructions manual. Briefly, the membrane was rinsed with ultrapure water and the Sensitizer solution was applied to the membrane. After 2 min of agitation on a rotary shaker, the Sensitizer solution was removed and the Reversible Stain solution was added to the membrane and left on a rotary shaker for 1 min. The Destain solution was then applied to remove the stain from the membrane and to visualise the protein bands. Finally, the Eraser solution was applied to the membrane to remove the stain from protein bands. The membrane was then washed twice with water to remove traces of gel, transfer buffer and staining kit components.

## 5.11. Immunodetection Protocol

Detection of Cav3.2 protein on the blot was performed using WesternDot 625 Goat Anti-Rabbit Western Blot Kit (Invitrogen) and anti-Cav3.2 primary antibodies (Alomone

Laboratories). The membrane was blocked in WesternDot Blocking Buffer for 1 hour on a rotary shaker. The membrane was then incubated overnight in a primary antibody solution (1 µg/mL anti-Cav3.2 rabbit antibody in Wash Buffer). After decantation of the primary antibody solution, the membrane was washed three times with Wash Buffer. The secondary antibody solution containing 4 µl of Biotin-conjugated-Goat anti-rabbit antibody in 8 mL of Wash Buffer was then added to the membrane and incubated for 1 hour. The membrane was washed again three times with Wash Buffer. The membrane was then incubated in 8 mL of Blocking Buffer with 4 µl Qdot 625 streptavidin conjugate for 1 hour. The membrane was washed three times with Wash Buffer. The bands were visualised by UV light using a GelDoc imaging system.

## 5.12. Immunocytochemistry

To investigate the cellular localisation of Cav3.2, immunostaining of cells was performed. Cells were grown on poly-L-lysine coated coverslips in 6 well plates. After reaching approximately 50 % of confluency, the cells were rinsed with PBS and fixed with 3 % paraformaldehyde for 15 min at room temperature. The coverslips were washed twice in ice-cold PBS. Cells were in PBS then permeabilized by 10 min incubation with 0.25 % Triton X-100 in PBS. Samples were then washed in PBS three times for 5 min on a rotary shaker. In order to minimize the non-specific binding of antibodies, the samples were blocked for 30 min with 1 % BSA in PBST (PBS with 0.1 % Tween 20) on a rotary shaker. The blocking solution was discarded and cells were incubated with primary antibody solution overnight at 4°C in a humidified chamber. The primary antibody solution was 1 % BSA/PBST containing 1 µg/ml anti-Cav3.2 mouse monoclonal antibody (Abcam). After incubation the antibody solution was discarded and the samples were washed three times for 5 min in PBS. The coverslips were then incubated with secondary antibody solution for 1 hour at room temperature in the dark. Secondary goat polyclonal anti-mouse antibody conjugated with FITC (Abcam) was diluted in 1 % BSA/PBST at concentration 1 µg/ml. After incubation with secondary antibody solution, the samples

were washed again three times in PBS. The coverslips were mounted with a drop of Fluoroshield Mounting Medium with DAPI (Abcam) and sealed with nail polish.

## 5.13. Fluorescence microscopy

The immunostained cells were observed using a fluorescence microscope (IX81 motorized inverted fluorescence microscope, Olympus Corporation). Visual analysis was performed using ocular lenses (this allowed for the observation of fluorescence colour) and the images were captured using a monochromatic camera mounted on the microscope. Images were analysed and coloured using Cell^M imaging software (Olympus Corporation).

## 5.14. Flow cytometry staining

Cells were detached by 5 min incubation with accutase (Sigma-Aldrich) and washed once with PBS. The cell number was determined using a Scepter Handheld Automatic Cell Counter (Millipore) and cells were resuspended at density 5 x $10^6$ cells/ml in ice cold PBS containing 10 % FCS. Cells were then divided into 1.5 ml Eppendorf tubes and fixed with 100 µl of 1 % paraformaldehyde in PBS. Cells were then spun down at 400 g for 5 min and washed with PBS. Permeabilisation of cell membrane to allow for staining of intracellular antigens was achieved by 15 min incubation with either 0.5 % Tween 20 in PBS or 0.5 % saponin in PBS.

The cells were then incubated with 1 µg/ml primary antibody in 3 % BSA/PBS for 1 hour on ice in the dark and they were washed three times with PBS and incubated with 1 µg/ml secondary antibody diluted in 3 % BSA/PBS for 1 hour on ice in the dark. After labelling, the cells were washed three times with PBS and immediately analysed on Guava EasyCyte flow cytometer.

## 5.15. Flow cytometry analysis

The Guava EasyCyte flow cytometer (Guava Technologies) was used to analyse expression of Cav3.2. Cells labelled with fluorescent antibodies were loaded on the 96-well plate (100 µl cell suspension per well) and analysed using the ExpressPlus assay. This assay allows for measurement of particle size and particle fluorescence.

## 5.16. Data analysis

The data presented in this thesis was analysed using Microsoft Excel 2013 and GraphPad Prism software. Data from experiment replicates was averaged and standard deviation (SD) was calculated using Microsoft Excel 2013. The number of replicates varied depending on availability of the reagents, therefore in certain cases only two replicates were performed. The p-values were calculated using unpaired t-test (software Microsoft Excel 2013). The area under curve (AUC) values were calculated using GraphPad Prism. The fluorescence data was normalised to the positive control, i.e. the value from a well in a given experiment was divided by the value of a positive control from the same experiment and presented as percentage.

# Part II

# Chapter 1: Analysis of Cav3.2 structure

# 1. Introduction

The identification of possible targets for antibody generation can only be achieved after thorough analysis of Cav3.2 structure. The starting point for a structural analysis of a protein is the amino acid sequence. Sequence data can be gathered either by direct protein sequencing (Edman degradation reaction and mass spectrometry) or deduced from the nucleotide sequence, if one is known. This data can then be used for structural studies. Direct analysis of three-dimensional protein structure is achieved mainly by X-ray crystallography although Nuclear Magnetic Resonance is also used. However, X-ray crystallography can only be used for proteins that form crystals which can then be analysed by X-ray diffraction. The vast majority of transmembrane proteins (including ion channels) do not form crystals and thus at present cannot be analysed by X-ray crystallography. Moreover, the interactions of transmembrane proteins with the lipid bilayer are crucial for adopting their tertiary structure. The structure of isolated and crystallised transmembrane proteins might significantly differ from their native structure. Nevertheless, some transmembrane proteins have been successfully crystallized and their structures described in detail. One of the first crystallized ion channels was KcsA, a bacterial potassium channel. This channel consists of four identical subunits arranged around the ion pore (Doyle *et al.,* 1998) and elucidation of its structure laid foundations for understanding the mechanism of the action of this and of other ion channels. Despite the aforementioned difficulties with crystallizing the transmembrane proteins, several transmembrane protein structures have been described and are deposited in the Protein Data Bank (PDB). As of July 2014, approximately 2400 empirical transmembrane protein structures have been deposited in the PDB – this is 2.5 % of the total structures deposited in the PDB (slightly over 100,000). Only 176 ion channel structures or their fragments have been published in the PDB, which accounts for 0.17 % of the total number of structures. New protein structures are added frequently.

Another approach to elucidating the transmembrane protein structure is based on computational methods. These methods can be roughly divided into two groups: (1) *ab initio* methods, where the protein conformation is computed solely on the basis of protein sequence; and (2) comparative modelling where a given protein model is created on the basis of sequence similarity to proteins with known structures (Filipek and Modzelewska, 2006). The *ab initio* methods assume that the protein folding process leads to minimization of the potential energy of the molecule. This energy can be calculated as a function of positions of all nuclei in the molecule and atom types (atomic number, hybridization, spin, character of bonds to other atoms). The terms of this function also include the stretching of molecular bonds, torsion angles, van der Waals and Coulombic interactions. A function gathering the above parameters is called force-field. Lower force-field values of a given conformation correspond to a more relaxed, hence more credible predicted structure. The comparative modelling of proteins relies mainly on global sequence alignment with homologous proteins of known structure. When no sufficient global alignment can be found, protein models can be created using 'threading' – attempts to fit the given protein sequence into a library of known folds and assessing its internal energy to assess whether a given conformation is feasible. These folds are then connected into the final structure. Another approach used in protein modelling is creating a series of local alignments that can detect highly conserved regions in proteins that would otherwise seem to be unrelated. Detecting these regions allows for creating partial models of the protein of interest which can then be developed using other methods of structural analysis (Filipek and Modzelewska, 2006).

Molecular modelling software such as ArgusLab (available at arguslab.com) is used for visualising molecule structure on the basis of available structural data or for creating new models on the basis of the chemical composition of a molecule. This software allows for creating models on the basis of user defined torsion angles (φ and ψ) in the protein backbone. Such models can then be used in computer-aided drug design, *e.g.* Virtual

Ligand Screening (a cheaper and faster method that could replace High-Throughput Screening) or Quantitative Structure Activity Relationship (QSAR) that investigates the binding between a given ligand and its target site (Fernández-Ballester *et al.,* 2011). Nevertheless, this approach can only be successful if the protein model accurately corresponds to the native structure of the channel. Currently protein models created *in silico* only without underlying empirical data are not accurate enough to allow for computer-assisted drug design (Fernández-Ballester *et al.,* 2011)

In addition to the above mentioned methods, the analysis of the sequence itself also provides information on the localisation of possible structures such as transmembrane segments, zinc fingers, leucine zippers etc. The transmembrane segments consist of mainly hydrophobic amino acids forming α-helix structure which is compatible with the hydrophobicity of the cell membrane (hydrophobic tails of phospholipids). The length of this hydrophobic section needs to be around 20 amino acids to match the thickness of the cell membrane (approximately 5-7 nm).

There are various methods and indexes for calculating the hydropathicity of protein sequences and predicting the localisation of transmembrane segments. The Kyte-Doolittle scale is one of the widely used methods (Qiagen Bioinformatics, 2014). In this system, each amino acid has an assigned hydropathicity value ranging from –4.5 for hydrophilic arginine to 4.5 for hydrophobic isoleucine. Kyte-Doolittle algorithm then calculates the hydrophobicity for each amino acid in the sequence by summation of the hydropathicity values for this given amino acid and the adjacent amino acids. The number of adjacent amino acids taken into account to calculate the hydrophobicity value (window size) is defined by the user and is in the range 3-21. Lower window sizes are used for the analysis of soluble proteins and searching for their hydrophilic regions that are likely to be on the surface of the protein. Larger window sizes (17-21) are used to search for putative transmembrane domains (Qiagen Bioinformatics, 2014).

The resulting hydropathicity value is then plotted against the position of the amino acid. Peaks on the plot indicate hydrophobic regions. The presence of membrane-spanning regions is suggested by hydropathicity values above 1. This algorithm proves useful in predicting the protein structure, however it must be emphasized that this method is computational only and does not probe the actual protein structure. Therefore the results obtained only suggest the possible structure of a given protein but cannot be a proof of the actual protein arrangement.

A further method used for the analysis of Cav3.2 structure is the antigenicity prediction tool – EMBOSS Antigenic available at http://emboss.bioinformatics.nl/. Antigenicity is an ability of a given peptide to elicit an immune response and bind antibodies. Antigenicity depends on sequence length, amino acid composition and conformation of a given peptide. Kolaskar and Tongaonkar (1990) investigated the most immunogenic regions of several proteins and built an algorithm analysing protein sequences and predicting the most immunogenic regions. The accuracy of this algorithm is approximately 75 % (Kolaskar and Tongaonkar 1990). This algorithm was used in the structural analysis of Cav3.2 to identify regions with higher chances of eliciting an immune response. Choosing more immunogenic regions for antibody generation would increase the chances of obtaining antibodies of high affinity and specificity.

Homology studies can aid in elucidating protein structure. Generally similar sequence implies similar structure and often similar mechanisms of action. One of the commonly used homology algorithms is ClustalW available at European Bioinformatics Institue website (ebi.ac.uk). It allows for pairwise and multiple alignments of both nucleotide and protein sequences. Protein alignment can be created using one of four matrices (BLOSUM, PAM, Gonnet and ID). These matrices contain the score for pairs of identical and similar amino acids. ClustalW algorithm creates the optimal alignment of sequences (maximum score), sometimes introducing gaps in the alignment. User-set parameters include penalties for gap opening, gap alignment and gap clustering.

## 2. Aims

The aim of this part of the project was to analyse the structure of Cav3.2 to identify the regions that are best suited as targets for antibody generation. This analysis was performed using available bioinformatics tools. Moreover, literature research aided in the selection of the target sequences by identifying the Cav3.2 motifs involved in the channel gating.

# 3. Results

The sequence of *Homo sapiens* Cav3.2 (recommended name: voltage-dependent T-type calcium channel subunit alpha-1H) was obtained from UniProt database, accession number O95180. This sequence was reported by Cribbs *et al.* (1998) with subsequent modifications by the same authors.

The full sequence length is 2353 amino acids and their arrangement into domains is shown in detail in Fig. 8 (image created using Protter 1.0). Two isoforms originating from alternative splicing have been proposed – isoform 2 differs from isoform 1 (canonical) by Glu→Lys substitution at residue 1593. Twenty five other naturally existing variants of Cav3.2 have been reported (Daniels *et al.,* 2001; Jagannathan *et al.,* 2002; Chen *at al.,* 2003; Heron *et al.,* 2004). The localisation of these variants is shown in Fig. 8.

Figure 8. **Amino acid sequence of Cav3.2 and its domain structure**

Protein sequence of voltage-dependent T-type calcium channel subunit alpha-1H (Cav3.2) was obtained from UniProt database, accession number O95180 (*Homo sapiens*; sequence length: 2353 amino acids). The overall view of the protein arrangement is presented below. An enlarged view of the fragments of this image is presented on subsequent pages. The orange area represents the plasma membrane. The extracellular portions of the protein are above the plasma membrane, the cytoplasmic regions are under the membrane. Blue numbers indicate transmembrane segment numbers. Black numbers indicate the position of amino acid in the sequence. The localisation of known variants is indicated by yellow diamonds. The localisation of possible N-glycosylation sites is indicated by green squares.

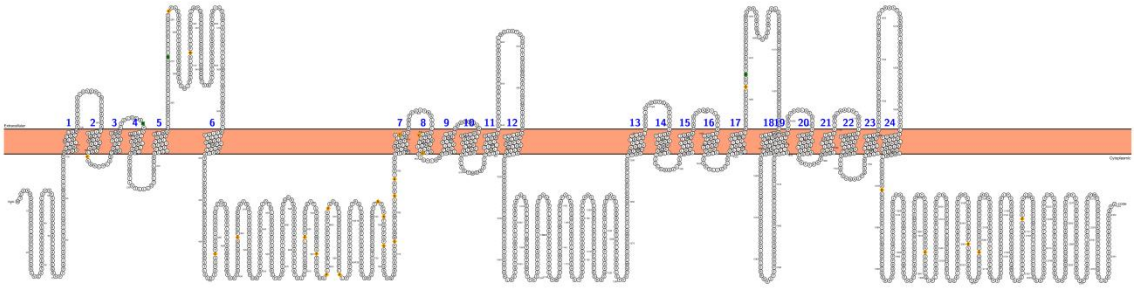

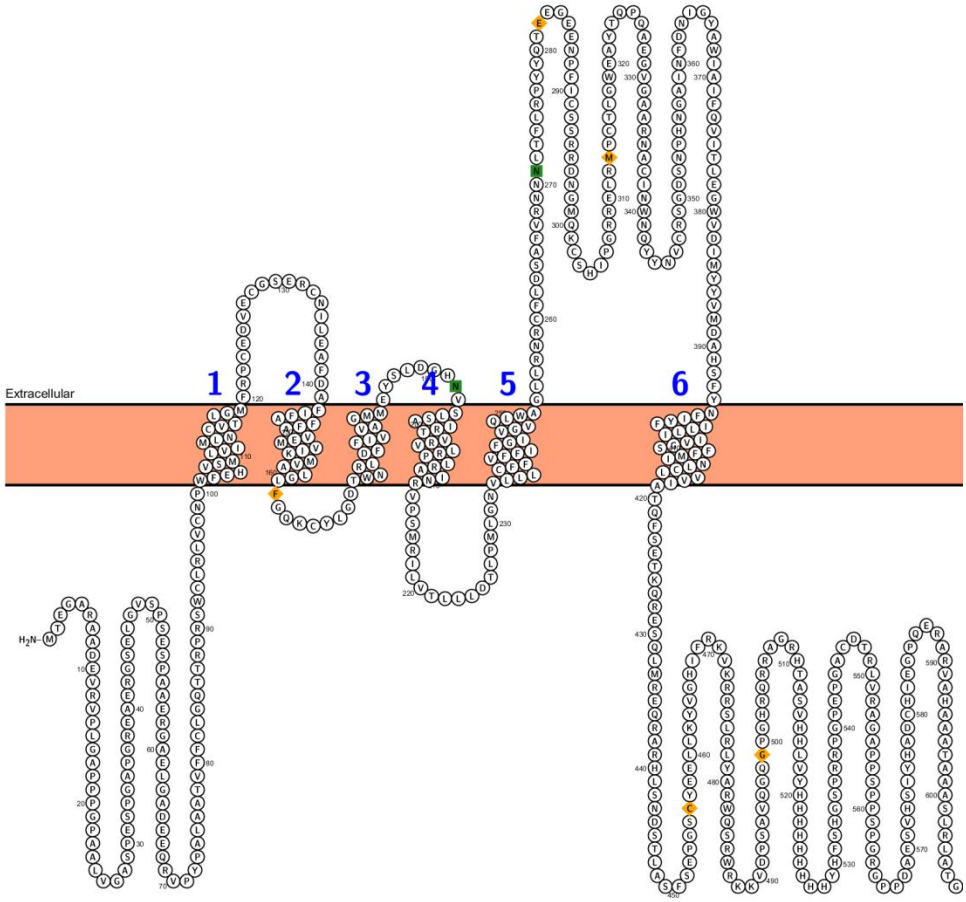
Extracellular
1
2
3
4
5
6
H2N-

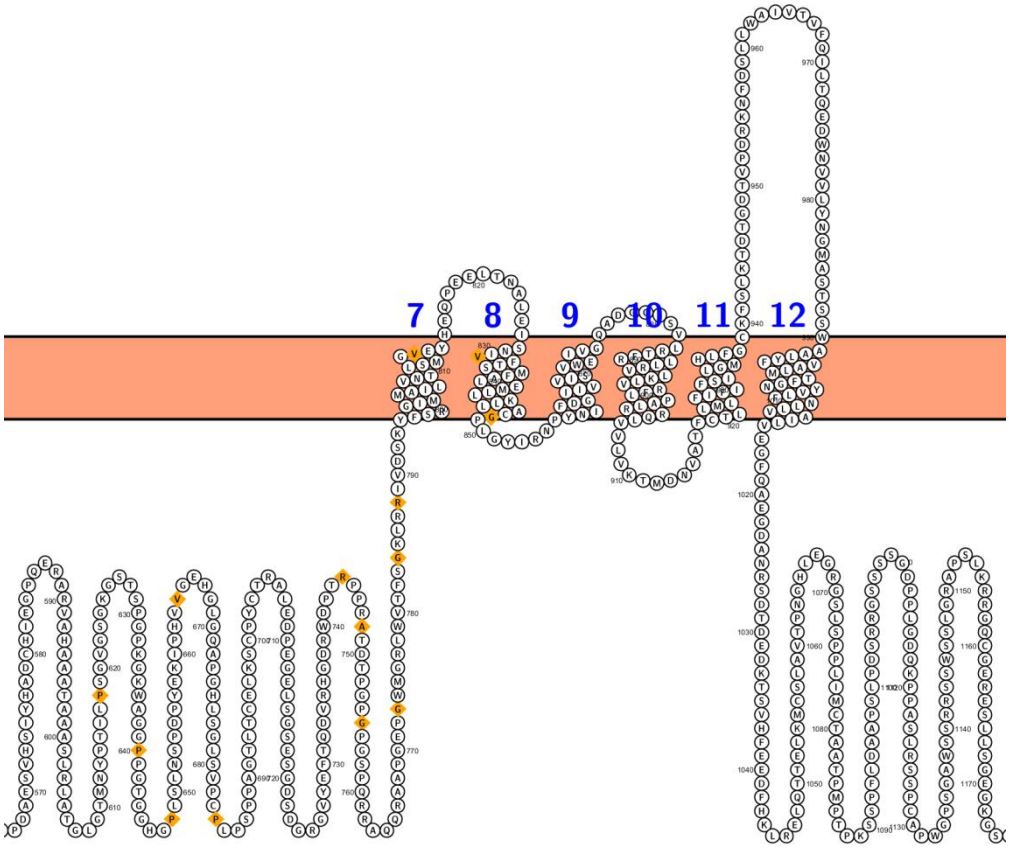
7
8
9
10
11
12

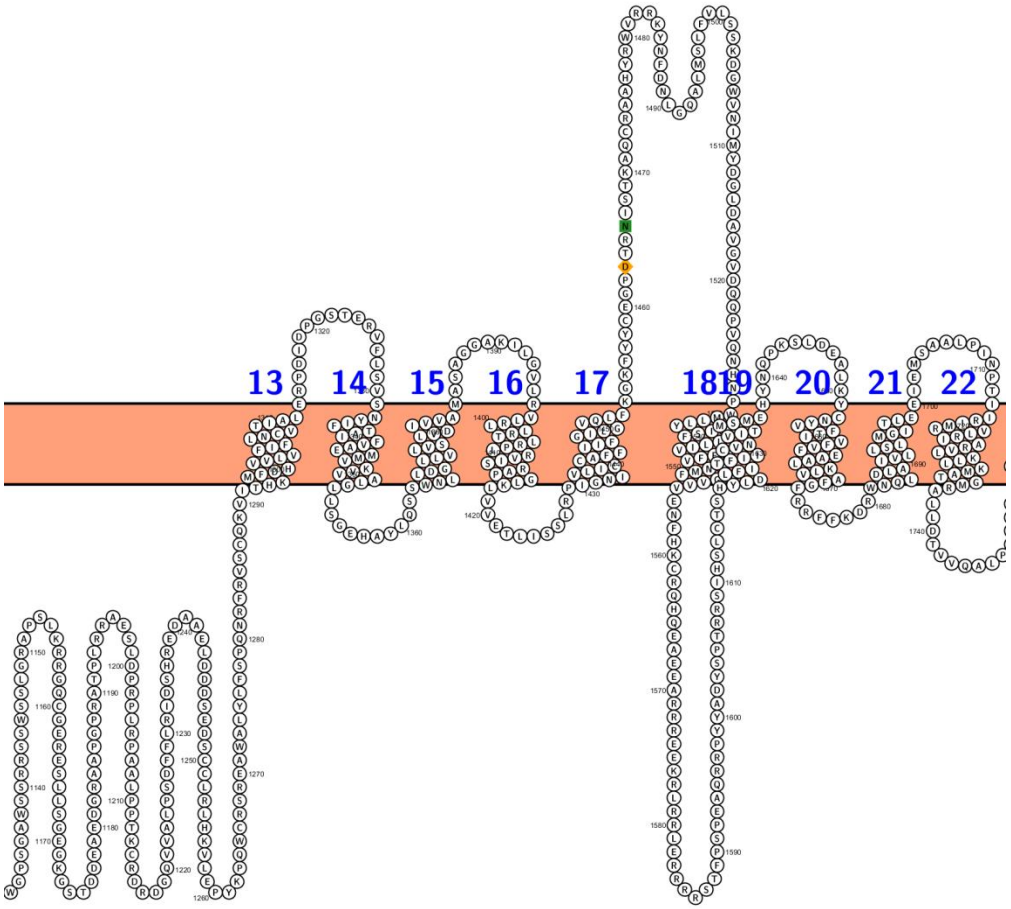
13
14
15
16
17
18
19
20
21
22

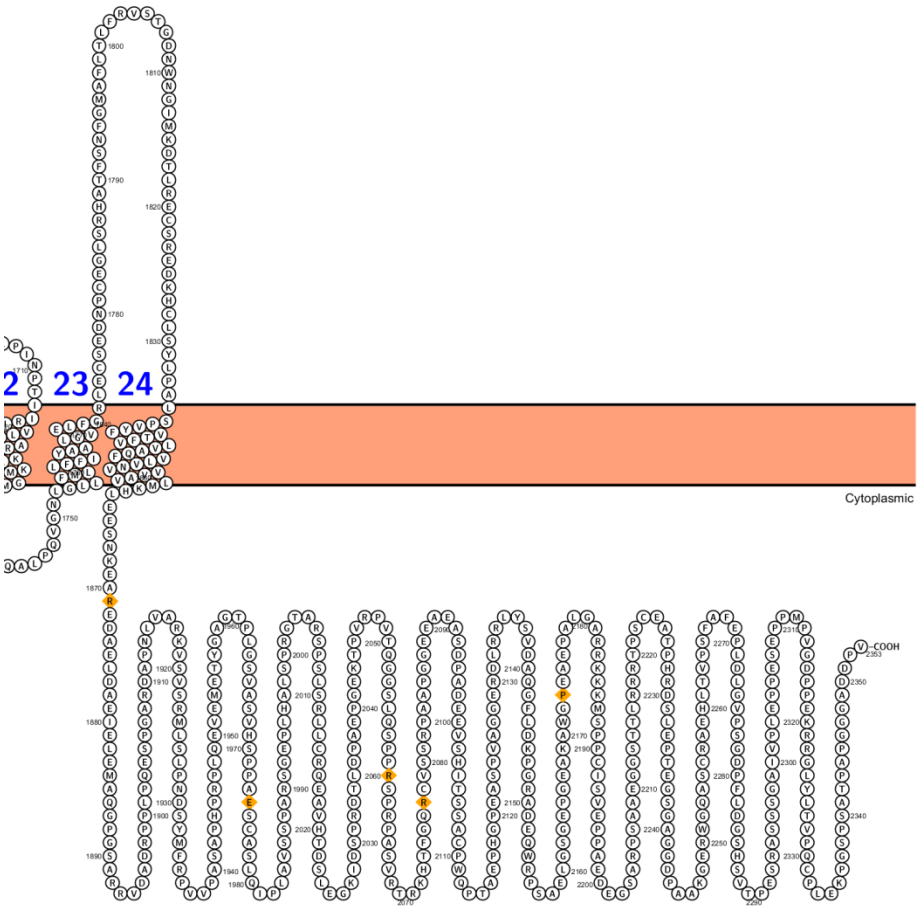
2
23
24
Cytoplasmic
-COOH

Human Cav3.2 is closely related to Cav3.1 and Cav3.3. Cav3.2 sequences of other mammals also are homologous to human Cav3.2. Moreover, Cav3.2 exhibits homology with other voltage-gated calcium channels and voltage-gated sodium channels *e.g.* Na1.5. The phylogenetic tree of Cav3.2 and other closely related ion channels is shown in Fig. 9. Amino acid alignment of human Cav3.2, Cav3.1, Cav3.3 and Nav1.5 is shown in Fig. 10. Pairwise alignment performed with ClustalW revealed that percent identity between Cav3.2 and Cav3.1 is 56.49 %, between Cav3.2 and Cav3.3 is 55.62 % and between Cav3.2 and Nav1.5 is 21.75 %.

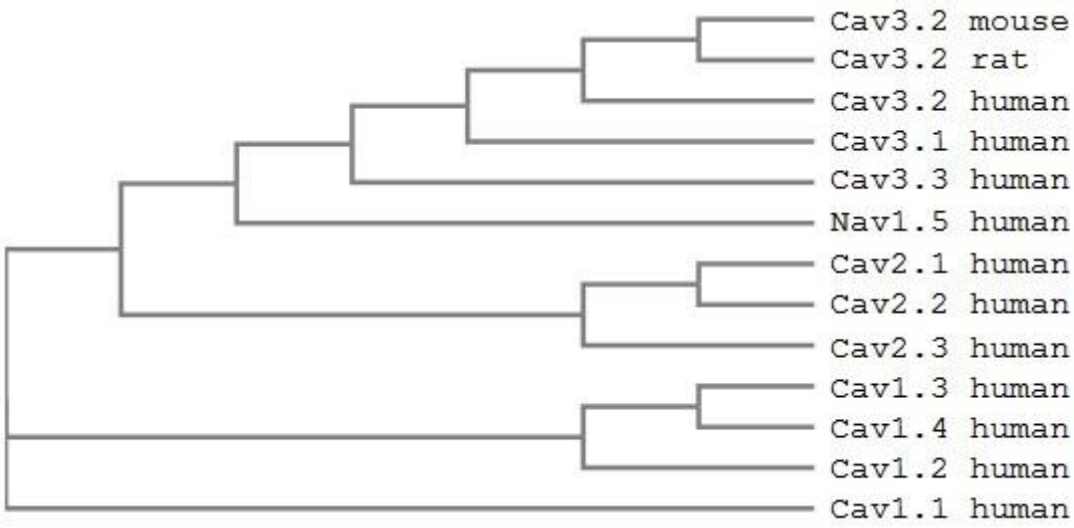


Figure 9. **Cladogram showing the relationship between mouse, rat and human Cav3.2 and other related ion channels**

The cladogram comparing the sequences of human Cav3.2 (O95180), mouse Cav3.2 (O88427), rat Cav3.2 (Q9EQ60), human Cav3.1 (O43497), human Cav3.3 (Q9P0X4), human Cav1.1 (Q13698), human Cav1.2 **(**Q13936), human Cav1.3 (Q01668), human Cav1.4 (O60840), human Cav2.1 (O00555), human Cav2.2 (Q00975), human Cav2.3 (Q15878) and human Nav1.5 sodium channel (Q14524) was obtained using ClustalW2 phylogeny tool (http://www.ebi.ac.uk/Tools/msa/clustalw2/).


Figure 10. **Amino acid alignment of human Cav3.1, Cav3.2, Cav3.3 and Nav1.5**

The amino acid sequence alignment of Cav3.1 (O43497), Cav3.2 (O95180), Cav3.3 (Q9P0X4) and Nav1.5 (Q14524) was obtained using ClustalW Multiple Sequence Alignment tool. A consensus sequence across all four proteins is indicated by asterisks under the alignment. Double dots under the alignment indicate amino acids with strongly similar properties (score above 0.5 in the Gonnet PAM 250 matrix). Single dots indicate weak conservation of amino acid properties. Red letters represent small and hydrophobic amino acids; blue letters represent acidic amino acids, pink letters denote basic amino acids and green letters indicate glycine and amino acids with hydroxyl, sulfhydryl and amine functional groups.

Figure 8 (continued). **Amino acid alignment of Cav3.1, Cav3.2, Cav3.3 and Nav1.5**

Analysis of Cav3.2 sequence hydrophobicity was performed using the Kyte-Doolittle algorithm and the results are shown in Fig. 11 and Table 1. The aim was to identify the membrane-spanning regions of the channel and the localisation of the pore; hence the window size used in computation was set at 17. The results show the arrangement of Cav3.2 into four domains, each of which has six transmembrane segments and a pore loop between fifth and sixth transmembrane segments. The N- and C- termini are most possibly cytoplasmic due to the lack of a signal peptide at the beginning of the sequence. The special structural features of Cav3.2 sequence such as zinc binding sites and potential N-glycosylation sites are included in Table 1. These results are in agreement with previously proposed by Perez Reyes (2003).

| | Amino acid residue number | Length | Putative structure |
|---|---|---|---|
| | 1-100 | 100 | N-terminus (cytoplasmic) |
| Domain 1 | 101-119 | 19 | Helical Transmembrane segment 1 |
| | 120-141 | 22 | Extracellular loop<br>→ Zn (residue 140) |
| | 142-160 | 19 | Helical Transmembrane segment 2 |
| | 161-169 | 9 | Cytoplasmic loop |
| | 170-184 | 15 | Helical Transmembrane segment 3 |
| | 185-193 | 9 | Extracellular loop<br>→ Zn (residues 189, 191)<br>→ GlcNAc (residue 192) |
| | 194-212 | 19 | Helical Transmembrane segment 4 |
| | 213-232 | 20 | Cytoplasmic loop |
| | 233-253 | 21 | Helical Transmembrane segment 5 |
| | 254-394 | 41 | Pore loop<br>→ GlcNAc (residue 271) |
| | 395-419 | 25 | Helical Transmembrane segment 6 |
| | 420-793 | 374 | Cytoplasmic loop – domain linker |
| Domain 2 | 794-814 | 21 | Helical Transmembrane segment 1 |
| | 815-827 | 13 | Extracellular loop |
| | 828-849 | 22 | Helical Transmembrane segment 2 |
| | 850-855 | 6 | Cytoplasmic loop |
| | 856-874 | 19 | Helical Transmembrane segment 3 |
| | 875-882 | 8 | Extracellular loop |
| | 883-906 | 24 | Helical Transmembrane segment 4 |
| | 907-917 | 11 | Cytoplasmic loop |
| | 918-938 | 21 | Helical Transmembrane segment 5 |
| | 939-990 | 52 | Pore loop |
| | 991-1015 | 25 | Helical Transmembrane segment 6 |
| | 1016-1290 | 275 | Cytoplasmic loop – domain linker |

Table 1.**Transmembrane segment localisation of Cav3.2 – Domains 1 and 2**
The Cav3.2 protein sequence, the localisation of transmembrane domains, glycosylation and zinc binding sites were extracted from UniProt database, accession number O95180. All the predicted transmembrane segments have at least 19 amino acid residues, except for the Segment 3 in Domain 1 (D1:S3). Zn indicate Zinc binding site; GlcNAc indicate potential N-glycosylation site.

| | Amino acid residue number | Length | Putative structure |
|---|---|---|---|
| Domain 3 | 1291-1313 | 23 | Helical Transmembrane segment 1 |
| | 1314-1331 | 18 | Extracellular loop |
| | 1332-1352 | 21 | Helical Transmembrane segment 2 |
| | 1353-1362 | 10 | Cytoplasmic loop |
| | 1363-1382 | 20 | Helical Transmembrane segment 3 |
| | 1383-1396 | 14 | Extracellular loop |
| | 1397-1418 | 22 | Helical Transmembrane segment 4 |
| | 1419-1428 | 10 | Cytoplasmic loop |
| | 1429-1452 | 24 | Helical Transmembrane segment 5 |
| | 1453-1529 | 77 | Pore loop<br>→ GlcNAc (residue 1466) |
| | 1530-1555 | 26 | Helical Transmembrane segment 6 |
| | 1556-1616 | 60 | Cytoplasmic loop – domain linker |
| Domain 4 | 1617-1637 | 21 | Helical Transmembrane segment 1 |
| | 1638-1651 | 14 | Extracellular loop |
| | 1652-1673 | 22 | Helical Transmembrane segment 2 |
| | 1674-1680 | 7 | Cytoplasmic loop |
| | 1681-1699 | 19 | Helical Transmembrane segment 3 |
| | 1700-1713 | 14 | Extracellular loop |
| | 1714-1737 | 24 | Helical Transmembrane segment 4 |
| | 1738-1751 | 14 | Cytoplasmic loop |
| | 1752-1772 | 21 | Helical Transmembrane segment 5 |
| | 1773-1835 | 63 | Pore loop |
| | 1836-1863 | 28 | Helical Transmembrane segment 6 |
| | 1864-2353 | 490 | C-terminus (cytoplasmic) |

Table 1 (continued). **Transmembrane segment localisation of Cav3.2 – Domains 3 and 4**

The Cav3.2 protein sequence, the localisation of transmembrane domains, glycosylation and zinc binding sites were extracted from UniProt database, accession number O95180. All the predicted transmembrane segments in Domains 3 and 4 have at least 19 amino acid residues. GlcNAc indicate potential N-glycosylation site.

A.

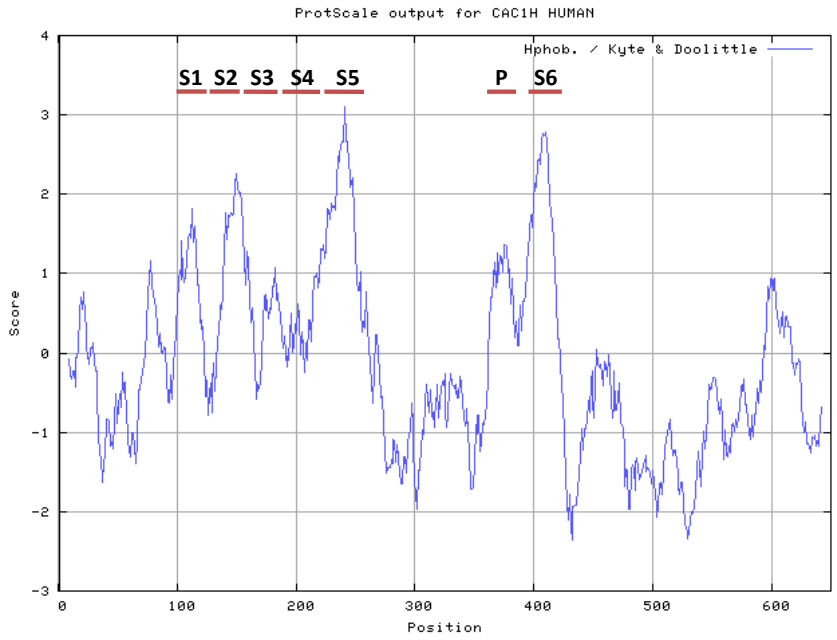


B.

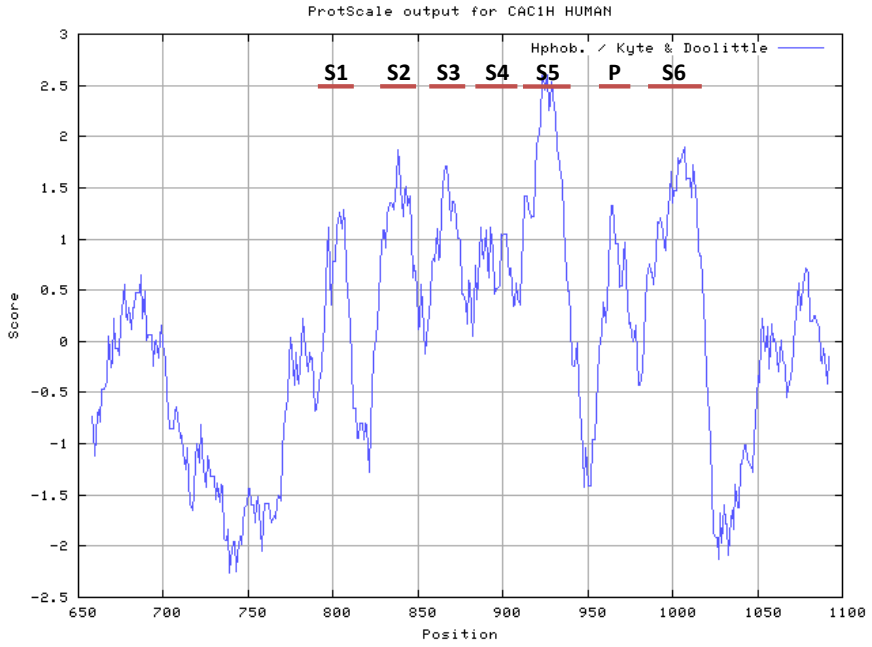


Figure 11. **Hydrophobicity analysis of Cav3.2**

ProtScale tool (http://web.expasy.org/protscale/) has been used to conduct hydrophobicity prediction plot based on Kyte & Doolittle scale. Window size was 17. The full length of human Cav3.2 has been divided into four parts to allow for clarity of the plots. Red bars above the plot indicate putative localisation of transmembrane segments and pore loops.

A. Fragment containing N-terminus and Domain 1 (1-650aa).

B. Fragment containing Domain 2 and D1-D2 linker (650-1100aa).

C.

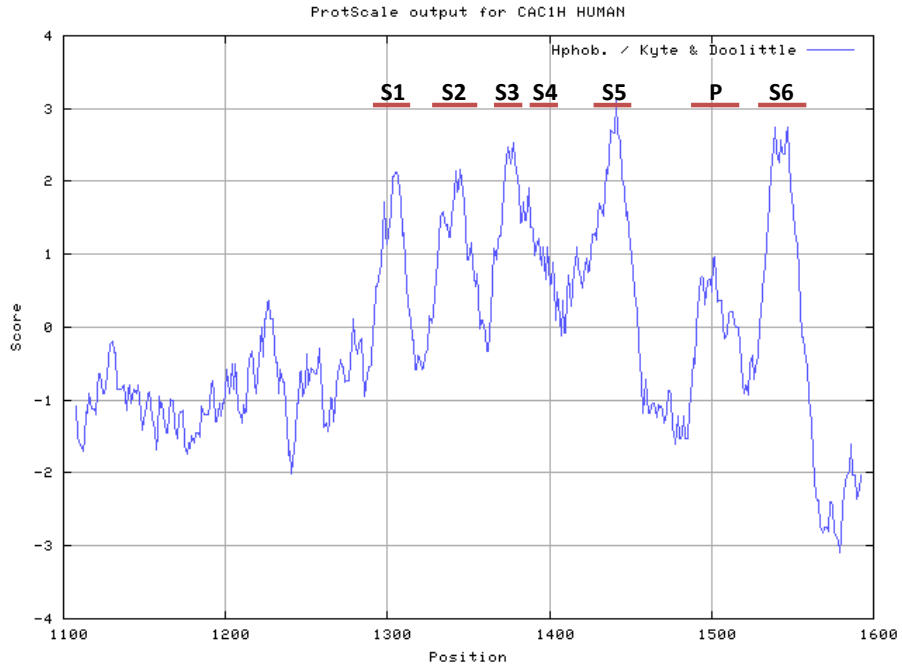


D.

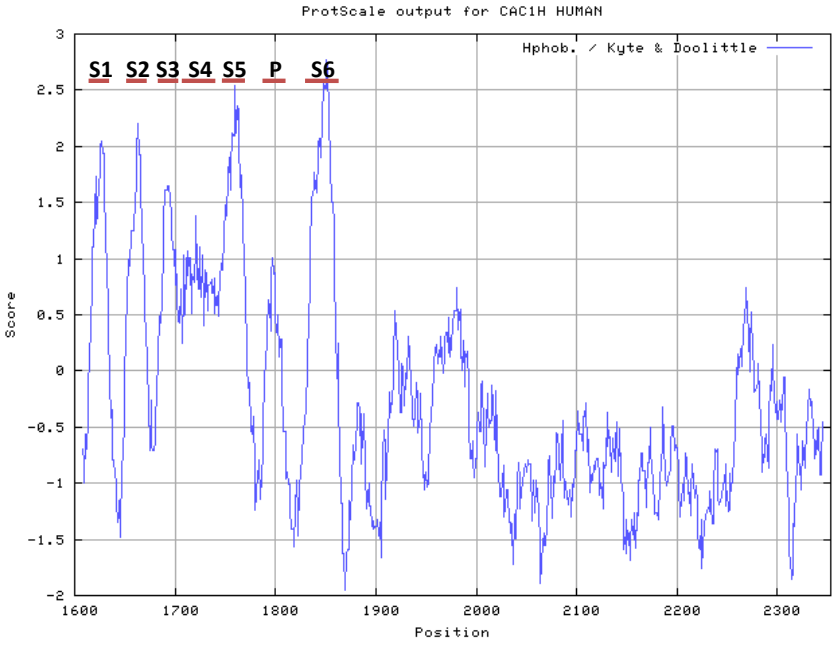


Figure 9 (continued). **Hydrophobicity analysis of Cav3.2**

C. Fragment containing Domain 3 and D3-D4 linker (1100-1600aa).

D. Fragment containing Domain 4 and C-terminus (1600-2353aa).

Overall, the Cav3.2 channel has 12 possible target regions for the generation of antibodies. These regions are the extracellular loops connecting transmembrane segments, *i.e.* the loops connecting the segments S1 with S2 and S3 with S4 in each of the domains. Moreover the pore loops in each domain are predicted to line the channel opening (Senatore, Zhorov and Spafford, 2012; Simms and Zamponi, 2014) and to be partially extracellular due to their length (41, 52, 77 and 63 amino acids in Domains 1 to 4, respectively).

The extracellular loops of Cav3.2 have been analysed using the EMBOSS Antigenic algorithm to assess their potential as antigens for the generation of antibodies. A score of 1 and above indicates regions with antigenic potential. Lower scores are returned as 0 and indicate no predicted antigenic potential of a given sequence.

The scores for each of the extracellular regions of Cav3.2 are presented in Table 2. The pore loop regions in all four domains exhibit significant antigenicity with scores in range 1.144-1.179. Only three of the short extracellular loops linking segments S1 with S2 and S3 with S4 have antigenic potential: both of the extracellular loops in Domain 1 and the S3/S4 loop in Domain 4.

| region | score | Sequence and maximum score position (underlined) |
|---|---|---|
| Cav3.2 maximum | 1.277 | EDKHCLSYLPALSPVYFVTFVLVAQFVLVNVVVAVLMKH |
| D1:S1/S2 | 1.120 | CEDVECGSE |
| D1:S3/S4 | 1.107 | LDGHNVSLS |
| D1:P | 1.144 | YAWIAIFQVITLEGW |
| D2:S1/S2 | 0 | - |
| D2:S3/S4 | 0 | - |
| D2:P | 1.169 | DSLLWAIVTVFQILT |
| D3:S1/S2 | 0 | - |
| D3:S3/S4 | 0 | - |
| D3:P | 1.152 | GQALMSLFVLSS |
| D4:S1/S2 | 0 | - |
| D4:S3/S4 | 1.062 | SAALPIN |
| D4:P | 1.179 | EDKHCLSYL |

Table 2. **Antigenicity prediction of Cav3.2 extracellular loops**

The antigenicity score for each of the Cav3.2 extracellular loops was calculated using EMBOSS Antigenic algorithm (http://emboss.bioinformatics.nl/cgi-bin/emboss/antigenic). Score above 1 indicate high antigenic potential.

The exclusion of regions with low predicted antigenicity leaves seven peptide sequences suitable as targets for antibody generation – all four pore loop regions, D1:S1/S2, D1:S3/S4 and D4:S3/S4. The extracellular loops between segments S3 and S4 are of particular interest for antibody target, due to the fact that segments S4 are thought to act as voltage sensors and move outwards when the channel is activated (Elliott *et al.,* 2004). The binding of antibodies may prevent this outward movement and therefore inhibit the channel activity. D1:S3/S4 is unique due to the presence of two zinc binding sites (residues 189 and 191 – Kang *et al.,* 2010) and one putative N-glycosylation site (sequence Asn-Val-Ser).

Previously published research indicated Cav3.2 regions that are implicated in the channel gating. Some of these regions are intracellular, *e.g.* the intracellular loop between Domains 1 and 2 was reported to act as a gating brake (Arias-Olguín *et. al.,* 2008). These intracellular regions cannot be readily used for generation of antibodies suitable for use on living cells, hence were not included in further research.

A review of the literature regarding only extracellular motifs of Cav3.2 implicated in Cav3.2 gating is summarized below.

## 3.1. Extracellular loop between segments S3 and S4 in Domain 4 (D4:S3/S4)

Ohkubo *et al.* (2010) investigated the differences in sensitivity of Cav3.1 and Cav3.2 to tarantula ProTx-I toxin. ProTx-I is a 35 amino acids long peptide toxin isolated from the venom of the tarantula *Thrixopelma pruriens*. The toxin has a characteristic structure similar to other peptide toxins such as hanatoxin. This structure consists of three pairs of cysteines forming three disulfide bonds – inhibitory cysteine knot (ICK). Moreover, hanatoxin has six hydrophobic amino acid residues that form a protruding cluster that has been proposed to intercalate into the cell membrane and reach the voltage-sensing S4 domain of the ion channel. ProTx-I has the ICK structure with the same positions of cysteines as hanatoxin and also has six hydrophobic amino acid residues at similar positions to hanatoxin. These residues may form an analogous cluster interacting with the voltage sensors of the ion channel. The similarities in structure of hanatoxin and ProTx-I suggest similar mechanisms of action. Hanatoxin has been reported to bind to the S3/S4 loop of voltage-gated Potassium channels (Ohkubo *et al.,* 2010). Both toxins have been reported to block diverse ion channels including T-type calcium channels, voltage-gated sodium channels (ProTx-I), voltage-gated Potassium channels and Cav2.1 (hanatoxin). This evidence suggested that ProTx-I may also bind to the S3/S4 loop of ion channels (Ohkubo *et al.,* 2010).

Cav3.1 is 160-fold more sensitive to ProTx-I than Cav3.2 ($IC_{50}$ = 0.2 μM and $IC_{50}$ = 32 μM, respectively; Ohkubo *et al.,* 2010). This difference makes ProTx-I useful in elucidating the functional differences between Cav3.1 and Cav3.2 as these channels are commonly coexpressed in the same cell type. Cav3.1 and Cav3.2 have a highly conserved structure, yet Cav3.1 is much more sensitive to ProTx-I. Analysis of the mechanism of ProTx-I action on these channels may pinpoint residues that are crucial for the gating properties of these channels and pave the way for the future development of the subtype specific channel inhibitors.

Ohkubo *et al.* (2010) investigated the mechanism of tarantula toxin ProTx-I action on Cav3.1 and Cav3.2 expressed in oocytes. The extracellular loop D4:S3/S4 of Cav3.1 and Cav3.2 has a similar structure to the S3/S4 linker of Kv2.1 Potassium channel and Nav1.2 sodium channel suggesting that this loop may participate in the binding of ProTx-I. The exchange of fourteen amino acids from loop D4:S3/S4 between Cav3.1 and Cav3.2 resulted in diminished sensitivity of Cav3.1/S3S4 chimera ($IC_{50}$ increase to 17.8 μM) and increased sensitivity of Cav3.2/S3S4 ($IC_{50}$ reduction to 15.8 μM). This is a significant increase in the sensitivity of Cav3.2, especially when taking into account that the D4:S3/S4 sequences of Cav3.1 and Cav3.2 differ by only four amino acid residues. However, the sensitivity of the recombinant Cav3.2 was still not approaching the level of the original Cav3.1, indicating that additional motifs are involved in the channel inhibition by ProTx-I. One of the differences between the D4:S3/S4 loops of these channels is the presence of putative N-glycosylation site in Cav3.1 which is absent in Cav3.2. It has not been elucidated whether this sequence is actually glycosylated and whether it may have any influence on toxin binding.

The mechanism of ProTx-I binding to Cav3.2 and Cav3.1 has not been fully elucidated. Nevertheless, this research confirmed the participation of D4:S3/S4 in gating of Cav3.1 and Cav3.2. Antibodies against D4:S3/S4 loop might bind to the channel in a similar manner to the ProTx-I and also affect the gating properties of the channel. The structure of the D4:S3/S4 loops of Cav3.1 and Cav3.2 is presented in Fig. 12. On the basis of this published research, the peptide sequence LMGITLEEIEMSAALPINPTII was chosen as a target for anti-Cav3.2 antibody generation.

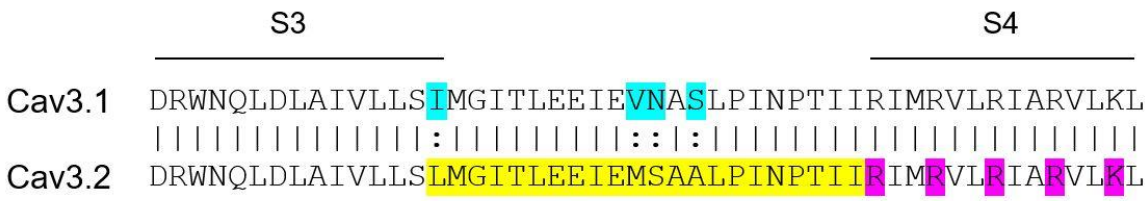


Figure 12. **Alignment of D4:S3/S4 of Cav3.1 and Cav3.2**

The EMBOSS Needle Alignment tool was used to compare Cav3.1 and Cav.3.2 sequences. Vertical bars indicate identical residues, double dots indicate similar residues. The peptide sequence used to raise antibodies is highlighted in yellow. The positively charged arginine and lysine residues in segment S4 are highlighted in pink. Differences between Cav3.1 and Cav3.2 sequence are highlighted in blue. The horizontal bars above the sequence indicate predicted transmembrane domains. The sequences of Cav3.1 and Cav3.2 were obtained from UniProt database accession numbers **O43497 and O95180** respectively.

## 3.2. Extracellular loop between segments S3 and S4 in Domain 1 (D1:S3/S4)

This loop contains histidine at position 191 which is crucial for the channel sensitivity to nickel, zinc, ascorbate and nitrous oxide. The mechanism of Cav3.2 sensitivity to nickel has been described by Lee *et al*. (1999) and Kang *et al.* (2006). Their research was based on structure comparison between two members of the LVA family: Cav3.1 and Cav3.2. These channels are highly homologous but Cav3.1 is not sensitive to nickel ($IC_{50}$ = 250 μM) while Cav3.2 is selectively blocked by nickel at low concentration ($IC_{50}$ = 12 μM). Chimeric constructs exchanging fragments of the protein between Cav3.1 and Cav3.2 have shown that D1:S3/S4 is crucial for $Ni^{2+}$ binding. Cav3.1 with D1:S3/S4 from Cav3.2 had increased sensitivity to nickel almost to the level of Cav3.2 whereas Cav3.2 with D1:S3/S4 from Cav3.1 lost sensitivity to nickel. Changes in other loops did not affect the $Ni^{2+}$ inhibitory effect. Point mutations of D1:S3/S4 have pinpointed His191 of Cav3.2 as being directly involved in binding nickel. Substitution of histidine with glutamine or alanine lowered the Cav3.2 sensitivity to level of Cav3.1. Mutation of a corresponding residue in Cav3.1 to histidine (Q172H) increased the channel sensitivity but not to the level of Cav3.2. Moreover binding of $Ni^{2+}$ to the original Cav3.2 delayed inactivation of the channel – $\tau_{inact}$ was increased from 8.6 ms to 11.9 ms. (Kang *et al.* 2006). Activation and inactivation curves were slightly shifted towards more positive potentials. Further chimeric studies (Kang *et al.,* 2010) revealed that His191 together with two preceding amino acids (Asp-Gly-His) is involved in nickel, zinc and copper sensitivity of Cav3.2. In addition to this sequence, a single aspartate residue in extracellular loop D1:S1/S2 is necessary to create the nickel binding pocket and achieve a full block of the channel. This study also suggested that electrostatic interactions between Asp140 in D1:S1/S2 and positively charged residues in D1:S3/S4 may influence the structural conformation of the channel and its trafficking to the cell membrane. This would explain the fact that oocyte expression of mutated Cav3.2 (D140A) was significantly reduced. The binding of

nickel or zinc to this epitope is thought to prevent movements associated with channel opening and stabilize the channel in its closed state.

Furthermore, D1:S3/S4 loop is also involved in Cav3.2 interaction with nitrous oxide ($N_2O$). $N_2O$ has long been used as an anaesthetic but its exact mechanism of action has not yet been elucidated. Orestes *et al.* (2011) proposed that the aforementioned nickel and zinc binding site can also bind iron and undergo metal-catalysed oxidation (MCO). $N_2O$ can react with bound iron producing hydrogen peroxide and other Reactive Oxygen Species (ROS), which in turn oxidise iron and the imidazole ring of His191 to 2-oxo-histidine. This modification may affect the channel conformation and reduce T-currents. Oxidised iron may then be reduced by electron donor system, allowing the cycle to restart. This hypothesis is supported by observation that $H_2O_2$ produces similar results in reducing Cav3.2 currents and this effect is non additive with $N_2O$ inhibition. Application of catalase and superoxide dismutase interrupted the inhibitory pathway of $N_2O$ suggesting that ROS are indeed involved in this mechanism. Mutation of His to Glu significantly reduces Cav3.2 sensitivity to $N_2O$ while the application of deferoxamine (potent iron chelator) increases Cav3.2 currents to 150 % of control indicating that iron bound to histidine is central in this mechanism. *In vivo* studies have shown that $N_2O$ mediated analgesic effect was absent in mutant mice lacking Cav3.2.

A similar mechanism underlies inhibition of Cav3.2 by ascorbate. Nelson *et al.* (2007a) found that ascorbate triggers MCO in D1:S3/S4 and Cav3.2 inhibition in acutely isolated dorsal root ganglion (DRG) neurons and transfected HEK293 cells expressing Cav3.2. The inhibition of T-type currents by ascorbate was higher in the HEK293 cells than in native environment in DRG cells. This can be attributed to the presence of an unidentified redox buffer system in neurons or the expression of more than one subtype of T-channels in DRG.

The MCO theory of Cav3.2 inhibition is further corroborated by experiments showing that Cav3.2 expressing nociceptors are sensitized by reducing agents such as DTT and L-

cysteine. Also T-type currents in HEK293/Cav3.2 cells are increased in presence of DTT and L-cysteine. These two agents are able to reduce cysteine residues and chelate metal ions. EDTA and DTPA that are not able to reduce cysteines, also increased T-currents, confirming that this effect is due to the removal of metal ion bound in D1:S3/S4 binding site.

Loop D1:S3/S4 is also involved in the gating of voltage-gated sodium channel Nav1.5, and antibodies against this loop block the sodium current. Chioni *et al*. (2005) investigated alternative splicing of Nav1.5. One splice form denoted Nav1.5 is predominantly expressed in adult tissues – brain, dorsal root ganglia and skeletal muscles. The other splice variant is expressed in the same tissues but mainly at the early stages of life and this variant is termed 'neonatal' Nav1.5 (nNav1.5). In mice, the switch from expressing nNav1.5 to expressing 'adult' Nav1.5 occurs before the $10^{th}$ day of life. Moreover, nNav1.5 is implicated in human cancer – re-expression of nNav1.5 in breast cancer has been reported by Fraser *et al.* (2005) and in prostate cancer by Djamgoz *et al.* (2001). Chioni *et al*. (2005) generated polyclonal antibodies using peptide which corresponds to D1:S3/S4 loop of nNav1.5. Immunofluorescent staining of tissues and Western Blotting confirmed that these antibodies (named NESOpAb) differentiate between the 'adult' and 'neonatal' splice variants of Nav1.5 despite these variants differing by only six amino acids. Moreover, NESOpAb significantly reduced nNav1.5 conductance. A 50 % block of the maximal current was achieved at less than 5 ng/ml concentration of NESOpAb. 'Adult' Na1.5 current was only diminished by 25 % and at much higher NESOpAb concentration – 250 ng/ml. The activation and inactivation thresholds of the channel were not affected by the binding of NESOpAb. These results show potential for the use of anti-Nav1.5 antibodies for future drug development and also for diagnostic purposes.

Sequence comparison of Nav1.5 and Cav3.2 has shown a high level of homology between these channels – 21.75 % overall sequence identity with higher sequence

conservation in some regions such as transmembrane segments. Sequences used for local alignment of Cav3.2 and nNav1.5 contain the D1:S3/S4 domains and flanking regions of 8-10 amino acids. EMBOSS Needle Alignment showed 56 % sequence similarity and 38 % identity in this region (Fig. 13) suggesting that its structural conformation and role in gating of both channels may be similar. This leads to hypothesis that antibodies specific to D1:S3/S4 loop of Cav3.2 may act in an analogous manner to NESOpAb. For immunization purposes a peptide containing amino acids numbered 186-199 was chosen. This peptide has the sequence YSLDGHNVSLSAIR.

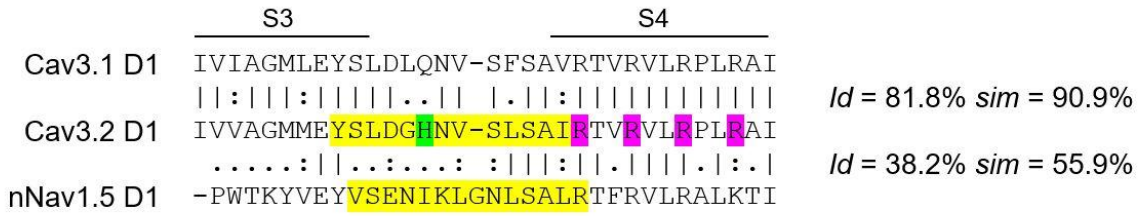


Figure 13. **Alignment of Cav3.1, Cav3.2 and nNav1.5**

The EMBOSS Needle Alignment tool was used to compare Cav3.1, Cav.3.2 and nNav1.5 sequences. Vertical bars indicate identical residues, double dots indicate similar residues and single dots indicate different residues. The peptide sequences used to raise antibodies are highlighted in yellow. The positively charged arginine residues in segment S4 are highlighted in pink. His191 in Cav3.2 is highlighted in green. The horizontal bars above the sequence indicate predicted transmembrane domains. *Id* and *sim* are identity and similarity percentage of these sequences calculated by EMBOSS using matrix EBLOSUM62. The sequences of Cav3.1, Cav3.2 and nNav1.5 are taken from UniProt database accession numbers **O43497, O95180 and Q8WWN6** respectively.

## 3.3. Extracellular loop between segment S5 and pore loop in Domain 1 (D1:S5/P)

Xu *et al.* (2005) have presented and tested a strategy for the generation of ion channels' inhibitors. They hypothesised that binding of antibodies to an extracellular loop which is directly after segment S5 in any ion channel can block the channel current. This extracellular loop was named E3. The hypothesis was tested on several ions channels. The authors focused on the TRPC5 calcium channel and Nav1.5 sodium channel. The former is a member of the Transient Receptor Potential family and consists of four identical protein units forming the channel; these polypeptides have six transmembrane domains structure with a pore loop between the fifth and sixth TM domain. The structure of the latter is more complex and the channel consists of one protein – four connected subunits containing six transmembrane domains each. Structural studies showed that the E3 loop after segment S5 was large enough to allow for the binding of antibodies, and polyclonal antibodies against E3 sequences have been produced in rabbits. The obtained antibodies were first tested for their specificity to a given ion channel and proved to distinguish between close members of the same family. Anti-TRPC5 antibodies recognized only TRPC5 and not TRPC4 or TRPC1 when tested by Western Blotting. Anti-Nav1.5 antibodies were used for immunostaining and did not bind to wild type cells (not expressing Nav1.5). Electrophysiological recordings of HEK293 expressing TRPC5 revealed that 10 min incubation of cells with anti-TRPC5 antibody caused a 50 % block of the channel current. The antibody was also effective in fluorescent assay measuring calcium influx. Anti-Nav1.5 antibodies caused 60 % block of the current after 20 min incubation with HEK293 expressing Nav1.5. This antibody did not affect the electrophysiological properties of Nav1.4 thus proving high selectivity. No detailed research has been conducted on the influence of the application of antibodies on the gating properties of these ion channels, *i.e.* no information about activation and inactivation thresholds and times was obtained. It is likely that the antibody simply obstructs the ion permeation pathway due to its close proximity to the pore loop. The

gating properties may remain unaffected as well as the channel exposure on the membrane. Channel internalisation may possibly occur upon binding of the antibody but it is unlikely due to the relatively short exposure of cells to the antibody (maximum 20 min).

Xu *et al*. (2005) also tested their hypothesis on another, not named, ion channel and claim a 100 % success rate in the production of blocking antibodies using this approach.

This concept was applied to Cav3.2. Structure analysis revealed that E3 (S5/P) regions in Domains 2, 3 and 4 are relatively short (16, 32 and 18aa) compared to E3 in Domain 1 (107 amino acids). Moreover, E3 in Domains 2, 3 and 4 of Cav3.2 are almost identical to Cav3.1 and Cav3.3. Antibodies against these loops would then lack the subtype specificity. S5/P loop in domain 1 is long and has regions of high diversity from Cav3.1 and Cav3.3. The peptide from Domain 1 close to the predicted pore loop was chosen to increase the chances of antibodies obstructing the pore. Another factor taken into account in design of the peptide was the presence of possible glycosylation sites. Posttranslational glycosylation of the extracellular loop would cause a steric hindrance preventing binding of the antibody. The sequence comparison between S5/P regions of Cav3.x family members is shown in Fig. 14. The peptide chosen for immunisation has the sequence: NVCRSGDSNPHNGAI. This sequence does not contain any N-glycosylation site although it contains two serine residues which can possibly be O-glycosylated.

The localisation of all three target peptides within the Cav3.2 molecule is shown in Fig. 15.


Figure 14. **Alignment of D1:S5/P of Cav3.1, Cav3.2 and Cav3.3**

The EMBOSS Needle Alignment tool was used to compare the regions immediately preceding the pore loop in Cav3.1, Cav3.2 and Cav3.3. Vertical bars indicate identical residues, double dots indicate similar residues and single dots indicate different residues. *Id* and *sim* are identity and similarity percentage of these sequences calculated by EMBOSS using matrix EBLOSUM62. The peptide sequence used to raise antibodies against Cav3.2 D1:S5/P is highlighted in yellow. The sequences of Cav3.1, Cav3.2 and Cav3.3 are taken from UniProt database accession numbers **O43497, O95180 and** Q9P0X4 respectively.

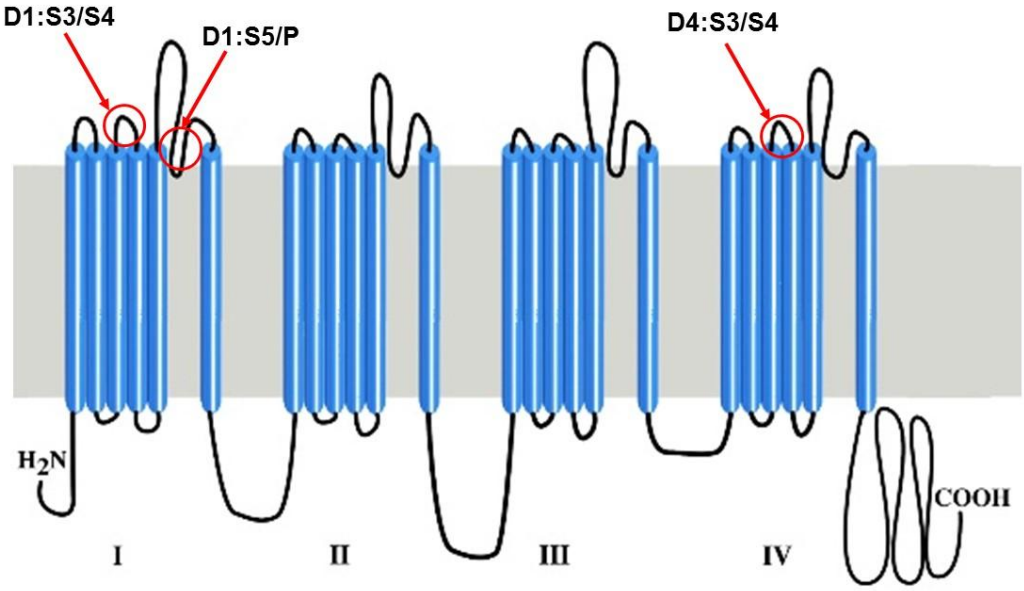


Figure 15. **Schematic structure of Cav3.2 indicating the localisation of the regions targeted by antibodies**

Three extracellular regions of Cav3.2 have been chosen as targets for the generation of the antibodies. D1:S3/S4 and D4:S3/S4 are loops connecting the third and fourth transmembrane segments in domains 1 and 4 respectively. D1:S5/P is a region immediately preceding the pore loop in domain 1. Image generated using GIMP 2.8.16 software.

The attempt to model parts of Cav3.2 structure was made using ArgusLab software. Due to the lack of structural data on Cav3.2 or any related ion channel, the models are highly theoretical and would not be suitable for computational drug design. The fragment of Domain 1 containing segments 3 and 4 and the putative extracellular loop is shown in Figure 14. The resulting structure has two alpha helices connected by a peptide with a beta-sheet structure. The modelling of transmembrane domains is relatively simple as it can be assumed that they adapt the alpha-helix structure. However, in the case of extracellular loops or intracellular domains, the secondary protein structure is unknown and can be only modelled based on homology with known structures. Cav3.2 has no homology to a known structure; hence it was assumed that this extracellular loop might adapt a flat beta-sheet structure. The likelihood of this model is further supported by the fact that the transmembrane helices are aligned in the same direction and are roughly parallel to each other, which would allow them to be embedded in the cell membrane without much stretching of the lipid bilayer. The attempt to model D4:S3/S4 was also performed using ArgusLab. In this case no satisfying structure could be obtained (results not shown). When flat beta-sheet structure was applied to the link between segments S3 and S4, this resulted in lack of alignment of these segments, which would exclude them from being embedded in the same cell membrane. This suggests that the link between those segments may adopt a non-standard structure. The D1:S5/P fragment is entirely extracellular with a part possibly lining the channel orifice, hence modelling of this region cannot be performed without structural data available.

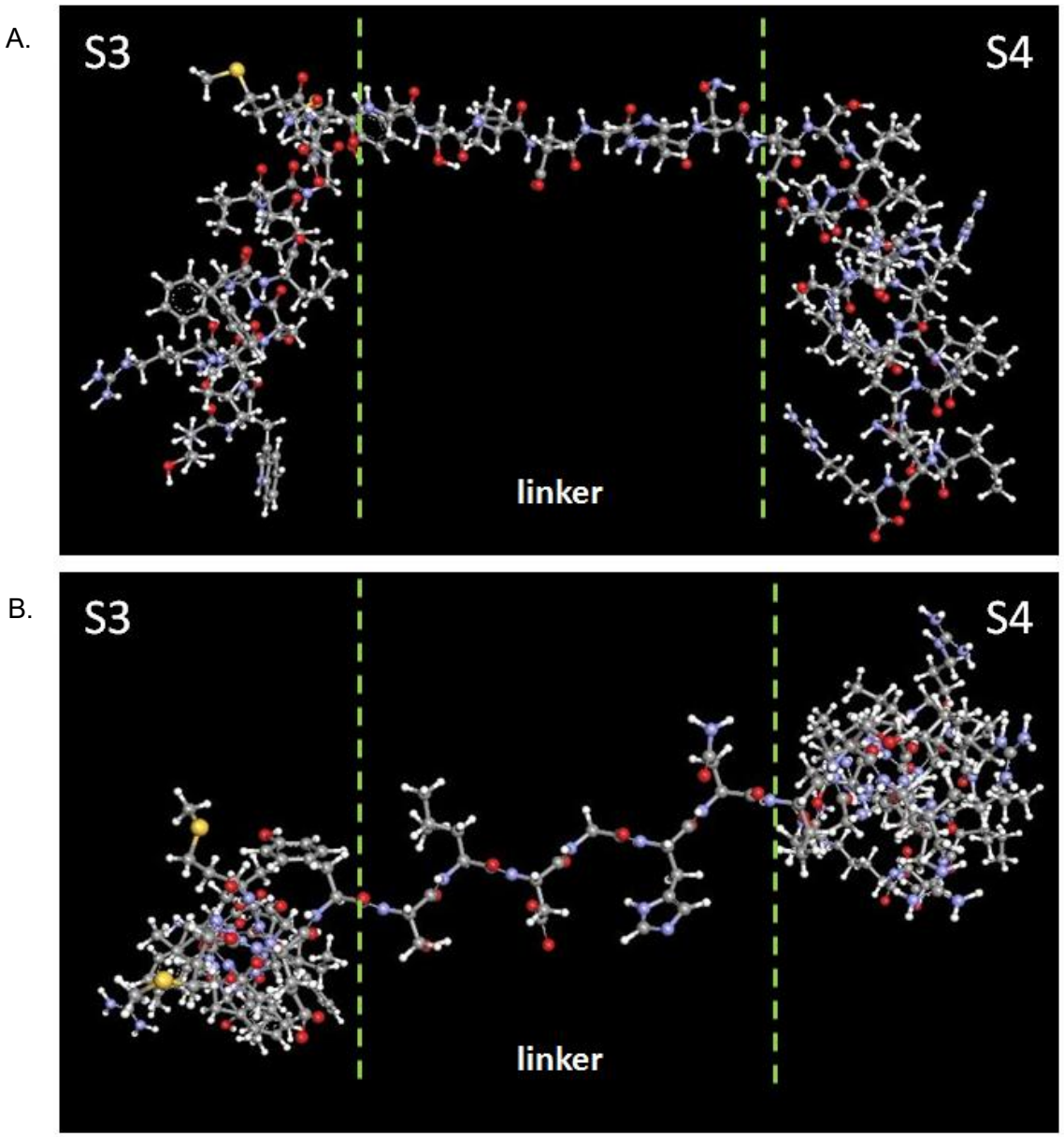


Figure 16. **Model of Domain 1 segments 3 and 4 and the extracellular loop D1:S3/S4 created with ArgusLab software**

A. Side view of the putative structure.

B. Top view of the putative structure.

Dotted lines divide intramembranous and extracellular fragments of the model. S3, S4 indicate transmembrane segments. Extracellular loop ('linker') connects the transmembrane segments.

The colour of the spheres indicate atom type: grey – carbon, white – hydrogen, blue – nitrogen, red – oxygen, yellow – sulphur.

# 4. Discussion

The objective of this structural research of Cav3.2 was to identify the structural motifs that would be promising targets for the generation of anti-Cav3.2 antibodies. Moreover, the aim was that the generated antibodies not only recognize and specifically bind Cav3.2 but also that they influence the Cav3.2 mechanism of action. Such antibodies whether inhibiting or enhancing the Cav3.2 activity would help to elucidate its mechanism of action and would have great potential for future drug design.

The first prerequisite was that antibodies are able to bind to Cav3.2 in living cells. Due to their size, antibodies are normally not able to penetrate into the cell membrane and cytoplasm without prior permeabilisation of the cell membrane. Such permeabilisation kills the cells and thwarts the functional studies. This significantly narrows the choice of peptides available for antibody design to the Cav3.2 motifs that are exposed on the extracellular side of the cell membrane. From Domain 1 only peptide D1:S3/S4 was chosen for antibody generation due to its vicinity to voltage sensor (S4) and for other reasons described earlier in this chapter. D4:S3/S4 in Domain 4 has been implicated in Cav3.2 blocking as described earlier and was also chosen as a target for antibody generation. The pore loop regions of all four domains are relatively long and exhibit significant antigenicity, making them potential targets for antibody generation. Moreover, the pore loop regions are thought to line the channel passage, hence the binding of a sizeable antibody molecule at this site would most likely result in the blocking of channel conductance. Research on pore-targeted antibodies blocking the channel permeability was described earlier in this chapter. Assuming that the pore loop regions of all four domains have an approximately equal share in lining the channel pore, binding of an antibody to any one of them would cause the same blocking effect. For this reason only D1:P region was chosen for antibody target.

The chosen extracellular loops appear to be crucial for Cav3.2 gating. Therefore antibodies binding to these regions may affect channel gating. Theoretically, binding of the antibodies may exert the following effects:

- Blocking of the channel pore – the D1:S5/P loop is in close proximity to the channel pore. The binding of a bulky antibody molecule should physically obstruct the channel pore thus blocking T-type currents. This effect is most likely to occur in the case of anti- D1:S5/P antibodies, although the other two antibodies binding at loops S3/S4 may also exert a similar effect. *In vivo* use of these antibodies would result in the disruption of many physiological properties due to the wide distribution of Cav3.2 and its multiple roles in a variety of cells.
- Alteration of gating properties without blocking the channel conductance – binding of antibodies to the D1:S3/S4 and D4:S3/S4 loops may not be sufficient to obstruct the channel pore but may affect movements of the channel domains, therefore altering its gating properties. The exact effect is difficult to foresee – it depends on whether the antibodies bind preferentially to the open or closed channels. If binding to a closed state they could *e.g.* increase activation threshold due to the need for more energy to force the channel open or lower the current amplitude due to the incomplete opening of the pore. If the antibodies bind to an open channel they could possibly stabilize the channel in an open state thus prolonging the inactivation time and increasing the tail current.
- Shielding the D1:S3/S4 loop – antibodies bound to Cav3.2 may not have any direct effect on the channel gating. The indirect effect could be due to the antibody "shielding" the D1:S3/S4 loop. As mentioned earlier, the histidine residue at position 191 within the loop participates in metal ion binding and MCO. This results in the stabilisation of the closed state. Binding of the antibody to this loop might displace bound metal ions thus removing the naturally present

inhibitors of Cav3.2 and sensitize the channel in a way described in Nelson *et al*. (2007).

- Combination of the aforementioned effects – *e.g.* shielding the D1:S3/S4 loop from MCO and simultaneous restriction of domain movements. This would result in the sensitisation balancing out the inhibition and apparent lack of effect or much lower effect than if any of these effects were entirely separated.
- Assuming that the antibodies have good affinity to the Cav3.2 channel, they could theoretically be used in the treatment of several diseases associated with the re-expression of Cav3.2 *e.g.* prostate and breast cancer. However, due to the wide distribution of Cav3.2 it could possibly cause several side effects.
- It is likely that one type of antibody will not cause a complete block of the channel but only a limited inhibition. However, the simultaneous application of all three types of antibodies may exert a more significant effect. Moreover this effect may be not only additive but synergistic, *i.e.* higher than it would be if the effects of separate antibodies were added.
- Delivery of antibodies to the central nervous system (CNS) still presents a major challenge; thus the anti-Cav3.2 antibodies may not be useful in binding to Cav3.2 in CNS but instead exert their effect only peripherally, either in the peripheral nervous system or in other cells such as cancer sites or adrenal glands.

## 5. Conclusion

Three motifs of Cav3.2 were chosen for generation of anti-Cav3.2 antibodies that should be able to recognize and bind Cav3.2 in living cells. These regions are: D1:S3/S4 (sequence YSLDGHNVSLSAIR), D1:P (NVCRSGDSNPHNGAI) and D4:S3/S4 (LMGITLEEIEMSAALPINPTII). The generation of antibodies against these peptides is described in Chapter 3.

# Chapter 2: The Validation of a Stable Cell Line expressing Cav3.2 (HEK/Cav3.2)

## 1. Introduction

Drug design process often involves the implementation of cell-based assays for the analysis of the efficacy and potency of a new drug *in vitro*. Cell-based assays are designed in a way which allows for the screening of many compounds in a relatively short time and for the measurement of the metabolic response brought about by the drug. Research on cells grown in culture also allows for the investigation of unknown metabolic pathways and of the role of many proteins and other compounds in the cellular metabolism. The cells used in such experiments must express the analysed protein that is the target of the particular drug or must be able to metabolise the drug.

Expression of the protein of interest can be endogenous – cells naturally expressing a given protein; or exogenous, where the cells used in the assay must be transfected to express the protein of interest. Both versions have their advantages and disadvantages. However, the endogenous expression of protein of interest tends to be regarded as the better option allowing for the investigation of the drug's effect on a metabolic pathway in a cellular environment most closely mimicking the natural functioning of cells in an organism. In cells naturally expressing a given protein, this protein is expressed at a certain, rather low level, regulated by the cell. Moreover, auxiliary subunits and other molecules linked to the functioning of the protein of interest, such as chaperones, specific kinases, phosphatases and G-proteins linking a membrane molecule to downstream signalling, are also expressed (Thomas and Smart, 2005). This feature of the native expression of analysed protein can be disadvantageous in case of any attempt to elucidate a role of a specific protein in cells. It might be difficult to pinpoint the exact role to a protein which is involved in a wider group of molecules in a single metabolic pathway. In such cases, the foreign expression of a protein can be an advantage as only the gene for the protein of interest is introduced into the cells. The expression of foreign DNA allows also for the manipulation of the DNA, for example the site-directed mutagenesis useful in the analysis of the relationship between the structure and function of proteins.

Moreover, cells with a native expression of certain proteins are often highly specialised, *e.g.* neurons and muscle tissue. These cells are often very difficult, if not impossible, to culture *in vitro* and often need to be prepared from laboratory animals. This technique, including the breeding of animals, is more difficult, expensive and time consuming compared to cell cultures *in vitro.* Additionally, the use of laboratory animals requires bioethics councils' approval, especially in cases where research causes suffering to animals. This limits the involvement of animal-derived specimens in high-throughput screening assays. The use of transfected cells expressing foreign protein circumvents the need for culturing cells with native expression of the protein of interest. It is important to choose the appropriate cell line for the expression of recombinant proteins to ensure a high fidelity of protein expression. The cell line chosen for this task should also possess certain characteristics such as ease of culture and transfection procedures, low maintenance costs (growth medium and supplement requirements). In the case of cells expressing recombinant ion channels it is also important that the chosen cell line does not express many other endogenous ion channels, as their presence confounds the electrophysiological recordings. The cells used for electrophysiological experiments should grow separately rather than in clusters to allow for experiments on individual cells. A high proportion of the necessary conditions required of the cell line used for exogenous protein expression can be found in HEK293 (Human Embryonic Kidney) cells.

HEK293 is one of the cell lines frequently used for expression of recombinant proteins due to the unique characteristics of these cells (Thomas and Smart, 2005).

HEK293 cells were created in the 1970's by the adenoviral transformation of foetal kidney cells performed by Frank Graham in Leiden, The Netherlands (Graham *et al.,* 1977). The cell line HEK293 was given the number of Graham's experiment, but these cells are also commonly known as HEK cells. These cells are hypotriploid – they have the average chromosome number 64 with the adenovirus sequences incorporated into chromosome 19 (ATCC, 2016). A modification of this cell line harbouring Epstein-Barr Virus gene 1 EBNA-1 is known as EBNA293 and was adapted to grow in suspension

rather than on the vessel surface as it is in the case of HEK293 (Baldi *et al.,* 2008). HEK293 is widely used for the transient and stable expression of foreign proteins and for large-scale recombinant protein production (Baldi *et al.,* 2008). This cell line expresses genes from plasmids regulated by cytomegalovirus (CMV) promoter. These plasmids effectively employ the cell machinery to synthesise relatively high amounts of the protein coded by the gene on the plasmid. HEK293 cells also provide a correct folding environment for the nascent protein and glycosylate the final protein products (Thomas and Smart, 2005). HEK293 cells are also thought to express only a limited number of ion channels on the cell membrane thus making electrophysiological experiments easier.

HEK293 cells are considered to be of epithelial origin, but surprisingly express a number of proteins normally seen in neuronal cells (Shaw *et al.,* 2002). Immunocytochemistry studies revealed the presence of neurofilament proteins NF-L, NF-M and α-internexin which are three of the four main constituents of neurofilaments. The fourth neurofilament protein NF-H was also detected, albeit at a very low level. HEK293 cells also expressed keratin 8, keratin 18 and vimentin. The expression of these filamentous proteins is characteristic in the early stage of neuronal differentiation. Their expression diminishes as the cells mature, and is replaced by the expression of α-internexin, then of NF-M, NF-L and NF-H. This suggests that HEK293 cells are actually of neuronal origin or that the adenoviral transformation causes the cells to express neuronal proteins via the activation of a neurogenic transcription factor which could be derived from the viral genes. However, the latter mechanism would also cause expression of many other neuronal genes and this was deemed unlikely (Shaw *et al.,* 2002). The hypothesis proposed by Shaw *et al.,* (2002) is that the adenovirus preferentially transforms neuronal cells and therefore the HEK293 cells are of neuronal origin rather than epithelial. This hypothesis is confirmed by other studies showing that HEK293 cells express mRNA and protein for a range of receptors normally found in neurons. These involve ligand gated and G-protein coupled receptors such as nicotinic and muscarinic acetylcholine receptors, glutamate, dopamine, corticotrophin, bradykinin and GABA receptors and Acid Sensing

Ion Channel ASIC (Thomas and Smart, 2005). HEK293 cells also express a variety of voltage gated ion channels: at least ten potassium channels, sodium channels BNaC2 and β1A and calcium channel subunits α2β and α2δ (Thomas and Smart, 2005).

HEK293 cells were therefore chosen for the expression of Cav3.2 in this project due to their unique properties described earlier. Firstly, the transient Cav3.2 expression was used. This is a simpler process involving only the transfection of cells with the plasmid of choice using an appropriate transfection procedure. The cells take up the plasmid and begin expressing the plasmid-encoded protein, provided the plasmid promoter is suitable for a given type of cells. The expression of the recombinant protein peaks usually within 2-3 days after which the level of expression diminishes as the cells continue to divide. The cells usually do not incorporate the plasmid into their genomes. The amount of protein produced in transient transfection can be high and may even allow for commercial production of recombinant proteins using HEK-EBNA293 cells (Meissner *et al.,* 2001). The level of protein expression reported in this case was >20 mg/L of a secreted IgG and 18 mg/L of *E.coli*-derived DNA binding protein that accumulates intracellularly. The membrane embedded serotonin receptor 5-$HT_3$ the receptor density was 3-6 x $10^6$ molecules in one cell – this result was achieved two days post-transfection (Meissner *et al.,* 2001). However, the efficiency of transfection and the subsequent level of protein expression can vary between 20-80 %, depending on many factors such as the condition of the cells, the degree of confluency, the presence of serum in growth medium, and the quality and quantity of the plasmid used for transfection (Thermo Fisher Scientific, 2015). In order to generate a stable cell line, the cells need to incorporate the foreign DNA into their genomes. Approximately 1 in $10^4$ cells transfected with circular plasmid incorporates the plasmid in its DNA (Thermo Fisher Scientific, 2015). These cells must then be isolated from other cells and expanded. This isolation can be performed by culturing cells in the presence of an antibiotic – the cells with the incorporated plasmid have antibiotic resistance encoded by the plasmid. The stable cell line obtained needs to be maintained in the presence of the antibiotic to prevent loss of the foreign DNA. The

level of protein expression can be as high as 4.7 g/L of yield accumulated over a period of three weeks of cell culture, with a daily productivity of up to 90 pg/cell (Wurm, 2004). This chapter describes the testing of transiently transfected cells and a stable cell line for the expression of Cav3.2. The transiently transfected cells were obtained in our lab using HEK293 cells, pcDNA3.1 plasmid carrying Cav3.2 gene and FuGENE 6 transfection reagent (Roche). The stable HEK293 cell line expressing Cav3.2 (HEK/Cav3.2) was a kind gift of Professor Edward Perez-Reyes from the University of Virginia, School of Medicine. This cell line has been previously confirmed to faithfully express functional Cav3.2 at a level suitable for electrophysiological experiments and the investigation of Cav3.2 function (Wolfe *et al.,* 2002; Xie *et al.,* 2007). The cells were cultured as per instructions obtained from Prof. Perez-Reyes. Western Blotting was used to confirm the expression of Cav3.2 in both transiently transfected cells and the stable cell line cells grown in our lab. The correct localisation of Cav3.2 to the cell membrane was confirmed by immunocytostaining.

## 2. Aims

The aim of this part of the project was to investigate the properties of a cell line stably expressing Cav3.2 (HEK/Cav3.2 cell line) and validate the usefulness of this line for fluorescence-based High-Throughput assays.

## 3. Results

Western Blotting confirmed the expression of Cav3.2. The protein on the blot was detected using primary rabbit anti-Cav3.2 antibodies (Alomone Labs) and WesternDot 625 Goat Anti-Rabbit Western Blot Kit (Invitrogen). The commercial anti-Cav3.2 antibody recognizes an intracellular peptide linking domains 1 and 2 (Alomone, 2016). The results indicate the presence of Cav3.2 in the cell lysates obtained from both transiently transfected cells and the stable cell line. Untransfected HEK293 cell lysate was used as a control and did not show the presence of Cav3.2 (Fig. 17). The Cav3.2 protein in the cell lysates was apparently fragmented, as the bands on the blot were only ~60 kDa instead of ~260 kDa which would indicate the complete protein molecule. However, these small bands seem to always appear in blots with Cav3.2 – it was reported by Alomone Labs (specification of product number ACC-025) and Sigma Aldrich (specification of product number C1868).

Flow cytometry of paraformaldehyde fixed and saponin-permeabilised cells was used to assess the level of expression of Cav3.2 in stable cell line and to confirm that Cav3.2 is not expressed in untransfected HEK293 cells (Fig. 18). Stable cell line HEK/Cav3.2 was confirmed to express Cav3.2 and to bind anti-Cav3.2 antibodies - 65.68 % of these cells showed significant green fluorescence when stained with primary anti-Cav3.2 (Alomone Labs) and secondary GFP-conjugated antibody contrasted with only 2.59 % of untransfected HEK293 cells.

Immunocytostaining was performed to assess the localisation of Cav3.2 in the stable HEK/Cav3.2 cells. The cells were stained with commercially available anti-Cav3.2 antibody (Alomone Labs) and with secondary anti-rabbit mouse GFP-labelled antibody. The GFP fluorescence was localised to the cell membrane, confirming that the Cav3.2 was correctly directed to the cell membrane in HEK/Cav3.2 cells. The untransfected HEK293 cells were used as a control and did not show any GFP fluorescence (Fig. 19).

Omission of primary antibody did not produce any fluorescence, indicating that non-specific binding of the secondary antibody did not occur (Fig. 19 D).

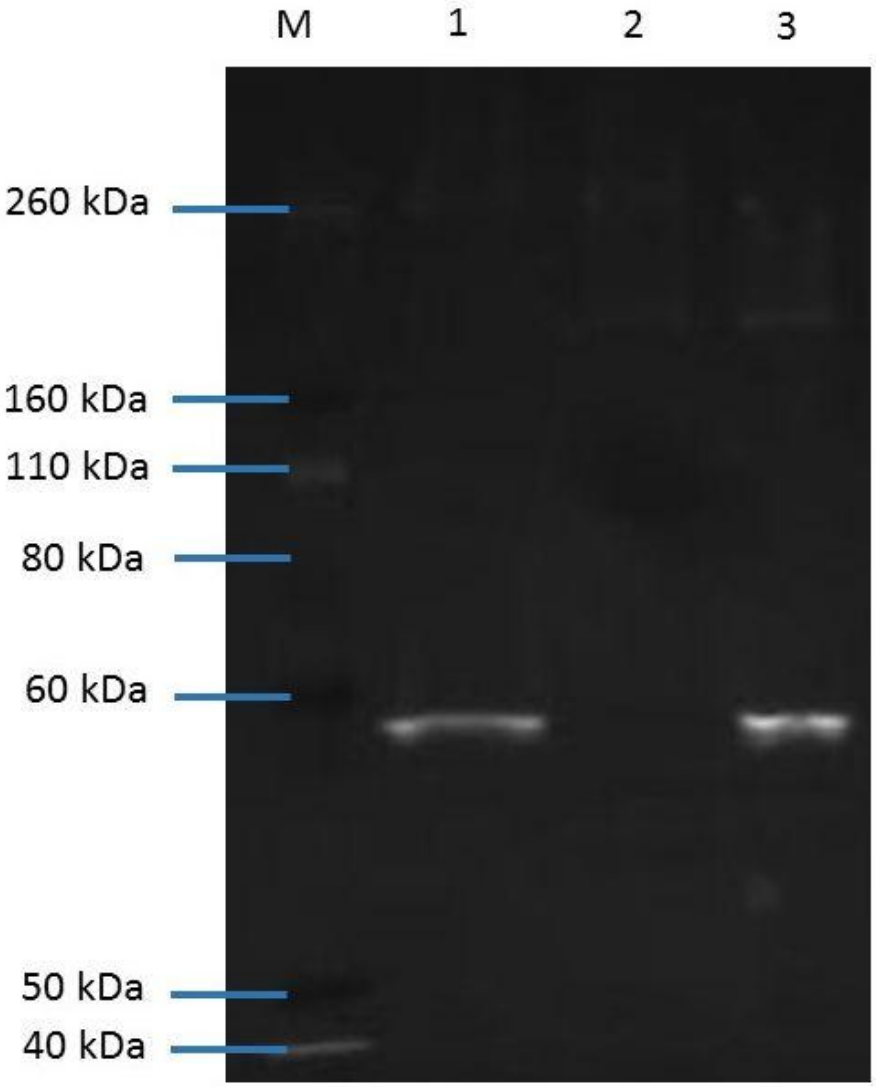


Figure 17. **Stable cell line and transiently transfected cells express Cav3.2**

The lysates of cells transiently transfected with Cav3.2 (lane 1) as well as cells stably expressing Cav3.2 (lane 3) were separated by SDS-PAGE and analysed by Western Blotting using anti-Cav3.2 antibody (Alomone Labs). The untransfected HEK293 cells were used as control (lane 2). The protein ladder (lane M) was Novex® Sharp Pre-Stained Protein Standard (Thermo Fisher Scientific). The fragment obtained in both cases was slightly smaller than 60 kDa instead of expected ~260 kDa for the whole Cav3.2 protein. This is most likely due to fragmentation of Cav3.2 molecule during cell lysate preparation. The results are similar to the ones reported in the product specification by the manufacturer (Alomone Labs).

A)

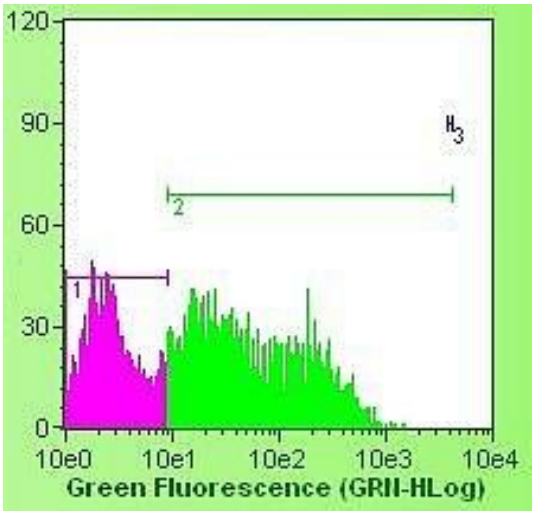


Marker 1 (pink): 34.32 %

Marker 2 (green): 65.68 %

B)

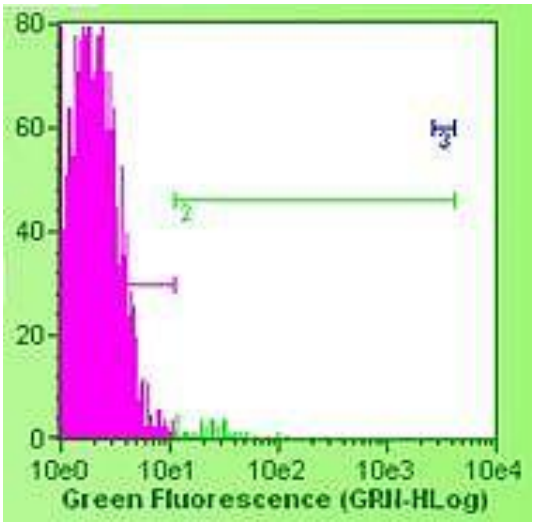


Marker 1 (pink): 97.41 %

Marker 2 (green): 2.59 %

Figure 18. **Stable HEK/Cav3.2 binds commercial anti-Cav3.2 antibodies**

The HEK/Cav3.2 stable cells and untransfected HEK293 cells were labelled with commercially available anti-Cav3.2 antibody (Alomone Labs) and stained with secondary anti-rabbit mouse GFP-labelled antibody. The stable HEK/Cav3.2 cells presented significant binding of anti-Cav3.2 antibodies: 65.68 % of cells exhibited substantial green fluorescence (A). Untransfected HEK293 cells did not exhibit significant fluorescence level – only 2.59 % of cells have shown some degree of fluorescence (B), but this can be attributed to non-specific binding of primary and/or secondary antibody.

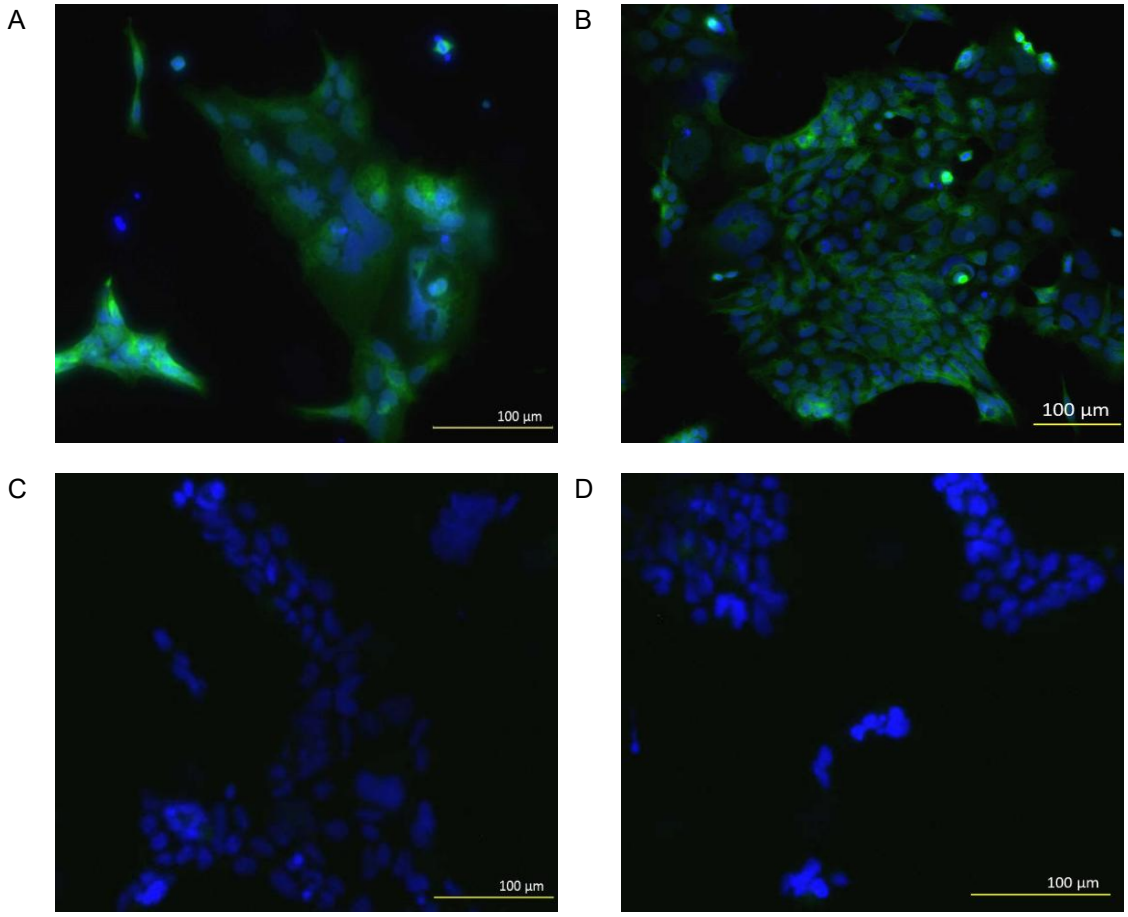


Figure 19. **HEK/Cav3.2 cells express Cav3.2 on the plasma membrane.**

Immunocytostaining with Alomone primary anti-Cav3.2 antibody and secondary GFP-labelled antibody confirmed abundant expression of Cav3.2 on the plasma membrane (A, B). Untransfected HEK293 cells did not show visible fluorescence when stained using the same protocol, indicating that the primary and secondary antibodies do not bind to any other protein native to HEK293 cells (negative control; C). HEK/Cav3.2 cells stained with secondary antibody only did not show green fluorescence, indicating that there is no non-specific binding of the secondary antibody to HEK/Cav3.2 cells (negative control; D). The cells were fixed with paraformaldehyde and permeabilised with saponin. Cell nuclei were stained with DAPI in all four images. The scale bars represent 100 µm.

# 4. Discussion

The HEK293 proved to be good host cells for exogenous expression of Cav3.2. Both transiently and stably transfected cells expressed significant levels of Cav3.2 which was confirmed using Western Blotting (Fig. 17). The protein is most likely fragmented during preparation of cell lysates. It is difficult to extract cell-membrane bound proteins (especially a large one with 24 transmembrane domains) without fragmentation during routine cell lysis procedure (own experience; informal discussion with supervisor and users of BioForum at protocol-online.org). It is also possible that the plasma membrane was not fully solubilised under the assay conditions and the centrifugation step during cell lysate preparation removed the membrane-bound protein. Modifications of the procedures did not improve the Western Blotting outcome. Nevertheless, the Western Blotting experiment produced results which are similar to the results published by two companies manufacturing anti-Cav3.2 antibodies and by several independent publications (*e.g.* Makarenko *et al.,* 2015; the Western Blot shown in this publication clearly contains a small band at about 60 kDa in addition to the band at 240-250 kDa). Immunoprecipitation was reported to be helpful in concentrating Cav3.2 protein in the cell lysate (Markandeya *et al.,* 2011).

The Western Blotting results raise a question about the accuracy of synthesis of Cav3.2 on the template of the pcDNA3.1 plasmid. It may be the case that the mRNA translation is terminated early for unknown reason and only the N-terminal fragment is produced. It may also be possible that the Cav3.2 protein fails to correctly embed in the cell membrane due to a lack of appropriate chaperones and is fragmented post-translationally. Fragmentation of Cav3.2 would most likely result in complete loss of function of this protein, which in turn would render the HEK/Cav3.2 cell line useless. However, the fluorescent assay described in later chapters proved that Cav3.2 was functional. Importantly, patch-clamp experiments on HEK/Cav3.2 cells were performed

by colleague Dr Vadim Volkov and confirmed the presence of an inward current typical for Cav3.2 (data not shown).

The reasons described above were sufficient for making an assumption that Cav3.2 is accurately transcribed, translated and folded in the HEK/Cav3.2 cells, and that the fragmentation observed on the blot resulted from destruction of the protein during cell lysis procedure.

The flow cytometry experiments described in this chapter confirmed the expression of Cav3.2 in stable HEK/Cav3.2 cell line (Fig. 18). The Cav3.2 protein was detected using commercially available antibodies (Alomone Labs) and secondary GFP-labelled antibodies. The cells were analysed using Guava EasyCyte. The percentage of cells showing significant green fluorescence was 65.68 % (Fig. 18 A). It is possible that the remaining 34.32 % of cells expressed Cav3.2 at low levels and were not stained strongly enough. Low level of Cav3.2 might occur for example shortly after cell division when the cells produce new membrane and the membrane proteins are added later in the development. It is also possible that in some cells, Cav3.2 expression is silenced for unknown reasons. This hypothesis seem to be confirmed by the immunocytostaining results that show a few cells not emitting green fluorescence (Fig. 19 A). Most of the cells show abundant and even expression of Cav3.2 on the cell membrane with slightly more intense staining in the perinuclear area in some cells. This may be due to the fact that the membrane on the edges of the adherent cells is more stretched than in the middle of the cell. The stronger staining may also represent the nascent Cav3.2 being synthesised in the endoplasmic reticulum near the nucleus.

The experiments presented in this chapter confirmed that HEK/Cav3.2 cells likely express Cav3.2 at levels sufficient for use of these cells in high-throughput screening assays described in the subsequent chapters.

Further experiments that would enhance the results presented in this chapter would include the use of a confocal miscroscope or immunocytostaining with plasma membrane markers such as anti-pan-cadherin antibodies that bind to plasma membrane

cadherins or fluorescently labelled concanavalin A that recognizes α-mannopyranosyl and α-glucopyranosyl residues in the outer leaflet of the plasma membrane (Chazotte, 2011). Without these experiments, the localisation of Cav3.2 to the plasma membrane cannot be fully ascertained.

# Chapter 3: The Production of Antibodies Targeting Selected Peptides within Cav3.2 Molecules

# 1. Introduction

Antibodies are proteins produced by the immune system that participate in the body's defence against various diseases. They specifically bind other molecules, such as proteins and polysaccharides – the molecules recognized by antibodies are called antigens. Antibodies (immunoglobulins) were discovered in 1923 by Michael Heidelberger and Oswald Avery who described the binding of bacterial polysaccharide antigens to proteins in serum (Van Epps, 2005). Since that day antibodies are still the subject of intensive research and have proved to be of paramount importance not only for the efficient functioning of the immune system but have also found many uses in medicine and science. The scientific uses of antibodies include their applications in countless immunoassays and biosensors where antibodies are employed to detect and sometimes quantify various molecules of interest (Lydyard, Whelan and Fanger, 2011). The underlying mechanism of immunoassays and biosensors is the reaction between the antigen and the specific antibody, and the ability to detect this reaction in the laboratory, using a variety of signal transducers, converters and readout methods. Immunoassays involve enzyme-linked immunosorbent assay (ELISA), radioimmunoassay (RIA), Western Blot, immunocytochemistry and immunohistochemistry. All of these assays are used not only in scientific and research setting but also in medical setting. Staining with antibodies can also be used in flow cytometry to visualize cells that express a particular antigen. Biosensors are increasingly used also outside of laboratory setting, for example to detect the presence of bacteria *Salmonella typhimurium* in meat (Byrne *et al.,* 2009). The use of antibodies in medicine is not limited to their immunoassay applications. Antibodies are also used as therapeutic agents. As of January 2015 there were 47 antibody-based therapeutics approved by the U.S. Food and Drug Administration, with the rate of new drugs approval of about four per year (Ecker *at al.,* 2015). The majority of the antibody-based drugs are used to treat various forms of cancer, but there are also antibody-based drugs for treatment of asthma,

psoriasis, multiple sclerosis, arthritis, Crohn disease and preventing transplant rejection (Carter, 2006). The variety of the disorders successfully treated with antibodies proves that these molecules appear to be ‘magic bullets’ that can be targeted at almost any molecule in the organism and disrupt a pathological pathway. However, the design and production processes of antibody therapeutics are complex and require careful planning.

## 1.1. Structure of antibodies

The basic structure of antibodies is tetrameric - two identical heavy chains and two identical light chains (Fig. 20). Three disulphide bridges link the heavy chains into a Y-shaped molecule. The light chains are attached to the sides of the heavy chains also by disulphide bonds. The light chains have two domains – constant ($C_L$) and variable ($V_L$). The heavy chains have four domains each – three constant ($C_H$) and one variable ($V_H$). The variable domains are crucial for binding antigens and for the specificity of the antibody to a particular antigen. The variable domains of both heavy and light chains are constituents of the $F_{ab}$ (fragment antigen-binding) that is responsible for the antibody's specific binding to a particular antigen (Delves *et al.,* 2011). There are two antigen binding regions in a single antibody molecule – at both arms of the Y. These regions are highly variable and each clone of antibodies has a different antigen binding structure that is spatially complementary to the antigen structure. Each antigen binding site (paratope) is made of six loops - complementarity determining regions (CDRs). The ability of CDRs to fit a particular antigen is achieved in a process called affinity maturation. The T-cells of the immune system present antigens to B-cells and the latter respond by producing antibodies of increasing affinity. This increase in affinity is achieved through two processes:

- Somatic hypermutation in the genes coding for antibody molecules
- Clonal selection of B-cells

The part of the antibody molecule that does not directly bind the antigens is termed $F_c$ (fragment crystallisable) and provides structural support to the $F_{ab}$ site. $F_c$ fragment also determines to which class an antibody belongs (five classes in placental mammals: IgA, IgD, IgE, IgG or IgM). Each antibody class has a slightly different function and appears at a different time in the development of an immune response. $F_c$ fragment is glycosylated at asparagine residue (Asn 297). The polysaccharide/glycan antenna consists of a core mannose and N-acetylglucosamine residues with some other optional

residues such as sialic acid, galactose and fucose. $F_c$ fragment is important in mediating effector functions of antibodies: the activation of complement-dependent cytotoxicity (CDC) and antibody-dependent cell-mediated cytotoxicity (ADCC) (Delves *et al.,* 2011). The half-life of antibodies in plasma depends on the binding of the $F_c$ portion with a salvage receptor FcRn that removes the circulating IgG antibodies thus protecting them from degradation (Ober *et al.,* 2001).

Antibodies are produced and secreted by B cells of the immune system upon appropriate stimulation with a foreign antigen. One clone of B cells produces identical antibodies, however, due to the presence of many different B cell clones in the body, the organism is able to produce over $10^9$ of immunoglobulins with different specificity (Delves *et al.,* 2011). Moreover, after invasion by a new unknown antigen, the body can produce new antibodies which are specific against this antigen. This feature of the immune system allows for the production of antibodies that can be used not only in the body's natural response against infection, but also for many other applications in medicine and science.

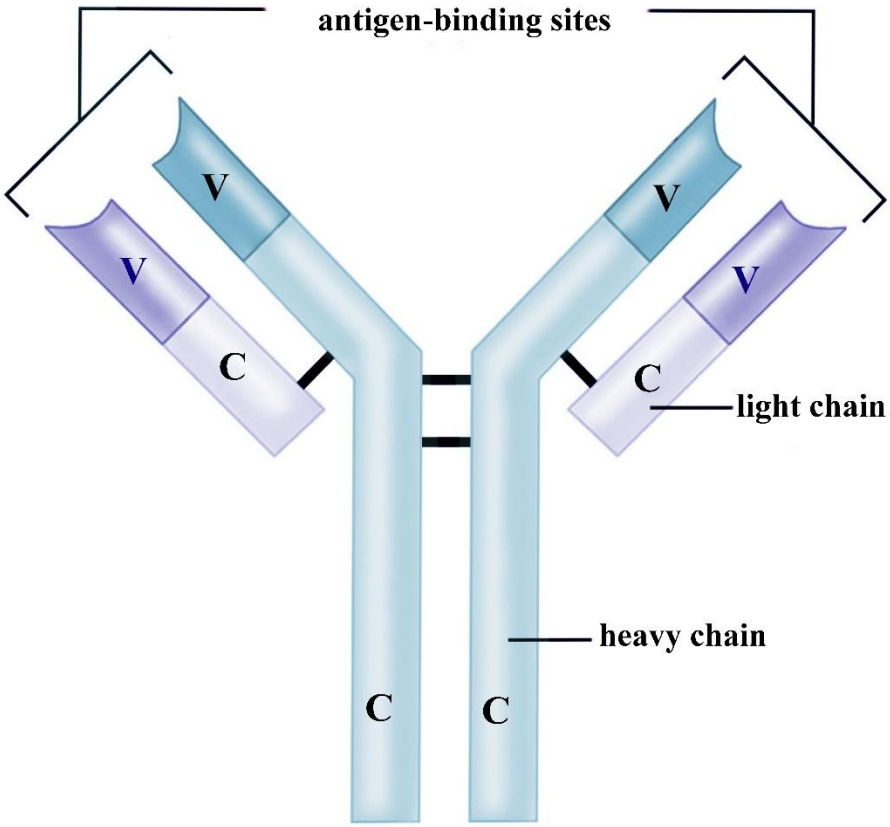


Figure 20. **Structure of an antibody**

A single antibody consists of two heavy (blue) and two light (purple) chains connected by disulphide bridges (black). The constant regions (C) have a defined sequence. The variable regions (V) are different for each clone of antibodies and determine the antibody specificity. Image generated using GIMP 2.8.16 software.

## 1.2. Production of antibodies for use in science and medicine

Antibody-based products used in medicine and research are most often monoclonal. This means that they have exactly the same sequence and are secreted by a single clone of cells. Resulting identical paratopes therefore bind to specified epitopes, for example specific short peptides within a protein molecule. On the other hand, polyclonal antibodies are produced by multiple clones of B cells upon immunisation with an antigen. Polyclonal antibodies generated against an immunogen such as protein molecule recognize several different sites within this molecule. Each clone of antibodies recognize a specific epitope, which can be either linear (continuous) or conformational. The length of a linear epitope recognised by antibodies varies between 5 and 21 amino acids. Conformational epitopes consist of peptides that are not adjacent in the primary sequence of an antigen, but are in spatial proximity (El-Manzalawy *et al.,* 2008).

The production of polyclonal antibodies is easier, cheaper and faster than the production of monoclonal antibodies and is also a necessary step before attempting to produce monoclonal antibodies. Polyclonal antibodies are obtained by the immunisation of animals of choice with the antigen of interest. Several factors must be taken into account in designing a successful immunisation procedure, such as the species of animal, the antigen formulation used, the route and timing of immunisation and the optional use of an adjuvant. Firstly, the chosen antigen must be foreign to the animal species to be immunised. Several species are used for the purpose of producing antibodies: rabbits, mice, rats, guinea pigs, hamsters, pigs, goats, sheep and even chickens (Larsson *et al.,* 2004). The animal should be chosen bearing in mind the required future application of the antibodies such as ELISA and the availability of secondary antibodies. Rabbits and mice are most commonly used because they are easy to bleed (Leenaars *et al.,* 1999). The use of outbred animals instead of inbred strains allows for a wider diversity in the immune response obtained. The animals used should be young adults – their immune systems are mature enough to produce a satisfactory response, and their immune

performance does not yet decline due to ageing processes (Leenaars *et al.,* 1999). The antigen chosen should be immunogenic enough, but it can be supported by a co-administration of an adjuvant such as Freund's complete adjuvant or aluminium salts. The immunisation protocol involves first the injection of the antigen which elicits a primary immune response, and usually two booster injections to improve antibody titre and their affinity to the antigen. After the first injection the B cells produce mainly antibodies belonging to the IgM class – these peak at 2-3 weeks following the injection. Subsequent doses induce a class switch to IgG and increase in antibody titre (Leenaars *et al.,* 1999). Once a satisfactory antibody production has been achieved, the animal can be bled and the antibodies purified from the serum. There are various methods that can be used for antibody purification (e.g. physicochemical fractionation such as differential precipitation and size-exclusion) but most common is affinity chromatography, where the antigen is used to capture the specific antibodies (Burnouf and Radosevich, 2001).

Monoclonal antibodies are produced by hybridomas, usually derived from mice. Immortalized myeloma cells are fused with spleen cells derived from immunized mice and the resulting hybrid cells are clonally expanded to obtain separate clones of cells producing identical antibodies. The cells are grown in a medium which selects the hybridomas and the produced antibodies are secreted into the medium from which they can be purified. This method is relatively inexpensive and allows for the generation of antibodies to a variety of antigens – they simply need to be injected into mice, sometimes with an adjuvant to stimulate an immune response. Murine monoclonal antibodies have multiple uses in molecular biology, biochemistry and drug discovery but are not found to be as useful in medicine. Very few marketed antibody drugs are monoclonal antibodies derived from mice. The reason for this is that these antibodies have a significantly different $F_c$ fragment to human antibodies. This causes them to be highly immunogenic in humans, which results in the production of human anti-mouse antibody (HAMA) and triggers side effects ranging from rash to severe allergic reaction and anaphylactic shock (Kricka, 1999). Moreover, murine antibodies have a short half-life of less than 20 hours

in human serum – this rapid clearance is due to their inability to bind with human salvage receptor FcRn (Carter, 2006). Different $F_c$ regions of mouse antibodies also affect the effector functions of such antibodies – they do not bind to human Fcγ receptors therefore are unable to participate in ADCC and complement activation (Guilliams *et al.,* 2014). These limitations of murine antibodies have been overcome by the production of chimeric, humanized, PRIMATIZED® and human antibodies (Reff *et al.,* 2002). Chimeric antibodies are those that have the constant part of the molecule derived from humans and the variable regions derived from mice or other species used for immunization. These antibodies are obtained using recombinant DNA technology and expressed in mammalian cell culture. Humanized antibodies are the next step in the development of antibody-based drugs and contain only foreign CDR sequences while the rest of the immunoglobulin molecule has the human sequence. In PRIMATIZED® antibodies the variable regions are derived from immunized monkeys and are more similar in sequence to human variable regions, therefore they do not elicit immune response when injected into humans. Fully human antibodies are produced by transgenic mice with engineered immunoglobulin genes – mouse genes are replaced with human ones, therefore the antibodies produced by such mice are indistinguishable from human antibodies (Reff *et al.,* 2002). PRIMATIZED® and fully human antibodies have the longest half-life in human serum: 10-13 days and 11-24 days respectively, and do not elicit an unwanted immune response in humans, making them most suitable for repeated/chronic therapy (Reff *et al.,* 2002).

The latest development in the production of antibody-based drugs is the phage display approach. The fusion of the sequence coding for the V-domain of a single light chain (scFv) with the pIII coat protein of the phage allows for a display of the antibody fragment on the surface of the phage (Conroy *et al.,* 2009). Phage libraries containing up to $10^{11}$ scFv fragments can be created by fusions of phage sequences with scFv sequences obtained by PCR amplification of sequences from human peripheral blood lymphocytes. Such phages are amplified in *E. coli* and phages displaying antibody fragments with an

affinity to a particular antigen are selected by binding to this antigen *in vitro*. Subsequent elution of bound phages, further amplification in *E. coli* and next rounds of panning allow for the enrichment of the phages with the highest affinity to the antigen. Such phages can then be sequenced and analysed to find the scFv fragment with optimal antigen binding properties (Conroy *et al.,* 2009).

## 1.3. Antibody design

Antibodies intended for medical use must be designed with the utmost care to obtain the right pharmacokinetic properties. The process of designing therapeutic antibodies can be divided into four stages: target selection, generation of antibodies, epitope selection and optimisation (Presta, 2005). The first stage, target selection, requires analysis of the physiological and pathological pathways and the selection of a molecule that is crucial for one of these pathways, but does not participate in any other pathway in the body. The target can be either an early stage target that has not yet been used in treatment, or it can be a target that is already clinically validated and confirmed by other therapeutic approaches (Carter, 2006) The chosen molecule should preferably be either secreted or displayed on the cell surface due to the limited internalization of antibodies and their limited activity within cells. Binding of immunoglobulins should prevent functioning of the molecule of interest or remove the molecule from the pathway of interest. For example, bevacizumab (Avastin produced by Genentech, Inc. and F.Hoffmann-LaRoche Ltd.) targets vascular endothelial growth factor A (VEGF-A) thus inhibiting angiogenesis which is essential for tumour progression. This drug is used to treat metastatic colorectal cancer and other metastatic cancers (Los *et al.,* 2009). Therapeutic antibodies can also be directed to cell membrane molecules such as cancer markers and carry toxins or radioactive isotopes that kill cancer cells with relatively mild damage to the healthy surrounding cells. One example of such an antibody is tositumomab (Bexxar; marketed by GlaxoSmithKline) labelled with radioactive 131-iodine isotope directed at CD20 antigen of B-cells, used in treatment of non-Hodgkin lymphoma (Fisher, 2005). Care must be taken that the antibodies produced are highly specific for the chosen molecule and do not interact with other molecules and pathways as this could lead to severe side effects (Presta, 2005).

The second stage is the production of antibodies against the chosen target. It usually involves the immunization of animals of choice and the production of either polyclonal or

monoclonal antibodies as described earlier. One major obstacle is the production of antibodies against proteins that have a high degree of homology between humans and rodents – in this case there are difficulties in obtaining a satisfactory immune response (Presta, 2005).

Following the successful production of a batch of antibodies directed at the whole antigen, it is necessary to choose antibodies that bind to the desired epitope within the molecule. The third stage is the choice of epitope, which depends on several factors such as the strength of interactions between an antibody and a given epitope, whether the antibody binds as a competitive or non-competitive ligand and whether the binding of the antibody to the particular target causes any further effects such as the internalization of the target or the blocking of target interactions with any other ligand. Moreover, if antibodies are targeted at a ligand-receptor pair, it is more effective if the antibodies bind to the molecule that is in limiting supply (Presta, 2005). This stage also allows for the selection of antibodies that exhibit species cross-reactivity, for example they bind to the same sequence in, *e.g.* monkey-derived antigens. This allows for pre-clinical studies to be performed in other species using the same antibodies and circumvents the need for generating similar antibodies targeting the corresponding antigen in animals (Carter, 2006). It is not always the highest affinity or the strength of antibody-epitope binding that make the best therapeutic antibodies. For example, antibodies that bind too strongly to the target molecule may have impaired tumour penetration, as was reported in the case of anti-HER-2 antibodies (Adams, *et al.,* 2001).

The final stage of antibody design is the optimisation of selected antibody clones. This is an iterative process requiring repeated exposure of the obtained antibodies to the antigen and the selection of the ones that exhibit optimal binding. Improvement in the desired properties of the antibodies can be achieved by various means, for example an increase or decrease in affinity or selectivity for the antigen may be achieved by site-directed mutations in the CDRs. Improving interactions between the paratopes of the optimized antibodies and their corresponding epitopes may be conducted with the aid of

molecular modelling tools. Bioinformatics tools have been successfully used to model interfaces between the epitope-paratope pairs and also to model the spatial orientation of heavy and light chains in the antibody molecule. Computational methods also allow for calculating the energetically favourable arrangements of atoms in antibody and antigen molecules and aid in finding the optimal configuration, which may then be used to introduce subtle changes in the antibody structure (Kuroda *et al.,* 2012).

The optimisation of antibodies may require a reduction in their immunogenicity which may be achieved by chimerization and humanization as described earlier.

Manipulations in $F_c$ region may improve the ADCC, complement binding and half-life of the antibody. For example, removal of the fucose residue from the glycan antenna at Asn 297 improves the ability of the antibodies to trigger ADCC when used at a lower concentration, compared to the fucosylated versions (Yamane-Ohnuki and Satoh, 2009). $F_c$ region may also be completely removed to produce $F_{ab}$ fragments – in this case the ADCC does not take place. Moreover, $F_{ab}$ and scFv fragments exhibit better tissue penetration than full-sized antibodies due to their smaller size (Nelson, 2010). However, due to the lack of the $F_c$ region these fragments have a much shorter half-life, which requires more frequent administration (Nelson, 2010).

## 2. Aims

The aim of this part of the project was to produce targeted anti-Cav3.2 antibodies and to investigate the properties of the generated antibodies.

# 3. Results

## 3.1. Antibody design and production

Three peptides have been chosen to raise polyclonal antibodies against them (described in detail in Chapter 1). The peptides of interest were produced by CovalAb S.A.S. (http://www.covalab.com/) using Fmoc strategy on solid phase. The obtained peptides were then analysed by HPLC to ensure purity and by mass spectrometry to determine their molecular mass (the experiment was conducted by CovalAb S.A.S.). The peptides were conjugated to a carrier protein Keyhole Limpet Haemocyanin. Each peptide conjugate was injected into two female New Zealand rabbits. Following immunization the rabbits' sera were obtained. The schedule of injections and bleeds is presented in Table 3. These procedures were carried out by CovalAb S.A.S.

The antibodies were immunopurified on sepharose columns (the experiment was conducted at LMU by the author). The columns were prepared by coupling the peptides to 1 ml of activated sepharose beads. The antisera were loaded onto the peptide-sepharose column and incubated for 1 hour at 37°C. After several washes of the columns, the elution of bound antibodies was performed using an elution buffer containing 0.02 % sodium azide. Fractions containing the antibodies were pooled and the final concentration of immunopurified antibodies was determined by reading the optical density at 280 nm using a UV spectrophotometer.

The immunoreactivity of the purified antibodies was determined by ELISA (the experiment was conducted at LMU by the author). A 96-well plate was coated with the peptide of interest (antigen). Eight dilutions of the antibody ranging from 1000 ng/ml to 8 ng/ml were prepared. Unpurified serum was used as a positive control. The titer was determined by the lowest concentration of antibody giving an optical density reading at 450 nm ≥1. 100 ng/ml was arbitrarily considered a good yield of specific and immunoreactive antibody.

| Day | Procedure |
|---|---|
| **0** | Preimmune bleed<br>First injection<br>(0.5 ml antigen + 0.5 ml complete Freund's adjuvant) |
| **21** | First boost<br>(0.5 ml antigen + 0.5 ml incomplete Freund's adjuvant) |
| **42** | Second boost<br>(0.5 ml antigen + 0.5 ml incomplete Freund's adjuvant) |
| **53** | First test bleed (4 - 5 ml) |
| **63** | Third boost<br>(0.5 ml antigen + 0.5 ml incomplete Freund's adjuvant) |
| **74** | Second test bleed (10 - 15 ml) |
| **88** | Final bleed (50-70 ml) |

Table 3. **Timetable of rabbit immunisation**

The procedure was carried out by CovalAb S.A.S. The antigen conjugate injected was supported with complete and incomplete Freund's adjuvants. The test bleeds were performed to assess the immune response and antibody affinity maturation.

## 3.2. Development of antibody affinity

The maturation of the antibody affinity was achieved by three boost injections performed at days 21, 42 and 63. First test bleed was performed at day 53 and the second test bleed was performed at day 74. The sera obtained from these test bleeds were tested using ELISA with the peptide antigen coated on the plate. These tests were performed by CovalAb – the company that conducted the rabbit immunisation for this project. The results for each rabbit are shown separately. The development of antibody reactivity against their respective peptides for anti-D1:S3/S4 antibodies is shown in Fig. 21, for anti-D1:S5/P antibodies in Fig. 22 and for anti-D4:S3/S4 antibodies in Fig. 23.

The antibodies from final bleed (day 88) were purified by CovalAb and delivered in 0.1 M Tris / Glycine pH 7.8 buffer containing 0.02 % sodium azide. The concentration of the antibodies varied depending on the efficacy of the purification: for anti-D1:S3/S4 antibodies the concentration was 11.5 µg/ml, for anti-D1:S5/P antibodies – 87.31 µg/ml and for anti-D4:S3/S4 antibodies – 238.05 µg/ml. The test bleed sera (unknown antibody concentration) were also delivered and used for purification of antibodies on sepharose column (experiments performed by the author).

## 3.3. Antibody binding to antigen *in vitro* - ELISA

The binding of the purified antibodies to their respective antigens was assayed using ELISA (the procedure was carried out at LMU by the author). The peptides of interest were coated on a 96 well plate at a concentration of 100 µg/ml. Eight two-fold serial dilutions of antibodies were used: 1000 ng/ml, 500 ng/ml, 250 ng/ml,125 ng/ml, 62.5 ng/ml, 31.25 ng/ml, 15.6 ng/ml and 8 ng/ml. The binding curves of the antibodies to their corresponding antigens are presented in Table 4 and Fig. 24.

A)

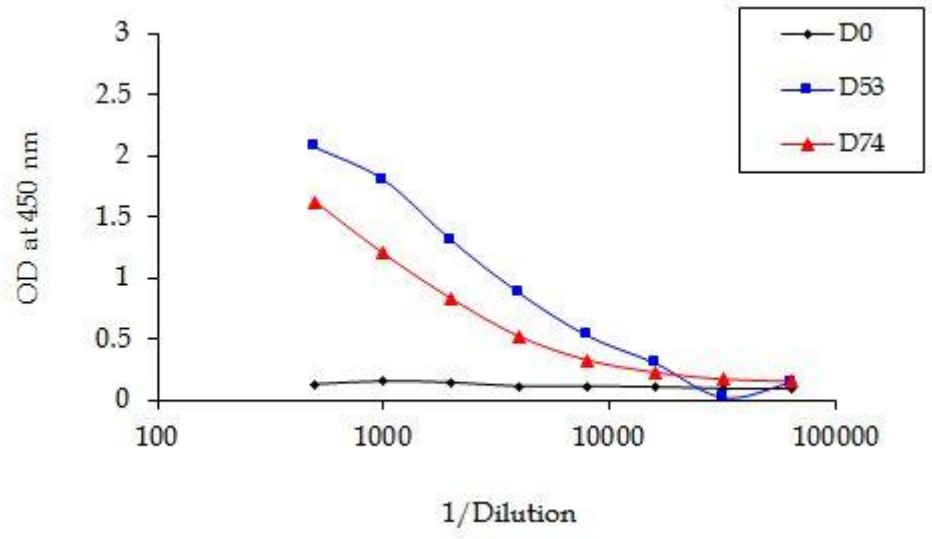


B)

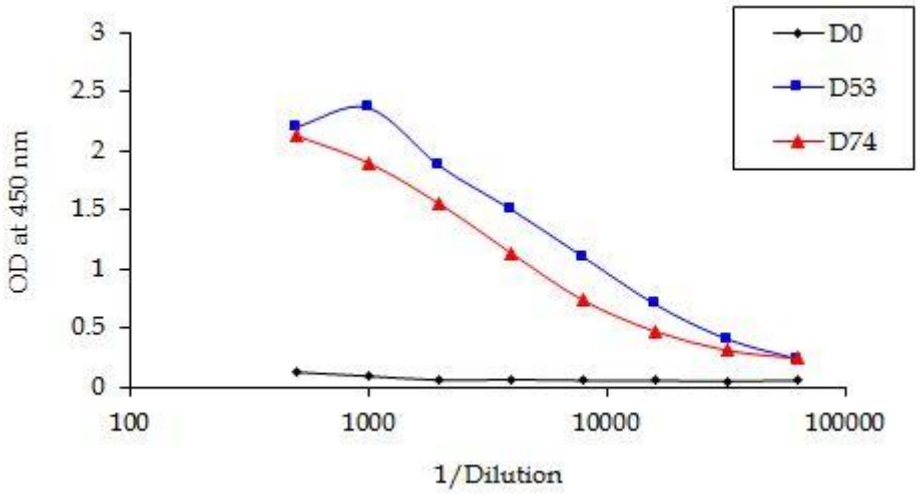


Figure 21. **Immunoractivity of rabbit serum against D1:S3/S4 peptide.**

The test bleeds were performed at day 53 and 74 following immunisation. The sera were tested using ELISA and compared with sera obtained before the start of the immunisation procedure. The animals immunised at this experiment were two New Zealand rabbits numbered #114006 (A) and #114021 (B). The experiment was performed by CovalAb S.A.S. and the presented data was obtained from CovalAb S.A.S.

A)

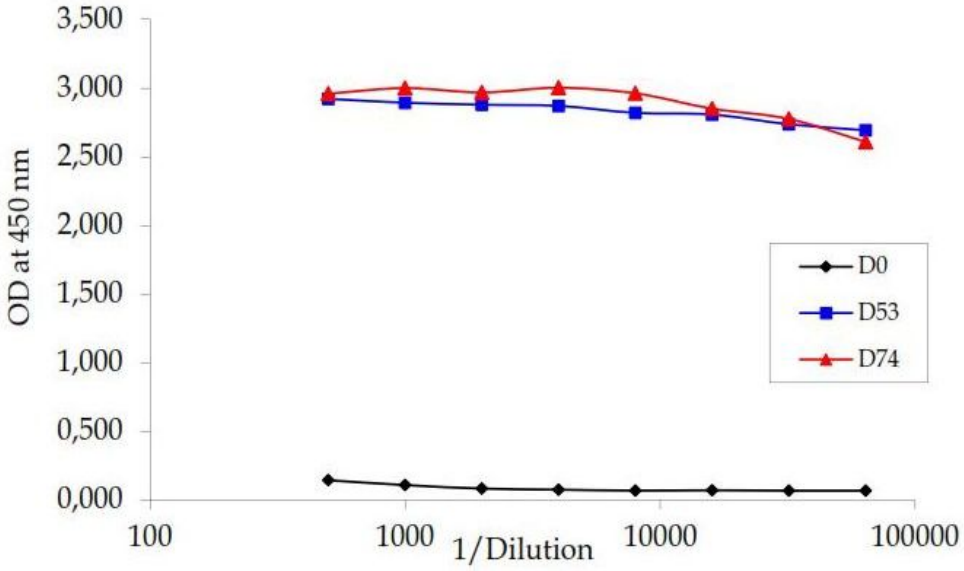


B)

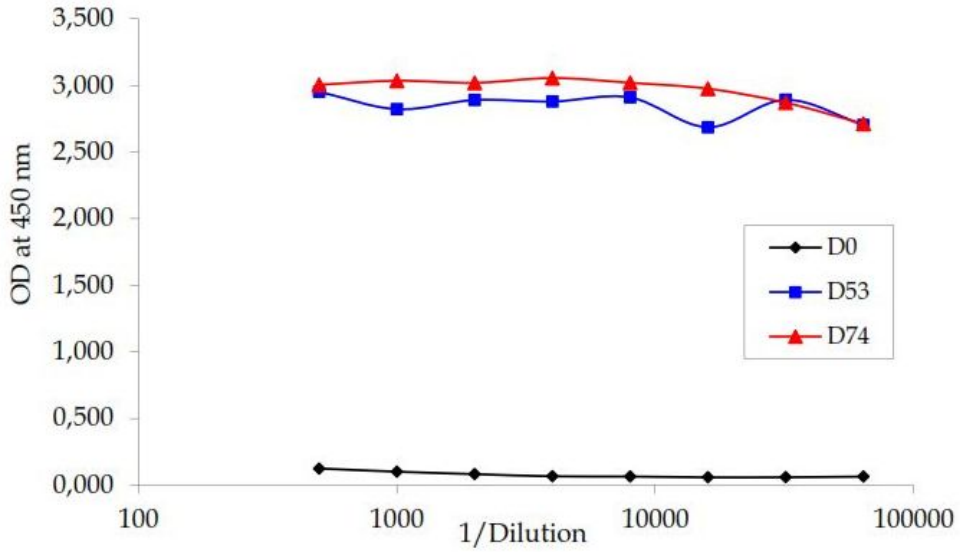


Figure 22. **Immunoractivity of rabbit serum against D1:S5/P peptide.**

The test bleeds were performed at day 53 and 74 following immunisation. The sera were tested using ELISA and compared with sera obtained before the start of the immunisation procedure. The animals immunised at this experiment were two New Zealand rabbits numbered #1230019 (A) and #1230021 (B). The experiment was performed by CovalAb S.A.S. and the presented data was obtained from CovalAb S.A.S.

A)

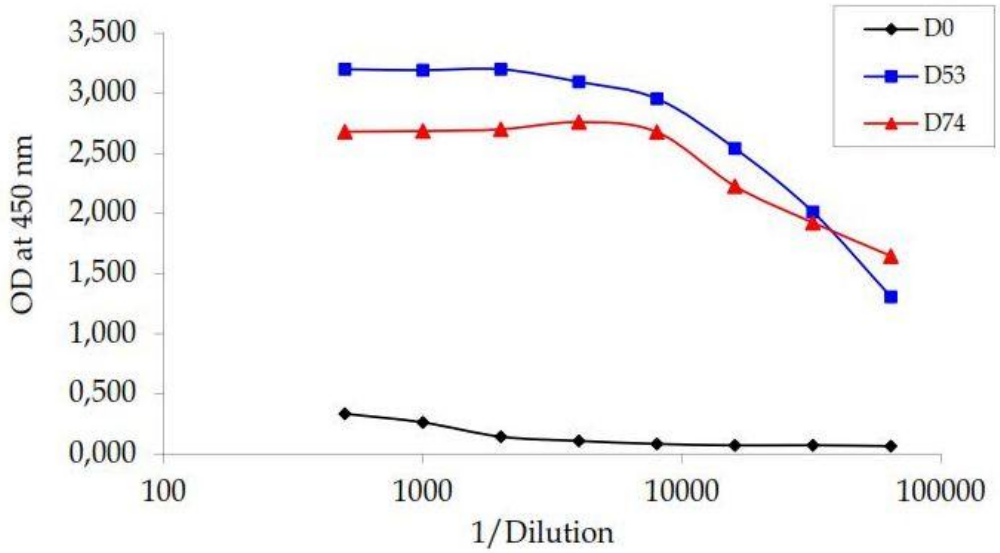


B)

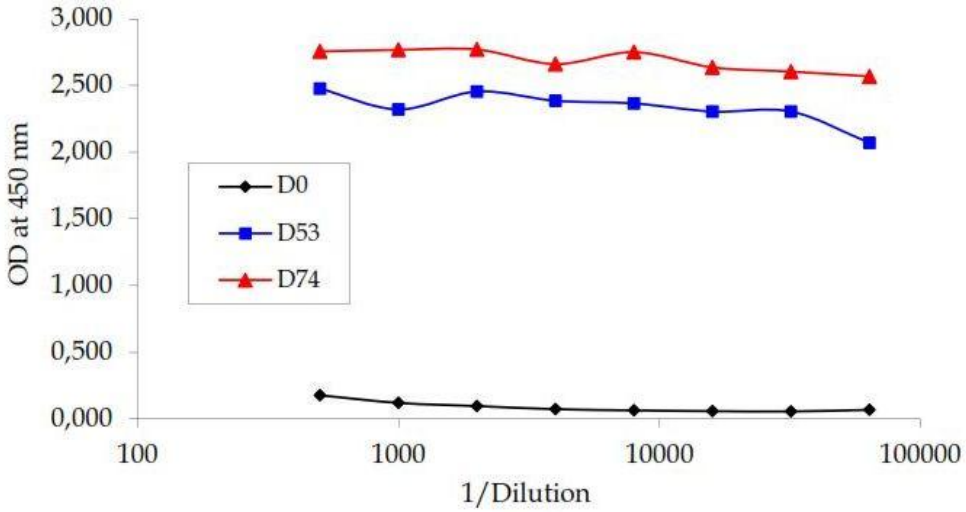


Figure 23. **Immunoractivity of rabbit serum against D4:S3/S4 peptide.**

The test bleeds were performed at day 53 and 74 following immunisation. The sera were tested using ELISA and compared with sera obtained before the start of the immunisation procedure. The animals immunised at this experiment were two New Zealand rabbits numbered #1223061 (A) and #1223063 (B). The experiment was performed by CovalAb S.A.S. and the presented data was obtained from CovalAb S.A.S.

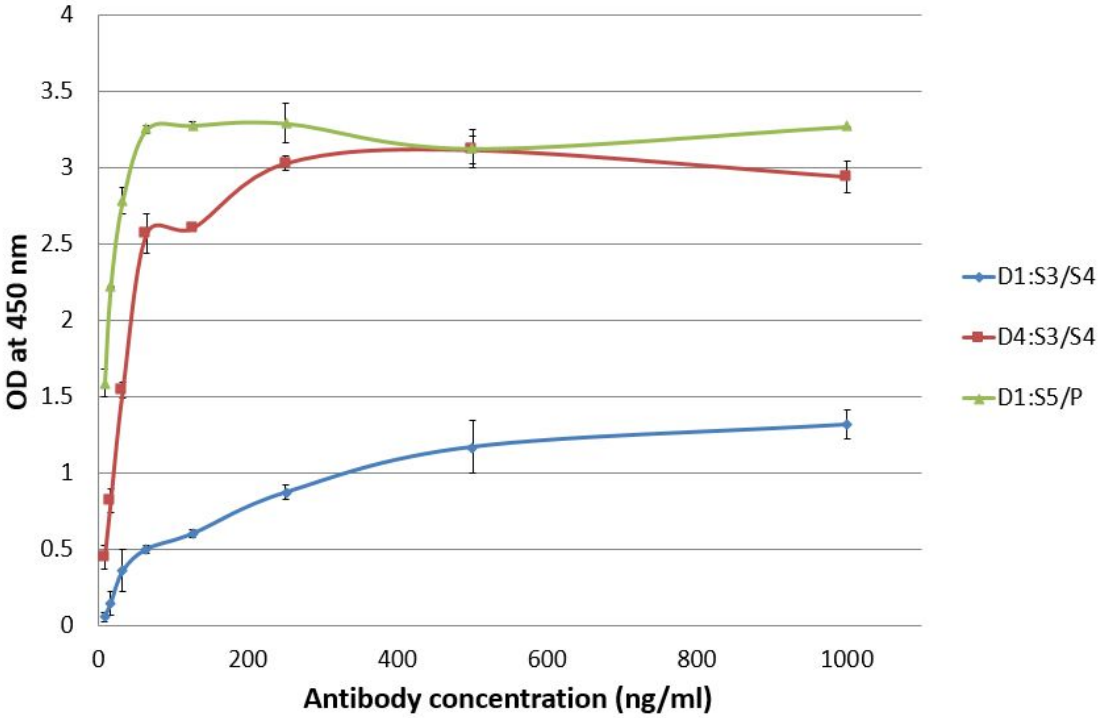


Figure 24. **ELISA results of antibody reactivity**

Antibodies produced against the three selected peptides were assayed for their ability to bind the antigen coated on microtiter plate. Indirect ELISAs were performed in duplicates with the three antigens coated on the microtiter plate. Each of the three generated antibodies was used as a primary antibody and detected using an anti-rabbit secondary antibody conjugated with HRP. TMB substrate was added to the wells and the reaction was stopped with the addition of sulfuric acid. The absorbance was read at 450 nm. The experiment was performed in duplicate and the error bars denote the standard deviation. The antibodies against the pore loop (D1:S5/P, grey line) proved to have the highest affinity to the corresponding peptide.

## 3.4. Antibody binding to antigen *in vitro* – flow cytometry

Flow cytometry was used to assess the binding of the generated antibodies to their corresponding peptides in their native conformation – on the surface of Cav3.2 expressing cells. The detailed protocol is provided in Methods (part I, 5.14, p. 56).The generated antibodies were used as primary antibodies to label the HEK/Cav3.2 cells. These antibodies were detected with mouse anti-rabbit secondary antibodies coupled with GFP for fluorescence detection using Guava EasyCyte flow cytometer. The antibodies against D1:S3/S4 sequence showed a limited degree of binding to cells expressing Cav3.2 – only 8.32 % were labelled with GFP (Fig. 25 A). The two other antibodies showed moderate binding to the HEK/Cav3.2 cells: the anti- D1:S5/P labelled 18.16 % and anti-D4:S3/S4 antibodies labelled 18.68 % of HEK/Cav3.2 cells (Fig. 26).

A)

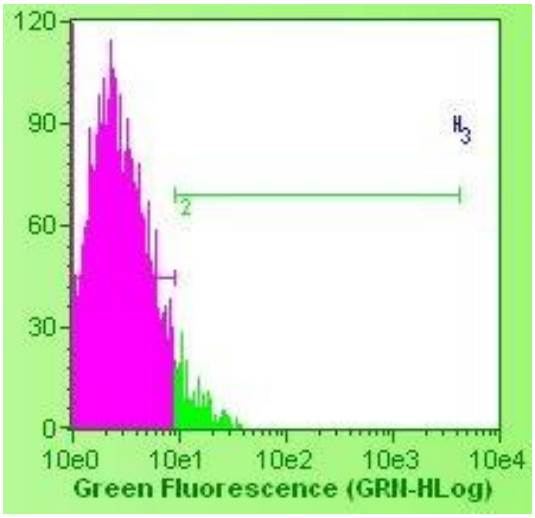


Marker 1 (pink): 91.68 %

Marker 2 (green): 8.32 %

B)

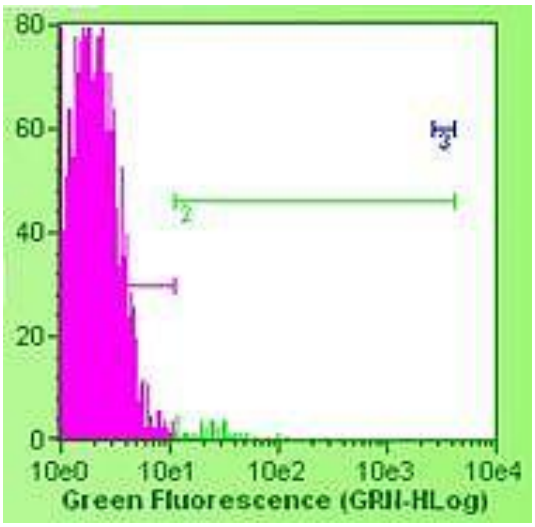


Marker 1 (pink): 97.41 %

Marker 2 (green): 2.59 %

Figure 25. **Binding of anti-D1:S3/S4 antibodies**

The HEK/Cav3.2 stable cells were labelled with anti- D1:S3/S4 antibody generated in this project and stained with secondary anti-rabbit mouse GFP-labelled antibody. These antibodies showed limited binding to their corresponding antigen in its native conformation – 8.32 % of cells exhibited green fluorescence (A). Untransfected HEK293 cells are shown for comparison – only 2.59 % of cells have shown some degree of fluorescence (B), which can be attributed to non-specific binding of primary and/or secondary antibody.

A)

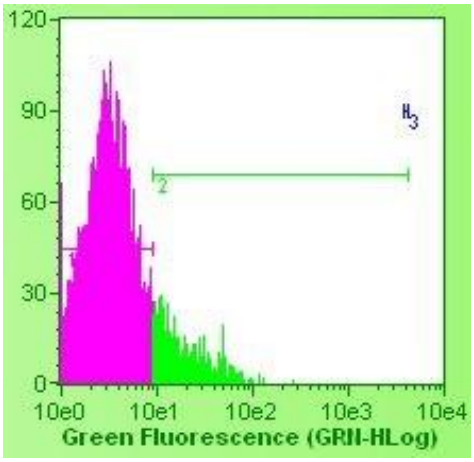


Marker 1 (pink): 81.84 %

Marker 2 (green): 18.16 %

B)

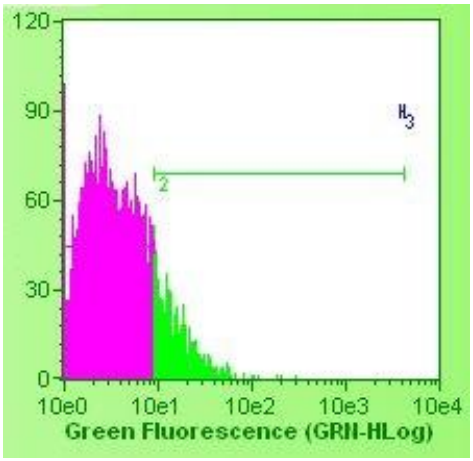


Marker 1 (pink): 81.32 %

Marker 2 (green): 18.68 %

C)

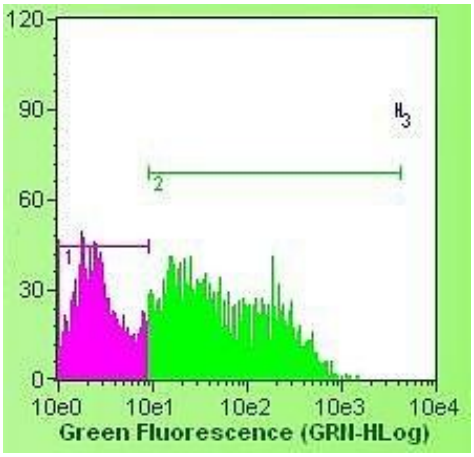


Marker 1 (pink): 34.32 %

Marker 2 (green): 65.68 %

Figure 26. **Binding of anti-D1:S5/P and anti-D4:S3/S4 antibodies**

The HEK/Cav3.2 stable cells were labelled with anti-D1:S5/P (A) and anti-D4:S3/S4 (B) antibodies generated in this project and stained with secondary anti-rabbit mouse GFP-labelled antibodies. These antibodies showed moderate binding to their corresponding antigen in their native conformation: 18.16 % and 18.68 % of cells showed increased fluorescence. The HEK/Cav3.2 stable cells stained with commercially available anti-Cav3.2 antibody are shown for comparison (C).

## 3.5. Antibody cross-reactivity

The antibodies were generated against three selected peptides located on the extracellular side of a Cav3.2 molecule. The antibodies should only bind to Cav3.2 in order to minimise possible side effects that could be associated with the use of antibodies that exhibit cross-reactivity with other proteins in humans. Moreover, if the antibodies produced exhibit cross-reactivity with other species, this would allow for their testing in animal models.

Protein BLAST was performed on the three peptides and the results are shown in Tables 5 (D1:S3/S4), 6 (D1:S5/P) and 7 (D4:S3/S4). Human pBLAST was performed to check for potential cross-reactivity with other human proteins. Non-human pBLAST was performed to assess the potential cross-reactivity of the generated antibodies in other species such as mice and monkeys. The query cover refers to the length of the peptide analysed that fully or partially matches the sequences found in published protein sequences. The percentage identity indicates how many residues in the peptide or the peptide fragment are identical with other published sequences. The expect value (E value) indicates how many matches with the same score could be expected in a given database purely by chance. The higher the E value, the less significant a match. E values close to 0 indicate a significant match (BLAST FAQ).

Table 4. **BLAST results of peptide YSLDGHNVSLSAIR (D1:S3/S4)**

| | Sequence name | % query cover | % identity | E value |
|---|---|---|---|---|
| Human pBLAST | voltage dependent t-type calcium channel alpha-1H subunit [Homo sapiens] | 100 % | 100 % | $10^{-7}$ |
| | voltage-dependent calcium channel T-type alpha 1I subunit [Homo sapiens] | 100 % | 71 % | 0.026 |
| | voltage-dependent T-type calcium channel subunit alpha-1G isoform 1 [Homo sapiens] | 100 % | 71 % | 0.15 |
| | 3'-phosphoadenosine 5'-phosphosulfate synthase 2 alpha [Homo sapiens] | 57% | 88 % | 19 |
| | calpain-10 isoform a [Homo sapiens] | 50 % | 100 % | 19 |
| Non-human pBLAST | voltage-dependent T-type calcium channel subunit alpha-1H [Cricetulus griseus] Chinese hamster | 100 % | 100 % | $4 \times 10^{-5}$ |
| | voltage-dependent T-type calcium channel subunit alpha-1H isoform X1 [Mus musculus] house mouse | 100 % | 100 % | $4 \times 10^{-5}$ |
| | calcium channel, voltage-dependent, T type, alpha 1H subunit [Rattus norvegicus] brown rat | 100 % | 100 % | $4 \times 10^{-5}$ |
| | voltage-dependent T-type calcium channel subunit alpha-1H isoform X5 [Chlorocebus sabaeus] green monkey | 100 % | 100 % | $4 \times 10^{-5}$ |
| | voltage-dependent T-type calcium channel subunit alpha-1H isoform X1 [Macaca mulatta] Rhesus macaque | 100 % | 100 % | $4 \times 10^{-5}$ |
| | voltage-dependent T-type calcium channel subunit alpha-1H isoform X1 [Papio anubis] olive baboon | 100 % | 100 % | $4 \times 10^{-5}$ |
| | voltage-dependent T-type calcium channel subunit alpha-1H isoform X1 [Gallus gallus] chicken | 100 % | 100 % | $4 \times 10^{-5}$ |

No match found for genus *Lagomorpha* (rabbits).

Table 5. **BLAST results of peptide NVCRSGDSNPHNGAI (D1:S5/P)**

| | Sequence name | % query cover | % identity | E value |
|---|---|---|---|---|
| Human pBLAST | voltage dependent t-type calcium channel alpha-1H subunit [Homo sapiens] | 100 % | 100 % | $5 \times 10^{-9}$ |
| | voltage-dependent T-type calcium channel subunit alpha-1I isoform a [Homo sapiens] | 100 % | 73 % | $5 \times 10^{-4}$ |
| | HZFw3 protein [Homo sapiens] | 60 % | 78 % | 46 |
| | SPG11 protein [Homo sapiens] | 66 % | 70 % | 66 |
| Non-human pBLAST | voltage-dependent T-type calcium channel subunit alpha-1H isoform X1 [Chlorocebus sabaeus] green monkey | 100 % | 100 % | $10^{-6}$ |
| | voltage-dependent T-type calcium channel subunit alpha-1H isoform X1 [Macaca mulatta] Rhesus macaque | 100 % | 100 % | $10^{-6}$ |
| | voltage-dependent T-type calcium channel subunit alpha-1H isoform X1 [Papio anubis] olive baboon | 100 % | 100 % | $10^{-6}$ |
| | voltage-dependent T-type calcium channel subunit alpha-1H [Gorilla gorilla gorilla] Western lowland gorilla | 100 % | 100 % | $10^{-6}$ |
| | voltage-dependent T-type calcium channel subunit alpha-1H [Equus caballus] horse | 100 % | 100 % | $10^{-6}$ |
| | voltage-dependent T-type calcium channel subunit alpha-1H-like isoform X1 [Ovis aries musimon] mouflon | 100 % | 100 % | $10^{-6}$ |

No match found for order *Lagomorpha* (rabbits), *Mus musculus* (mouse) and *Rattus norvegicus* (brown rat).

Table 6. **BLAST results of peptide LMGITLEEIEMSAALPINPTII (D4:S3/S4)**

| | Sequence name | % query cover | % identity | E value |
|---|---|---|---|---|
| Human pBLAST | voltage dependent t-type calcium channel alpha-1H subunit [Homo sapiens] | 100 % | 100 % | $6 \times 10^{-17}$ |
| | voltage-dependent T-type calcium channel subunit alpha-1I isoform a [Homo sapiens] | 95 % | 90 % | $3 \times 10^{-13}$ |
| | KIAA1120 protein [Homo sapiens] | 95 % | 90 % | $3 \times 10^{-13}$ |
| | voltage-dependent T-type calcium channel subunit alpha-1G isoform 1 [Homo sapiens] | 95 % | 86 % | $2 \times 10^{-12}$ |
| | olfactory receptor 8H2 [Homo sapiens] | 68 % | 69 % | 0.18 |
| | dynein heavy chain 7, axonemal isoform X11 [Homo sapiens] | 54 % | 100 % | 4.0 |
| Non-human pBLAST | voltage-dependent T-type calcium channel subunit alpha-1H isoform X1 [Macaca mulatta] Rhesus macaque | 100 % | 100 % | $10^{-14}$ |
| | voltage-dependent T-type calcium channel subunit alpha-1H isoform X1 [Chlorocebus sabaeus] | 100 % | 100 % | $10^{-14}$ |
| | voltage-dependent T-type calcium channel subunit alpha-1H isoform X1 [Papio anubis] olive baboon | 100 % | 100 % | $10^{-14}$ |
| | voltage-dependent T-type calcium channel subunit alpha-1H isoform X1 [Pan paniscus] Bonobo | 100 % | 100 % | $10^{-14}$ |
| | voltage-dependent T-type calcium channel subunit alpha-1H [Gorilla gorilla gorilla] Western lowland gorilla | 100 % | 100 % | $10^{-14}$ |

No match found for order *Lagomorpha* (rabbits), *Mus musculus* (mouse) and *Rattus norvegicus* (brown rat).

# 4. Discussion

## 4.1. Modifications to the antibody design process

The generation of polyclonal antibodies described in this chapter does not exactly follow the design process described by Presta (2005), which comprises of four stages: target selection (1), generation of antibodies (2), epitope selection (3) and optimisation (4). In the experiment described here, the design process was changed. The target selected was chosen not only for its potential targeting by therapeutics. The involvement of Cav3.2 in various physiological and pathological pathways has been demonstrated, but the exact role of this channel and its cooperation with other molecules is not yet fully understood. The antibodies generated are more likely to help in elucidating the function of Cav3.2 rather than being developed as therapeutic agents.

Another change in the design process was that in this experiment stages two and three proposed by Presta (2005) have been carried out in reverse order. The epitope selection has been done *a priori* and the antibody production was directed only at these three chosen epitopes, instead of generating antibodies against the whole protein. This approach circumvented the need for antigen extraction and purification in native conformation, which would be rather difficult in this case, due to Cav3.2 being membrane-bound. Moreover, *in silico* analysis of Cav3.2 structure allowed for pinpointing stretches of the molecule which may be involved in the channel gating. It is hoped that antibodies directed against these epitopes may induce changes in the channel conductivity.

The antibodies generated and tested in this project were polyclonal. This option was more affordable and allowed for the generation of antibodies against three chosen peptides. The antibodies' paratopes most likely do not cover whole peptide sequences, but rather polyclonal antibodies generated against a particular peptide comprise of several clones with slightly differing coverage and affinity. This increases the chances that some of these antibodies would bind at a crucial site, with higher affinity and with a

particularly effective orientation on the Cav3.2 molecule embedded in the membrane. The antibodies were generated against linear peptides, while in Cav3.2 these peptides are likely to have some degree of secondary and tertiary structure stabilised by interactions with the remaining part of the protein and the cell membrane. It is also likely that the opening and closing of the channel changes the conformation of these peptides. The generation of polyclonal antibodies increases the chances that some of these antibodies would bind to the peptides in their native conformation.

The last difference between the published design process and this project is that the polyclonal antibodies cannot be optimised. The optimisation process involves production of monoclonal antibodies and their sequencing, which would exceed the scope of this research project.

## 4.2. Reactivity of the generated antibodies

The generation of all three types of polyclonal antibodies in rabbits was successful (Figs. 19-22). The antibodies generated had good affinity to the peptides when tested in ELISA format. The antibody with the highest affinity to the corresponding peptide were the antibodies directed against the pore loop (D1:S5/P) (Fig. 22), closely followed by the antibodies targeting the loop in Domain IV (D4:S3/S4) (Fig. 23). The antibodies directed against loop in Domain I (D1:S3/S4) proved to have a lower affinity to the peptide in ELISA (Fig. 21). This assumption is only valid assuming that the peptides themselves have identical attraction to the surface of the microtiter plate. It is theoretically possible that antibodies against D1:S3/S4 have very high affinity to the peptide but the peptide exhibits only weak binding to the microtiter plate.

Flow cytometry was used to measure the degree of binding of the generated antibodies to their corresponding peptides within the Cav3.2 molecule. This experiment was important to elucidate whether the antibodies recognize these peptides in their native conformation. As mentioned above, the peptides used for immunisation were linear and the same strings of amino acids within the protein molecule have a certain spatial

arrangement and rigidity, and are generally not accessible from all sides. A short extracellular loop could possibly be positioned rather flat on the cell membrane, thus being only partially accessible to the antibodies. Moreover, the sequences used for immunisation are putatively extracellular – their exposure on the cell membrane was predicted using bioinformatics tools but was not confirmed with any practical experiments such as NMR or X-ray crystallography. Therefore it is possible that Cav3.2 does not have the exact structure predicted by the algorithms. Flow cytometry experiments can contribute to elucidation of the actual structure of Cav3.2.

The binding of antibodies to D1:S3/S4 loop in flow cytometry experiment was limited – only 8.32 % of cells exhibited green fluorescence when stained with the custom antibodies. This is slightly higher than the non-specific binding of commercial antibodies to the untransfected HEK293 cells (2.59 %). The percentage of HEK/Cav3.2 cells stained with commercial anti-Cav3.2 antibodies was 65.68 %. This indicates that the generated antibodies do not have high affinity to the D1:S3/S4 loop. This is probably due to low immunogenicity of this peptide and is in agreement with the ELISA results. The purified antibodies and the sera at days 53 and 74 for peptide D1:S3/S4 had significantly lower affinity to the peptide than the other two antibodies had to their peptides.

The binding of the other two generated antibodies showed a moderate level of GFP fluorescence: 18.68 % in the case of anti-D4:S3/S4 antibodies and 18.16 % in the case of anti-D1:S5/P antibodies; this compares to 65.68 % of HEK/Cav3.2 cells stained with the commercial antibodies and seems to be a rather low level of staining. Nevertheless, this is a significant degree of the antibody binding, clearly distinguishable from the non-specific binding of antibodies to the untransfected HEK293 cells. Moreover, it is possible that the extracellular stretches of protein were damaged during cell fixation and permeabilisation. These procedures are performed with paraformaldehyde and detergents such as saponin, Triton X-100 and Tween-20. Fixation with paraformaldehyde preserves the cell structure due to the formation of methylene cross bridges between protein molecules (Schnell *et al.,* 2012). After paraformaldehyde

fixation, the cells need to be permeabilised with the aforementioned detergents to allow for antibody access (Schnell *et al.,* 2012). Saponin and digitonin selectively remove cholesterol from the membranes (Schnell *et al.,* 2012). Triton X-100 and Tween 20 make holes in the cell membrane and elution of some lipids, thus allowing the antibodies to stain antigens in the cytoplasm but they may also remove some proteins (Jamur and Oliver, 2009). Fixation with PFA and the use of detergents are standard methods used in immunocytostaining and flow cytometry, however, they may produce some artefacts. Ideally, a live cell imaging should be used to fully describe protein localisation, because immunostaining procedures on dead cells may lead to protein extraction or relocalisation (Schnell *et al.,* 2012). Staining of live cells could be performed with the antibodies generated in this project, as they target regions that are predicted to be extracellular and accessible in live cells.

The degree of the antibody binding described here appears to be rather low, nevertheless, it may be more than enough to block the channel conductance. Furthermore, the binding of the generated antibodies may be relatively low in the flow cytometry protocol that involves triple washing between staining with primary and secondary antibodies, which may elute moderately binding antibodies. However, when the antibodies are incubated with the cells and not washed out, the majority of them may remain bound to Cav3.2.

## 4.3. Prediction of antibody selectivity

The BLAST results confirmed that the peptides selected are present in human Cav3.2 (shown in BLAST results as T-type calcium channel subunit α-1H). Unfortunately, all three peptides have similarities in Cav3.1 and Cav3.3. The peptide from Domain I S3/S4 has 71 % identity with sequences found in both Cav3.1 and Cav3.3. This peptide also has some sequence identity with 3'-phosphoadenosine 5'-phosphosulfate synthase 2 (PAPS2) and calpain-10. The peptide identity is only partial, nevertheless, the antibodies raised against the long peptide may only bind to part of it which could happen to be the

same as in PAPS2 or calpain-10. The use of such antibodies in humans could cause unpredictable side effects. Peptide for D1:S3/S4 is also present in Cav3.2 of other species such as mice, Chinese hamsters, rats and monkeys. This would allow for the use of these antibodies also in other species to test for systemic effects of blocking Cav3.2.

The peptide generated against the pore loop (D1:S5/P) has shown 73 % identity with a peptide from Cav3.3, but did not return any similarities with the Cav3.1 structure. This would suggest that the generated antibodies would bind to Cav3.2 and Cav3.3 only – in this way they could be useful in differentiating between the functions of Cav3.1 and Cav3.2 – their expression often overlaps, making it difficult to distinguish between the effects caused by these two channels. The D1:S5/P peptide has shown some identity with proteins HZFw3 and SPG11, but the identity was low enough and the E value was very high, indicating that the similarity with these proteins may not be significant. The amino acid sequence is also present in Cav3.2 in other species, mostly monkeys, but not mice, rats and rabbits.

The peptide from Domain IV S3/S4 is only present in human Cav3.2. The corresponding peptide in Cav3.3 has only 90 % identity with the peptide from Cav3.2 – two amino acids in the middle of the loops are different. Cav3.1 loop similarity to Cav3.2 peptide is 86 % with three different amino acids in the middle of the loop. The investigated peptide also has some identity with olfactory receptor 8H2 and an isoform of dynein heavy chain. Both of these proteins may be affected by antibodies generated against the D4:S3/S4 peptide. However, these proteins have limited sequence identity and query cover together with limited expression – these factors would probably minimise the possible interactions of the antibodies with these proteins and cause minimal side effects.

## 4.4. Possible further experiments

The process of generating antibodies against the selected peptides proved to be successful. The obtained antibodies had satisfactory properties and could be further

used in Cav3.2 experiments *in vitro.* The experiments described in this chapter could be further enhanced. For example, the reactivity of the generated antibodies against denatured Cav3.2 molecules could be assessed using Western Blotting. Flow cytometry experiments should include controls with the generated antibodies used after pre-incubation with their corresponding peptides (peptide competition assay). This would block the antigen binding sites of the generated antibodies. The use of such neutralised antibody alongside free antibodies allows for identification of specific staining. The non-specific staining would be visible in both samples, while the specific staining would be absent from the sample where the neutralised antibodies were used. Another type of control would be to use cells expressing Cav3.3 and Cav3.1 which are the proteins with the highest similarity to Cav3.2 as shown by BLAST results. In such cases cross-reactivity may occur and the generated antibodies could also bind to Cav3.3 and Cav3.1. Unfortunately, due to the limited amount of antibodies available and also lack of cell expressing Cav3.3 and Cav3.1 in our lab, such controls were not performed. Similarly, the generated antibodies could have been used for immunocytochemistry, but this technique requires a rather significant amount of the primary antibody. For this reason immunocytochemistry was only performed using Alomone anti-Cav3.2 antibodies and not the antibodies generated in this project.

# Chapter 4: Fluorescent Assay for Measuring the Kinetics of Cav3.2

# 1. Introduction

The involvement of ion channels in cellular and organismal metabolism can be investigated using a range of methods. The localisation and expression patterns of ion channels can be assessed using molecular biology methods such as immunostaining and mRNA analysis. The analysis of expression patterns sheds some light on the possible role of a given ion channel in metabolism; however, to elucidate its exact role it is crucial to understand the gating kinetics of this channel. Ion channels have different gating properties depending on the activation mode (ligand or voltage-gated), activation and inactivation thresholds and times.

There are several methods allowing for the measurement of ion channel gating. Ion channels are interesting drug targets and they are often investigated in the pharmaceutical industry. From a pharmacological point of view the methods used in investigating ion channel kinetics and their interaction with various drugs should be simple and easily scalable to allow for the investigation of multiple components against a chosen target within a reasonably short time (High Throughput Screening). High Throughput Screening (HTS) is the first step in drug development. HTS involves the development and validation of an *in vitro* model system that mimics the *in vivo* pathways. The ideal model system must be easy to create and should allow for the investigation of numerous compounds in a relatively short time, and must also allow for the choice of lead compounds with desired chemical and pharmacological properties. The use of such a model would allow for the screening of the effect of multiple compounds on a given target. HTS may involve cell-based or cell-free assays. Cell-free assays only measure ligand-target interactions (binding) but usually do not identify agonists, antagonists and the mechanisms of the action of the tested compounds. Cell-based assays are sometimes performed on native tissue sections but usually utilise cell lines that are easy for culturing and genetic manipulations. These cell lines are transfected with a gene

coding for the protein of interest (drug target) and the ligand-compound interactions are studied in a physiologically relevant environment.

Various methods may be implemented in the HTS for ion channels. In the case of Cav3.2 there are two main groups of methods suitable for analysis of channel kinetics: electrophysiological analysis and fluorescence-based methods. These methods are described in the subsequent sections.

## 1.1. Electrophysiological method of measuring ion channel kinetics

The most advanced techniques that deliver the most information about channel gating are the electrophysiological methods such as patch clamp and voltage clamp. These techniques rely on the detection of electrical currents flowing through the cell membrane. Electrophysiological recording was first used to detect single-channel currents in frog muscle fibre (Neher and Sakmann, 1976). In recent years the method has been further improved and optimised. In a patch clamp method a glass pipette filled with electrolyte solution is attached to the cell membrane in such a way as to allow for the formation of a seal between the pipette tip and the membrane. This seal has very high resistance (>10GΩ) and is called a gigaseal. Depending on the desired configuration, the membrane patch enclosed by the pipette can be pulled away from the cell resulting in a so-called “inside-out” configuration. The intracellular side of the membrane is exposed to the bath environment and the extracellular side is facing the pipette interior. The currents flowing through the ion channels in that membrane fragment are measured by an attached voltage amplifier. This mode is mainly used to record single-channel kinetics. Another configuration is called “whole-cell recording mode”. In this case suction is applied through the pipette resulting in a rupture of the cell membrane fragment enclosed by the pipette. The cytoplasm then comes into contact with the pipette solution and the rest of the cell remains attached to the pipette. In this mode the electrical activity of the whole cell is recorded. Another possible configuration is “outside-out” when the pipette attached in the whole-cell recording mode is pulled away from the cell tearing a piece of the membrane which then reseals with the cytoplasmic side facing the pipette interior. The patch-clamp configurations are presented in Fig. 27.

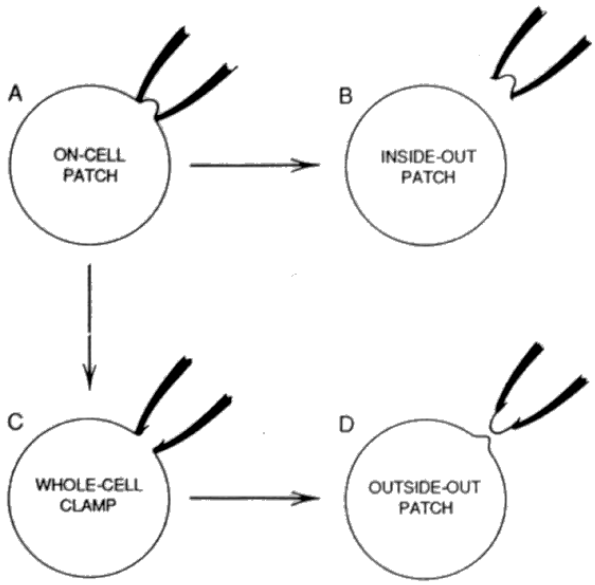


Figure 27. **Possible patch clamp configurations**

Various configurations of patch clamp experiment can be utilised to allow for the gathering of channel gating data. Cell attached patch allows for the measurement of single channel currents without disturbing the cell membrane integrity (A). Inside-out patch (B) involves pulling away a part of the membrane with the cytoplasmic side facing the bath solution. Whole-cell clamp allows for the recording of the electrical activity of the whole cell (C). In outside-out patch the membrane pulled from the cell reseals on the pipette and the cytoplasmic side faces the interior of the pipette (D). Adapted from Fulton (2008).

The patch clamp technique allows for precise measurements of virtually all of the channel properties: conductance, current, activation and inactivation thresholds and times. Analysing a given channel using patch clamp is the most detailed and accurate method but it has several disadvantages, which include the cost of the equipment required and the need for highly skilled operator. Moreover, patch clamp experiments are time-consuming and can be performed only on one cell at a time. Automated patch clamp systems allow for the investigation of more cells at a time and does not require an operator to perform all measurements. This method is still rather expensive and does not achieve the very high capacity that is required for HTS. The electrophysiological techniques are therefore good for investigating the channel kinetics in native cells but less useful in cases where multiple compounds need to be tested for their influence on the channel gating, as in HTS. The patch clamp technique is most appropriate for detailed investigation of the channel kinetics but not best suited for HTS assays. Once the gating properties of a channel are well described, other methods may be used to measure changes in the channel gating in response to drug application.

## 1.2. Fluorescence-based investigation of Cav3.2 kinetics.

Alternative methods for measuring channel activity have been developed, relying on the alternative detection of ion influx that can be used for HTS. There are three such methods reported for measuring Cav3.2 activity. All of them rely on fluorescent detection of calcium ion influx into cells expressing recombinant Cav3.2. Two of these methods also involve manipulation of the cell membrane potential in order to activate Cav3.2 channels. The main challenge in developing a model for Cav3.2 screening is the fact that these channels have specific kinetics of activation and inactivation. The spontaneous resting membrane potential (RMP) for non-excitable cells is relatively positive, *e.g.* for HEK293 cells it is between -40 and -20 mV (Belardetti *et al.* 2009). Thus at resting membrane potential of many cell lines routinely used for screening purposes, Cav3.2 channels are largely inactivated. However, as described by Chemin *et al.* (2000), the activation and inactivation curves for Cav3.2 intersect at about -60 mV thus creating the so-called 'window current' that allows for calcium ion influx at the resting membrane potential of HEK293 cells. It was possible to measure this current using path-clamp without the need for altering the membrane potential (Xie *et al.,* 2007). The intracellular $Ca^{2+}$ concentration was increased in cells expressing Cav3.2 and detected with a calcium-sensitive fluorescent dye such as Fura-2 used in this study. Subsequent increases in extracellular $Ca^{2+}$ concentration resulted in the increased influx of calcium ions into the cells and fluorescence increase that was maintained at a stable level until the end of recording (Fig. 28). This current as well as calcium level changes have been abolished by the application of mibefradil (Fig. 28), thus confirming that the window current of Cav3.2 was the cause of these changes. In this way, the HEK293 cells expressing Cav3.2 can be used for screening novel compounds which inhibit Cav3.2 activity.

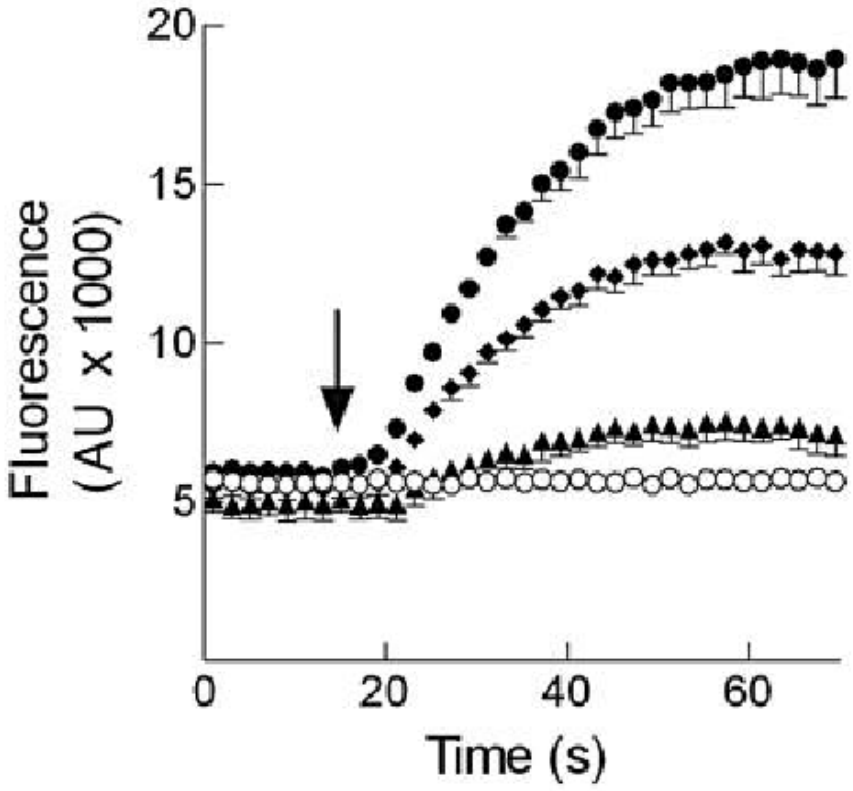


Figure 28. **Fluorescent assay for Cav3.2 activity (Xie *et al.,* 2007)**

The cells expressing Cav3.2 increased their $Ca^{2+}$ content when extracellular concentration of this cation was rapidly increased by a bolus of $Ca^{2+}$ (arrow) that increased $Ca^{2+}$ concentration to 10 mM. This resulted in fluorescence rise in these cells (filled circles). Cells not expressing Cav3.2 were insensitive to extracellular $Ca^{2+}$ rise (empty circles). Pre-treatment with 10 μM mibefradil caused an almost complete block of fluorescence rise in cells expressing Cav3.2 (filled triangles). Pre-treatment with 0.3 μM mibefradil caused half-maximal block of fluorescence rise in cells expressing Cav3.2 (filled diamonds).

A different approach to this challenge was presented in work by Belardetti *et al*. (2009). The problem with higher RMP can be overcome by artificially altering the membrane potential using gramicidin. This peptide forms pores in the cell membrane that are selective for small monovalent cations *i.e.* $H^+$, $NH_4^+$, $Cs^+$, $Rb^+$, $K^+$, $Na^+$, $Li^+$ and tetramethylammonium ion. By varying the concentration of ions in the extracellular medium, it was possible to lower the membrane potential to a desired value. In the absence of small monovalent positive cations in the extracellular buffer, there was net Potassium ion efflux out of the cells through gramicidin pores. This increased the membrane polarisation to -90 mV at which the Cav3.2 channel inactivation is removed and the channels switch to a resting state. Subsequent increases in potassium ion concentration in the extracellular media cause a rise in membrane potential up to -60 mV, which causes the Cav3.2 channel to open thus allowing the influx of $Ca^{2+}$ ions. This influx was visualised by preloading the cells with a calcium sensitive fluorescent dye and the measurement of calcium-induced fluorescence. A similar approach involving manipulation of cell membrane potential was later described by Prigge, Rösler and Hegemann (2010). In their experiment HEK293 cells expressing Cav3.2 were additionally transfected with mTrek potassium channel and channelrhodopsin-2 (ChR2). The mTrek channels are voltage-insensitive and allow for potassium efflux thus decreasing the membrane potential to the required level. Channelrhodopsin-2 conducts monovalent cations and is activated with blue light causing depolarization of the cell membrane. This allows for repetitive activation of Cav3.2 in same cells and for measuring the calcium-induced fluorescence of Fura-2 dye.

## 1.3. Implementation of a fluorescent assay for measuring Cav3.2 kinetics

The experiment presented in this chapter and subsequently used to investigate the antibodies' effect on the Cav3.2 kinetics had been adjusted from the research published by Xie *et al.* (2007) and validated for use in our laboratory.

The HEK293 cells expressing Cav3.2 were grown to confluency on a 96-well plate and incubated in the Fluo-4-AM loading buffer. Fluo-4-AM is a calcium-sensitive fluorescent dye that is used for the detection of changes in intracellular calcium concentration. The dye is absorbed by the cells and the acetoxymethyl ester is hydrolysed thus releasing the active dye. After loading with the dye the cells were placed in an Omega plate reader and the fluorescence changes were recorded for 60 s for each well. After 10 s of recording the baseline fluorescence, a bolus of high $Ca^{2+}$ solution was automatically added by the machine to each of the wells. A high concentration of external $Ca^{2+}$ ions caused calcium ion influx to the cell cytoplasm in cells expressing Cav3.2 due to the window current. This caused an increase in fluorescence of the dye – these cells constituted a positive control for the experiment. This fluorescence increase rapidly reached a plateau and was then sustained until the end of the recordings for each well. The reason for the fluorescence plateau was that the equilibrium between intracytoplasmic and extracytoplasmic $Ca^{2+}$ concentration is achieved and there is no further net movement of calcium ions across the cell membrane. For negative control, HEK293 cells not transfected with Cav3.2 were used to ensure that fluorescence increase after addition of $Ca^{2+}$ is not due to $Ca^{2+}$ influx through any other unidentified calcium channel. Moreover, the tested compounds could potentially affect the Fluo-4 fluorescence, hence this control was used alongside the cells expressing Cav3.2. After initial implementation and testing, the modification of the assay was also attempted. Calcium ions in the cells are mainly stored in the endoplasmic/sarcoplasmic reticulum. In physiological circumstances the increase in cytoplasmic level of $Ca^{2+}$ activates the calcium re-uptake pumps in the endoplasmic/sarcoplasmic reticulum (SERCA) that

remove these ions from the cytoplasm. Another mechanism of reducing $Ca^{2+}$ level is the activation of plasma membrane calcium ATPase (PMCA) that actively pump $Ca^{2+}$ out of the cell. In order to increase the distance between the baseline fluorescence and the response fluorescence, the calcium re-uptake inhibitors were added to the wells and the assay was tested again.

The resting membrane potential and the level of Cav3.2 expression may slightly vary between cells thus resulting in differences in baseline and response fluorescence. Moreover, the condition of the cells may also affect the $Ca^{2+}$ influx rate. Therefore the measured fluorescence needs to be normalized by baseline correction. The cellular response to the elevated $Ca^{2+}$ and the fluorescence rise was quantified by the integration of the area under the curve (AUC). In pharmacokinetics, the AUC represents bioavailability of a drug. Similarly, calculation of the area under the fluorescence response curve represents the total amount of $Ca^{2+}$ that reached the cytoplasm.

## 1.4. Modification of the published assay format

The fluorescence-based assay was developed on the basis of the research published by Xie *et al.* (2007). The initial assay settings were as published by Xie *et al.* (2007). Attempts to optimize the assay included changes in the cell seeding protocols (cell density), time of pre-incubation with the fluorescent dye, the dye type and concentration; and times of incubation with the tested drugs such as mibefradil and other known Cav3.2 inhibitors. Two cell types were tested for their suitability for the assay: transiently transfected cells and a stable cell line expressing Cav3.2. Moreover, changes in the fluorescence recording protocol were attempted to increase the assay sensitivity.

### 1.4.1. Cell line and seeding protocol

Cells stably expressing Cav3.2 have been used in all three published assays investigating this channel kinetics. The experiments described in this thesis use mainly a stable cell line HEK/Cav3.2 obtained from the research team of Prof Edward Perez-Reyes (University of Virginia, School of Medicine). This cell line was also used in the experiments described by Xie *et al.* (2007). HEK cells transiently transfected with Cav3.2 plasmid were also used for comparison with the stable cell line. The advantage of a transient transfection over a permanent transfection lies mainly in the expression levels of a protein. The transiently transfected cells usually harbour multiple copies of the plasmid and thus express higher levels of protein than stably transfected cells (Kim and Eberwine 2010). The transiently transfected cells usually show some level of the recombinant protein expression after one day and up until seven days post-transfection, however, the transfection reagent protocols recommend harvesting the cells in 24-96 hours (Life Technologies Lipofectamine® protocol). Transiently transfected cells do not incorporate the recombinant DNA sequence in their genomes, therefore the likelihood of this DNA disrupting other important genes is minimal. Due to the short period of harbouring the foreign DNA, the likelihood of mutations in the sequence of interest is lower. Paradoxically, the disadvantages of the transiently transfected cells also stem

from the level of protein expression – it is usually unstable, highly variable between individual cells and variable during the period in which the protein is expressed. During cell division the introduced DNA is often lost, thus resulting in an increasing proportion of cells not expressing the recombinant protein. The stably transfected cells, on the other hand, incorporate the foreign DNA into their genomes and pass the new DNA to the progeny. The stable cell lines are usually derived from a single cell (monoclonal expansion), therefore the descendant cells have the recombinant DNA incorporated at the same location, under the control of the same promoter and expressing the same level of the protein of interest. The main disadvantage of the stable cell lines is their degeneration over time and lowering proliferation rate with increasing passage number. An antibiotic needs to be added to cell medium for the maintenance of the gene of interest. However, the addition of antibiotic may exert side effects on the cellular metabolism thus affecting the cell response to other compounds in any assay. It is difficult to predict whether the performance of stable cell line or the transiently transfected cells is better suited for implementation in the Cav3.2 fluorescent assay. The experiment described here compares the use of both types of cells.

The Cav3.2 fluorescent assay involves seeding the cells in a 96-well plate and performing measurements after the cells have attached to the bottom of the wells and formed a monolayer. Usually the wells need to be first coated with an agent that enhances the cell adherence to the polystyrene surface of the microtiter plate. This is especially important in cases where the assay requires several washes of the cells and changes of the solutions in the wells. The compound chosen for well coating in this assay was poly-D-lysine. The seeding density of the cells may affect the formation of the monolayer. In the case of too high initial density, the cells may form clumps – this would result in increased fluorescence from a given area. Too low seeding density would require a longer period of culturing for the cells to reach a confluent monolayer of cells. The confluent monolayer is of paramount importance for this assay reproducibility, as the occurrence of gaps between cells would result in no fluorescence being recorded for

a given area in the well and the lowering of the average fluorescence recorded for the whole well. Variable seeding densities were tested to find the optimal one allowing the formation of the cell monolayer in 24 hours post-seeding.

### 1.4.2. Fluorescent dye

Two fluorescent dyes were tested in the assay to assess the differences in the assay sensitivity: Fluo-4-AM and Calcium Green-AM (both from Life Technologies). Both dyes are advertised as relatively non-toxic to cells and are supposed not to interfere with the cellular metabolism and signalling.

### 1.4.3. Dye concentration

The dye concentration needs to be adjusted to allow for efficient loading into the cells but to avoid dye-induced toxicity. The Life Technologies protocol recommends the use of Fluo-4-AM in range 1–5 μM. In addition to the dye, it is usually necessary to use the non-ionic detergent Pluronic® F-127 (Life Technologies) to aid with the Fluo-4-AM dispersion in the aqueous solvent. A range of dye concentrations was tested in this experiment to find the optimal dye concentration that allows for the visualisation of the fluorescent response.

### 1.4.4. Incubation time

The incubation time is of crucial importance in this assay. There are two incubation periods: the first is meant to load the cells with the fluorescent dye and to allow for the dye de-esterification. This period should be long enough to allow for efficient dye uptake and hydrolysis. The prolonged incubation time with the dye increases the toxic effects of the dye and causes dye leakage from the cells or dye compartmentalization within the cells. After the loading time the cells are washed off to remove the excess dye that has not been absorbed.

The second incubation period is important for the efficient binding of the tested compounds and inhibitors, *e.g.* mibefradil. Mibefradil binding to Cav3.2 is relatively well understood and it only requires approximately 20 min for the compound to block the fluorescence response. However, the time to reach equilibrium in the case of other tested

compounds is not well known, and some molecules, such as antibodies, may require longer time to bind to Cav3.2.

## 1.5. Validation of a fluorescent assay for measuring Cav3.2 kinetics

The values of AUC obtained during four independent experiment repeats for HEK293 cells (negative control) and HEK/Cav3.2 cells (positive control) treated with $Ca^{2+}$ bolus are shown in Table 7. The suitability of the assay was further confirmed by the application of a known Cav3.2 blocker – mibefradil at concentration 10 μM.

An example of raw traces and a single well plot obtained during the experiments are shown in Fig. 30. For additional control, HBSS-HEPES buffer was administered instead of the high $Ca^{2+}$ buffer for HEK/Cav3.2 cells to ensure that the increase in fluorescence was not stimulated by fluid flow disturbances – no fluorescence increase was observed in those cells (data not shown).

The suitability of this fluorescence-based essay was confirmed by the calculation of Z-factor. The Z-factor, also called a screening window coefficient, is a statistical parameter used for the validation and optimisation of HTS assays. This factor defines the signal window, also called the assay dynamic range that is available in a particular test. The Z-factor calculations take into account the average values of positive and negative controls and the errors of these averages (standard deviation). Assuming that the positive and negative controls obey the normal (Gaussian) distribution profile, 99.7 % of the control values should lie within three standard deviations of the mean. The relative distance between the means for the positive and negative controls is also important in estimating the usefulness of an assay for HTS. The formula for calculating the Z-factor is shown below (Zhang, Chung and Oldenburg, 1999):

$$Z = 1 - \frac{3\sigma_{+c} + 3\sigma_{-c}}{|\mu_{+c} - \mu_{-c}|}$$

Where:

$\sigma_{+c}$ – standard deviation of positive control

$\sigma_{-c}$ – standard deviation of negative control

$\mu_{+c}$ – mean of positive control

$\mu_{-c}$ – mean of negative control

The values of the Z-factor determine the suitability of an assay to use in HTS. An ideal assay has a Z-factor value of 1, which means that $\sigma_{+c}$ and $\sigma_{-c}$ are equal to 0, *i.e.* there is no deviation from the recorded values of controls. Z-factor in range $1 > Z \geq 0.5$ indicate an excellent assay with a large separation band between the positive and negative controls. If the Z-factor value is lower than 0.5, the assay has a limited usability and should be improved (Zhang, Chung and Oldenburg, 1999).

## 2. Aims

The aims of this part of the project was to implement and validate a fluorescence-based High-Throughput Screening assay for the Cav3.2 modulators. Previously published fluorescence-based assays for measuring the kinetics of Cav3.2 were compared and evaluated.

# 3. Results

The assay for measuring Cav3.2 activity in cells expressing this channel was adapted from Xie *et al.* (2007). An attempt to use the method proposed by Belardetti *et al.* (2009) was made but the results were inconsistent due to an unidentified error.

The initial settings of the assay were set up according to Xie *et al.* (2007). In an attempt to improve the fluorescence response, several parameters were modified. The results of these modifications are presented below:

## 3.1. Cell seeding protocol

The use of transiently transfected cells for the assay proved to be difficult due to inconsistencies in the fluorescent response. The cells were transfected in the wells of the 96-well plate as described in *Methods* (Part I, 5.7, p. 50). The variability between fluorescence responses in individual wells was too high to be considered. In the wells where the transfection reaction was successful, the fluorescence change was high and easily observed upon adding $Ca^{2+}$. In other wells the transfection procedure did not work for unknown reasons and therefore no fluorescence response was observed (Fig. 29). In the case of the stable cell line expressing Cav3.2 there was no significant variability between the wells on the same plate (Fig. 30), although there was some variability between experiments performed with different batches of cells on different days.

The cell seeding density that proved to be optimal was 5 x $10^4$ cells per well of a 96-well plate. After 24 hours incubation at 37 ºC in the usual medium, the cells were well attached and covering almost the whole bottom of the well (approximately 90 % confluency assessed visually; data not shown).

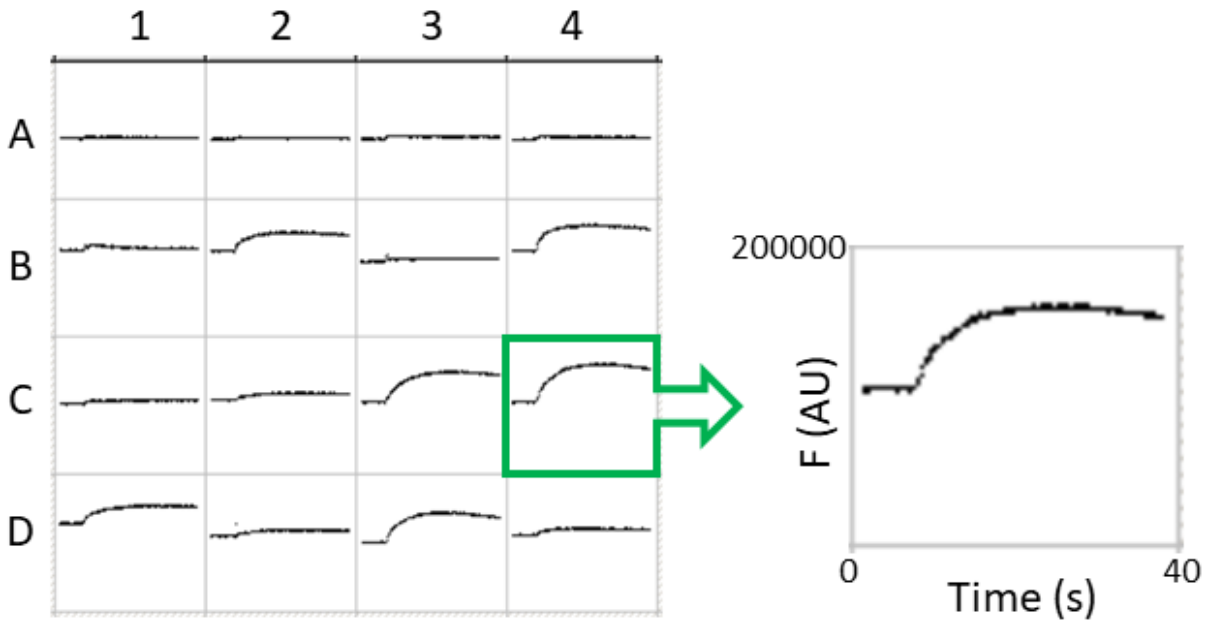


Figure 29. **Fluorescent response in transiently transfected cells expressing Cav3.2**

The cells transiently transfected with Cav3.2 proved to have too high variability in the level of Cav3.2 expression, and therefore showed fluorescence increase in some wells while not showing any reaction in other wells. A 96-well plate fragment is shown. Control untransfected cells (row A) did not exhibit fluorescence after stimulation with 20 mM $Ca^{2+}$. Cells transiently transfected with plasmid containing Cav3.2 (rows B, C and D) showed highly variable fluorescence response after addition of the same high $Ca^{2+}$ solution (final $Ca^{2+}$ concentration in wells was 10 mM). Magnified recording from one well is shown on the right side. The fluorescence (F) in each well was measured in arbitrary units (AU) for 40 s.

## 3.2. The fluorescent dye

Two fluorescent dyes were tested in the assay to assess differences in the assay sensitivity: Fluo-4-AM and Calcium Green-AM (both from Life Technologies). Calcium Green proved to be less useful in the microplate assay due to a lower increase in fluorescence upon binding of $Ca^{2+}$ – only approximately 14-fold increase in fluorescence in calcium-bound form versus the unbound form. Fluo-4 increases the fluorescence over 100-fold in the presence of calcium ions. This allowed for the observation of a more pronounced increase in fluorescence levels in cells loaded with Fluo-4 instead of Calcium Green, therefore the former dye was chosen for subsequent applications.

## 3.3. Dye concentration

The optimal dye concentration was found to be 2 μM – higher dye concentration did not increase the fluorescence response. However, no negative effects were observed from the higher dye concentration.

## 3.4. Incubation time

A range of incubation times was tested to identify the optimal time frame allowing for efficient dye loading and efficient binding of the tested compounds. The final incubation time was 20 min for the loading of Fluo-4-AM, followed by removal of the unabsorbed dye by washing with HBSS-HEPES. The tested antibodies were then incubated with the cells for 20 min.

## 3.5. Fluorescence recording settings

The final settings of the fluorescence recording protocol were as follows: fluorescence readings were performed using Omega FluoStar plate reader. The fluorescence was excited with light at 485 nm and recorded at 520 nm every 0.2 s for 40 s. Obtained data was baseline-corrected using the Omega in-house software. The data was then exported

to Microsoft Excel and GraphPad Prism and plotted. The area under the curve was calculated using GraphPad Prism (Fig. 30).

A.

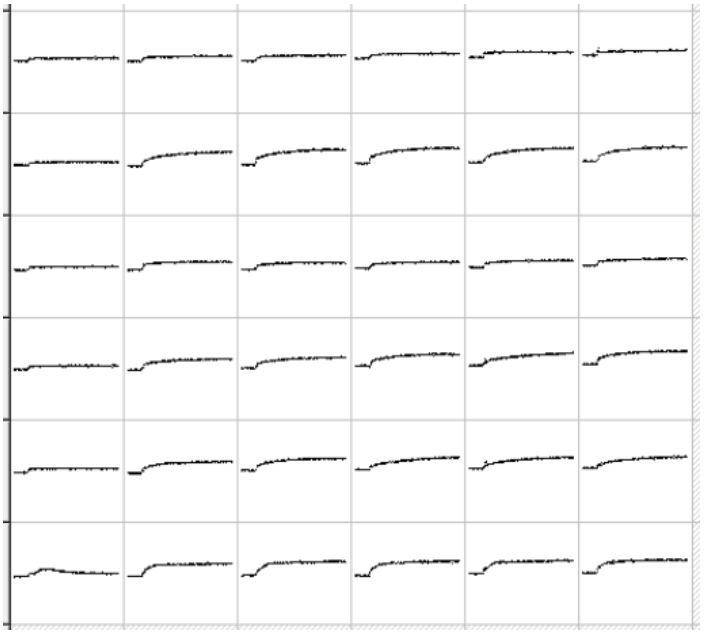

B.

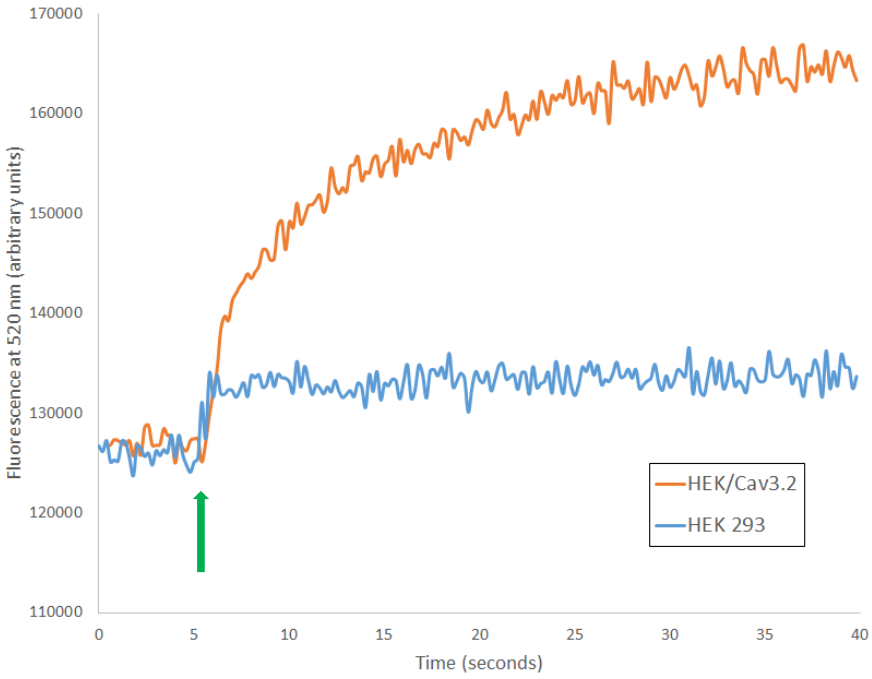


Figure 30. **A typical example of results obtained using optimized fluorescence-based assay for Cav3.2 kinetics**

A. Raw traces of a plate fragment.

B. Data from two wells exported and analysed using Microsoft Excel. The orange curve shows fluorescence changes in HEK/Cav3.2 cells (positive control). The blue curve shows fluorescence recording for HEK293 cells (negative control). The arrow (at 5s) indicates the addition of 20mM $Ca^{2+}$ HBSS-HEPES solution which raised the Ca2+ concentration in wells to 10 mM.

| | HEK/Cav3.2 cells | HEK293 cells | HEK/Cav3.2 cells + mibefradil |
|---|---|---|---|
| Area under the curve | 696399 | 184199 | 226297 |
| | 745451 | 192362 | 343695 |
| | 687199 | 161299 | 201198 |
| | 727734 | 178339 | 286168 |

Z-factor = 0.774

Table 7. **Assay validation – cumulative fluorescence of positive and negative controls**

The table shows the area under the curve values for positive control (HEK/Cav3.2 cells), negative control (HEK293 cells) and mibefradil pre-treated HEK/Cav3.2 cells. The Z-factor was calculated on the basis of positive and negative controls and proves that the assay is suitable for use in High-Throughput screening.

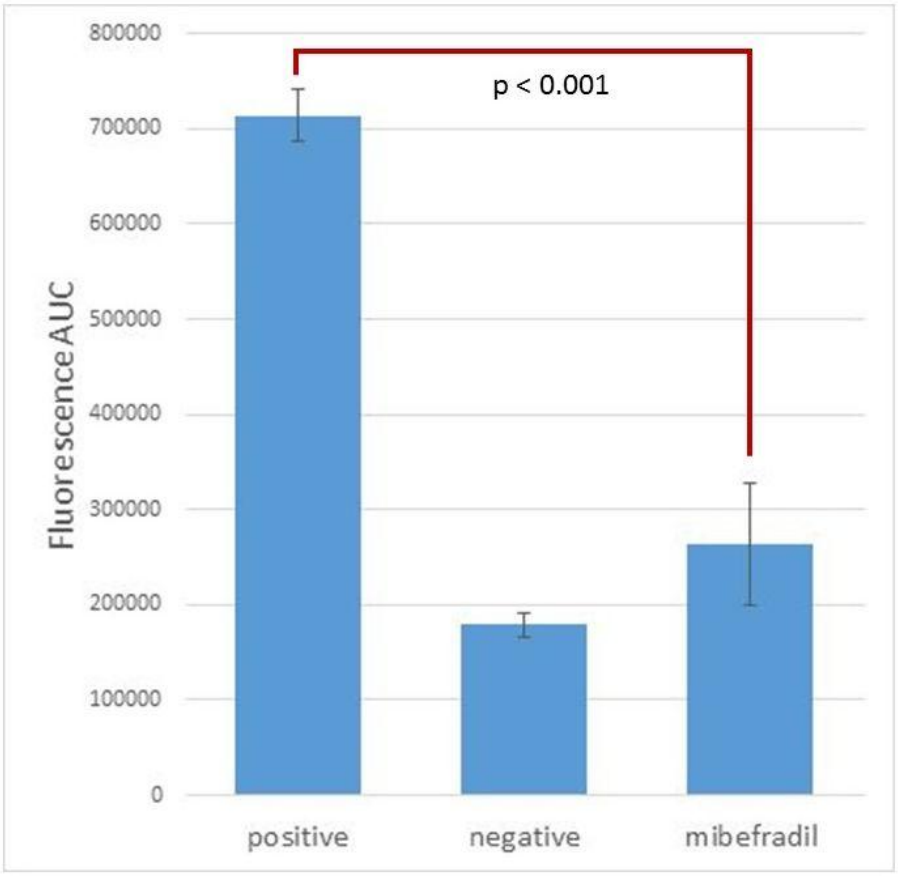


Figure 31. **Assay validation – comparison of cumulative fluorescence**

Fluorescence area under the curve values for positive and negative controls and for mibefradil-treated HEK/Cav3.2 cells. The data presented are mean ± SD of four replicates. Statistical analysis of the presented data was performed by the t-test (unpaired) using Microsoft Excel 2013 software. The p value < 0.001 for positive control and mibefradil treated cells showed that the difference between these results is statistically highly significant.

# 4. Discussion

The aim of this part of the thesis was to implement and validate a fluorescent assay for measurement of Cav3.2 activity. Ion channels are involved in many metabolic processes and new ways in which ion channels are involved in pathophysiology are continuously being discovered. This makes ion channels important drug targets and requires the development of screening assays for these molecules. The current lack of HTS assays for ion channels, especially prominent in the case of voltage-gated ion channels, hampers the drug development efforts. Electrophysiological methods are not amenable for incorporation in HTS assays; therefore other approaches are necessary. In recent years a few fluorescence-based assays for investigation of voltage-gated calcium channels have been proposed. They rely on detection of $Ca^{2+}$ influx using fluorescent dyes. There are three such published assays developed for investigation of Cav3.2 (described in this chapter's Introduction). Two of these assays were tested by the author of this thesis: the assay published by Xie *et al.* (2007) and Belardetti *et al.* (2009). The assay published by Prigge, Rösler and Hegemann (2010) was not tested due to the requirement of co-transfection of cells with three ion channels (Cav3.2, mTrek and channelrhodopsin-2) and the difficulties in obtaining the plasmids coding for these channels.

The assay published by Belardetti *et al.* (2009) required the use of gramicidin in order to create pores in the cell membrane and allow for the modification of the membrane potential with the aid of various buffers. This assay proved to be difficult to implement due to a significant degree of response in HEK293 cells not transfected with Cav3.2. This response might be due to osmotic imbalances in the buffers which could drive $Ca^{2+}$ ions into the cells through gramicidin pores.

The assay published by Xie *et al.* (2007) is simpler than the aforementioned assays and does not require the use of several buffers and drugs, all of which could potentially affect

the Cav3.2 gating properties. This thesis employs the assay published by Xie *et al.* (2007) but with some modifications. The assay described in this chapter was utilized in the subsequent part of this thesis to assess whether the binding of anti-Cav3.2 antibodies influences Cav3.2 conductance.

The initial settings of the assay presented in this chapter were as published by Xie *et al.* (2007). The tested modifications were designed to improve the assay sensitivity and reproducibility.

The first modification tested was the use of transiently transfected cells expressing Cav3.2 instead of a stable cell line. Transiently transfected cells would offer several advantages over stably transfected cells. The most interesting feature would be the possibility to generate a variety of mutated Cav3.2 sequences that could then be introduced into cells and quickly tested for changes in their gating properties without the need for generating a stable cell line. Other advantages include a higher level of target protein expression than in the case of a stable recombinant cell line. Unfortunately the transiently transfected cells proved to be difficult to use in this assay due to a variable level of Cav3.2 expression and the resulting variability in the fluorescence signal obtained.

The second modification was the attempt to use another fluorescent dye to measure the cellular response. Two dyes: Calcium Green-AM and Fluo-4-Am were tested. Fluo-4-AM was selected for the assay due to its high fluorescence increase (approximately 100-fold) upon binding of $Ca^{2+}$ ions. The dye has low toxicity and is easy to load into the cells. The background fluorescence is low because the acetoxymethyl ester is only hydrolysed intracellularly, thus releasing the calcium-sensitive form intracellularly. The optimal incubation time was found to be 20 min and the chosen dye concentration was 2 μM. The cells were loaded with the dye in the incubator at 37 ºC – this speeds up the dye uptake and hydrolysis. After loading with the dye the cells were transferred to room temperature for the rest of the experiment on a given batch of cells. This limits the cellular stress caused by temperature changes. The subcellular compartmentalization of the dye

and dye exclusion from cells was lower at room temperature. The published assay involved the use of probenecid (organic anion-transport inhibitor) to prevent dye leakage from cells into the medium. In our case the use of probenecid was not necessary therefore it was not used. The use of probenecid could possibly affect the cell metabolism to some extent and interact with the compounds tested in the assay.

The extracellular $Ca^{2+}$ concentration was initially 1 mM to maintain adherence of the cells. The increased concentration of $Ca^{2+}$ that was used to elicit a fluorescence response was set at 10 mM. This resulted in a rapid and significant fluorescence increase. A higher concentration of $Ca^{2+}$ was also considered as it allowed for an even more pronounced fluorescence rise. However, a high concentration of $Ca^{2+}$ and other divalent cations could affect the binding of drugs and antibodies to Cav3.2, therefore the 10 mM of $Ca^{2+}$ was found to be the optimal concentration. These conditions proved to be sufficient for eliciting a satisfactory fluorescence response.

The concentration of mibefradil used in the assay to suppress the fluorescence increase was 10 μM. This concentration is much higher that the $IC_{50}$ of approximately 3 μM. This higher concentration of mibefradil allowed for an almost complete blocking of the Ca-induced Fluo-4 fluorescence rise within a relatively short incubation time of 20 min.

The implementation of the assay proved to be successful and the assay achieved a very good Z-factor result that is a measure of the assay suitability for HTS. A good assay that is useful for HTS purposes should have the Z-factor above 0.5. Values approaching 1 indicate a near-perfect assay with a wide distance between the values obtained for positive and negative controls. The assay published by Xie *et al.* (2007) had a Z-factor result 0.5. A similar fluorescence based assay for a closely related channel Cav3.1 had a Z-factor of 0.66 (Kim *et al.,* 2009). The assay presented in this chapter has a Z-factor of 0.774, indicating a significant improvement in the assay dynamic range.

The assay presented here compares favourably with the patch clamp method of measuring Cav3.2 kinetics – it is less time-consuming and does not require the use of advanced electrophysiological equipment. A variety of compounds can be easily tested

using microtiter plates, either in 96-well or 384-well format. The essay is reproducible and reliable.

It is important to note that in this case, when the RMP of the cell is not manipulated and is approximately -40 mV, only about 2 % of the Cav3.2 channels are open. Therefore the drugs bind to a closed state of the channel and possibly prevent the channel opening. This may be useful in cases where excessive firing of Cav3.2 may contribute to pain syndromes. In order to investigate the drugs binding to an open state of the channel, it would be necessary to invent a system allowing for the opening of a significant majority of the Cav3.2 channels.

In summary, the assay presented in this chapter is a reliable method for the screening of compounds possessing anti-Cav3.2 activity and can be used for investigating whether the anti-Cav3.2 antibodies have the ability to modify Cav3.2 gating properties.

# Chapter 5: Analysing the Influence of Anti-Cav3.2 Antibodies on Cav3.2 Channel Conductance

## 1. Introduction

The reactivity of the generated antibodies to Cav3.2 were measured and found to be satisfactory (Chapter 3). These results suggest that the binding of antibodies to the recombinant Cav3.2 occurs *in vitro*. The results in this chapter describe experiments to determine whether the antibodies are capable of blocking the conductance produced by the Cav3.2 channel.

Antibodies against voltage-gated ion channels that block the channel conductance have been previously reported.

Gómez-Varela *et al.* (2007) described the generation of a monoclonal antibody against human ether à go-go potassium channel (hEag1). A range of monoclonal antibodies were generated against the E3 region of the channel – the linker between the fifth and sixth transmembrane segments. These antibodies were tested separately for their activity against this channel and a clone mAb56 proved to be successful in blocking the channel current. This antibody binds to a linear region of the channel with a sequence GSGSGKWEG. Antibodies against other sequences of the E3 segment had affinity towards the channel as documented by immunofluorescence imaging, but did not affect the channel gating. The application of mAb56 to HEK293 cells transfected with hEag1 reduced the potassium current by 40 % within 10 min of superfusion with 45 µg/mL of the antibody. This current change was measured using whole-cell patch clamp. Similar effects were obtained using *Xenopus* oocytes and cells naturally expressing hEag1 – neuroblastoma cell line SH-SY5Y (~45 % inhibition within 5 min of superfusion with 45 µg/mL of the antibody). The antibody was highly specific against hEag1 and did not bind to closely related hEag2 and HERG channels.

Chioni *et al*. (2005) generated polyclonal antibodies using peptide VSENIKLGNLSALR which corresponds to D1:S3/S4 loop of nNav1.5 (neonatal Nav1.5, expressed in breast cancer cell line MDA-MB-231). Immunofluorescent staining of tissues and Western Blotting confirmed that these antibodies (named NESOpAb) differentiate between the

'adult' and 'neonatal' splice variants of Nav1.5 despite these variants differing only by six amino acids. Moreover, NESOpAb significantly reduced the nNav1.5 conductance. The block achieved by antibodies was 50 % of the maximal current and was achieved at less than 5 ng/ml concentration of NESOpAb. 'Adult' Na1.5 current was only diminished by 25 % and at much higher NESOpAb concentration – 250 ng/ml. The activation and inactivation thresholds of the channel were not affected by the binding of NESOpAb. These results show the potential of antibodies for future drug development and for diagnostic purposes.

Xu *et al.* (2005) have presented and tested a novel strategy for the generation of ion channel inhibitors. They focused on the TRPC5 calcium channel and Nav1.5 sodium channel. The former is a member of the Transient Receptor Potential family and consists of four identical protein units forming the channel; these polypeptides have a six transmembrane domains structure with a pore loop between the fifth and sixth TM domain. The structure of the latter is more complex and the channel consists of one protein – four connected subunits containing six transmembrane domains each. Structural studies on these channels have revealed the existence of an extracellular loop (named E3) between transmembrane segment S5 and the pore loop of the channel. This E3 loop was large enough to allow for the binding of antibodies. Polyclonal antibodies against E3 sequences were produced in rabbits. The obtained antibodies were first tested for their specificity to a given ion channel and proved to distinguish between close members of the same family. Anti-TRPC5 antibodies recognized only TRPC5 and not TRPC4 or TRPC1 when tested by Western Blotting. Anti-Nav1.5 antibodies were used for immunostaining and did not bind to wild type cells (not expressing Nav1.5). Electrophysiological recordings of HEK293 expressing TRPC5 revealed that 10 min incubation of cells with anti-TRPC5 antibody caused 50 % block of the channel current. The antibody was also effective in fluorescent assay measuring calcium influx. Anti-Nav1.5 antibodies caused 60 % block of the current after 20 min incubation with HEK293 expressing Nav1.5. This antibody did not affect the electrophysiological properties of

Nav1.4 thus proving high selectivity. No detailed research has been conducted on the influence of the application of antibodies on the gating properties of these ion channels, *i.e.* no information about activation and inactivation thresholds and times has been obtained. It is likely that the antibodies simply obstruct the ion permeation pathway due to its close proximity to the pore loop. The gating properties may remain unaffected as well as the channel exposure on the membrane. Channel internalisation may possibly occur upon binding of the antibody but it is unlikely due to relatively short exposure of cells to the antibody (maximum 20 min).

Xu *et al*. (2005) also tested their hypothesis on another, not named ion channel and claim a 100 % success rate in the production of blocking antibodies using this approach.

Zhou, Ma and Huang (1998) described the generation of polyclonal anti-Kv1.2 and anti-Kv3.1 antibodies that blocked the potassium channel current. The anti-Kv1.2 was generated using sequence FAEADERDSQFPSIP located between the transmembrane segment S5 and the pore loop and corresponds to the external vestibule of the channel mouth. This antibody reduced the whole-cell patch clamp recorded Kv1.2 current by ~70 % within 7-15 min of incubation with 250 nM of the antibody. The $IC_{50}$ of the antibodies was determined to be 54 nM, which is comparable with potassium channel neurotoxins (Zhou, Ma and Huang, 1998). Preincubation of this antibody with the corresponding peptide used for antibody generation removed the block. The addition of other, non-specific antibodies slightly reduced the channel current but required the antibodies to be added at a high concentration - over 1000 nM to achieve 20 % current block (Zhou, Ma and Huang, 1998). The binding of anti-Kv1.2 antibodies also prevented the binding of dendrotoxin to this channel in a dose-dependent manner. Anti-Kv1.2 antibodies were also effective against endogenous Kv1.2 currents measured in NG108-15 neuroblastoma-glioma hybrid cell line – a 76 % block was achieved within 10-15 min using 250 nM of the antibody (Zhou, Ma and Huang, 1998). The authors also produced anti-Kv3.1 antibodies against the external vestibule in this channel, using a peptide of sequence GAQPNDPSASEHTH. This antibody at 250 nM caused 79 % current reduction

in HEK293 cells expressing Kv3.1. The IC50 was reported to be 58 nM (Zhou, Ma and Huang, 1998).

The above studies confirm that antibodies against voltage-gated ion channels have the potential to block the channel conductance. However, most of the above mentioned antibodies were directed against monovalent cation channels which may suggest that these channels are easier to block. Only anti-TRPC5 antibodies were able to block the calcium current. The TRPC5 channel is homomultimeric and can also form heteromultimers with TRPC1 channels (Xu *et al.,* 2008). The homomultimeric channels would have more than one repeat of the target sequence and this could result in binding more than one antibody molecule to the functional channel. This may result in a more efficient blocking of such a channel compared to a monomeric channel with four different domains such as Cav3.2.

## 2. Aims

The aim of this chapter was to measure and describe the effects of the generated anti-Cav3.2 antibodies on the channel conductance of Cav3.2.

## 3. Results

The fluorescent assay described in Chapter 4 was used to measure the effects of the three anti-Cav3.2 antibodies on the channel conductance. The detailed protocol is provided in *Methods* (part I, 5.6, p. 50). Briefly, the cells growing on a 96 well plate were preincubated with antibodies or mibefradil for 15 min and the fluorescence response was evoked by the addition of a high $Ca^{2+}$ solution that raised the extracellular $Ca^{2+}$ concentration and caused ion influx to the cells mainly through Cav3.2 channels and other native ion channels.

| | | | | | | |
|---|---|---|---|---|---|---|
| HEK293 | A1 | A2 | A3 | A4 | A5 | A6 |
| HEK/Cav3.2 | B1 | B2 | B3 | B4 | B5 | B6 |
| HEK/Cav3.2 + Abs tested | C1 | C2 | C3 | C4 | C5 | C6 |
| HEK/Cav3.2 + Abs control | D1 | D2 | D3 | D4 | D5 | D6 |
| HEK/Cav3.2 + mibefradil | E1 | E2 | E3 | E4 | E5 | E6 |

Figure 32. **The layout of a multiwell plate used for Cav3.2 assays**

A 96-well plate was used for measuring the capability of anti-Cav3.2 antibodies to block Cav3.2 conductance. Wells in row A contained HEK293 cells not expressing Cav3.2 – negative control. HEK/Cav3.2 cells were seeded in row B and used as a positive control, without addition of any antibody. Row C contained HEK/Cav3.2 cells incubated with the investigated antibody. The antibody solution was diluted 1:2 from the original concentration, i.e. it was 5.8 µg/ml for anti-D1:S3/S4, 59.5 µg/ml for anti-D4:S3/S4 and 43.7 µg/ml for anti-D1:S5/P antibodies, therefore sodium azide concentration in wells was 0.01 %. Row D contained HEK/Cav3.2 cells incubated with a control antibody against Nav1.5 ion channel – produced by CovalAb in the same way as the anti-Cav3.2 antibodies and containing 0.02 % sodium azide. This antibody was diluted 1:2 giving the antibody concentration of 39.4 µg/ml and the final concentration of sodium azide of 0.01 %. In row E, HEK/Cav3.2 cells were incubated with mibefradil. HBSS/HEPES buffer with high [$Ca^{2+}$] (final concentration in wells 10 mM) was added to wells in columns 2 – 6 (red arrows). Plain HBSS/HEPES buffer was added to column 1 for control purposes (blue arrow).

## 3.1. Example of results calculation

### 3.1.1. Raw results

Fluorescence readings were performed using an Omega FluoStar plate reader. The fluorescence was excited with light at 485 nm and recorded at 520 nm every 0.2 s for 40 s (200 recordings of each well). The baseline fluorescence was read for 5 s in each well and followed by an automatic injection of HBSS/HEPES buffer with high [$Ca^{2+}$] to elicit a fluorescence response. Plain HBSS/HEPES buffer was injected in the first column of cells to ensure that any mechanical medium disturbance caused by the injection does not produce any changes in fluorescence. The data obtained was baseline-corrected using the Omega in-house software. The data was then exported to GraphPad Prism and the area under the curve (AUC) was calculated. The AUC values for every well were exported to Excel. The AUC values for each well are shown in Table 8.

| | Col 2 | Col 3 | Col 4 | Col 5 | Col 6 | Avg | SD |
|---|---|---|---|---|---|---|---|
| *HEK293* | 192596 | 203694 | 165874 | 184167 | 215031 | 192272 | 16799 |
| *Cav3.2* | 859696 | 756912 | 761088 | 782290 | 822177 | 796433 | 39182 |
| *Abs* | 502634 | 598347 | 552381 | 495741 | 586244 | 547069 | 41955 |
| *Abs control* | 625360 | 839566 | 872247 | 874038 | 598283 | 761898 | 123448 |
| *Mibefr* | 205672 | 198652 | 248193 | 175737 | 216893 | 209029 | 23761 |

Table 8. **AUC values for individual wells – experiment investigating the influence of D4:S3/S4 antibodies on Cav3.2-mediated calcium influx**

The values of fluorescence response elicited by the addition of HBSS/HEPES buffer with 10 mM final $Ca^{2+}$ concentration are shown in columns 2-6. The AUC values for each well were collected. Row 1 shows values for untransfected HEK293 cells, row 2 – for HEK/Cav3.2 cells with no antibody (positive control). Row 3 (Abs) shows values obtained for HEK/Cav3.2 cells treated with the D4:S3/S4 antibodies. Row 4 (Abs control) contained HEK/Cav3.2 cells treated with control antibody against Nav1.5. Row 5 shows values obtained for HEK/Cav3.2 cells treated with mibefradil (negative control). The average (Avg) and standard deviation (SD) in each row were calculated.

#### *3.1.1.1. Anti-D1:S3/S4 antibody*

The concentration of the purified antibody against the S3/S4 extracellular loop of Cav3.2 in Domain 1 was 11.5 µg/ml. The antibody solution was diluted 1:2 when incubated with cells, giving a final concentration in wells of 5.8 µg/ml. The anti-D1:S3/S4 antibody reduced the $Ca^{2+}$ induced fluorescence compared to the fluorescence response evoked in cells not treated with the antibody. The results of four independent experiments are shown in Fig. 33.

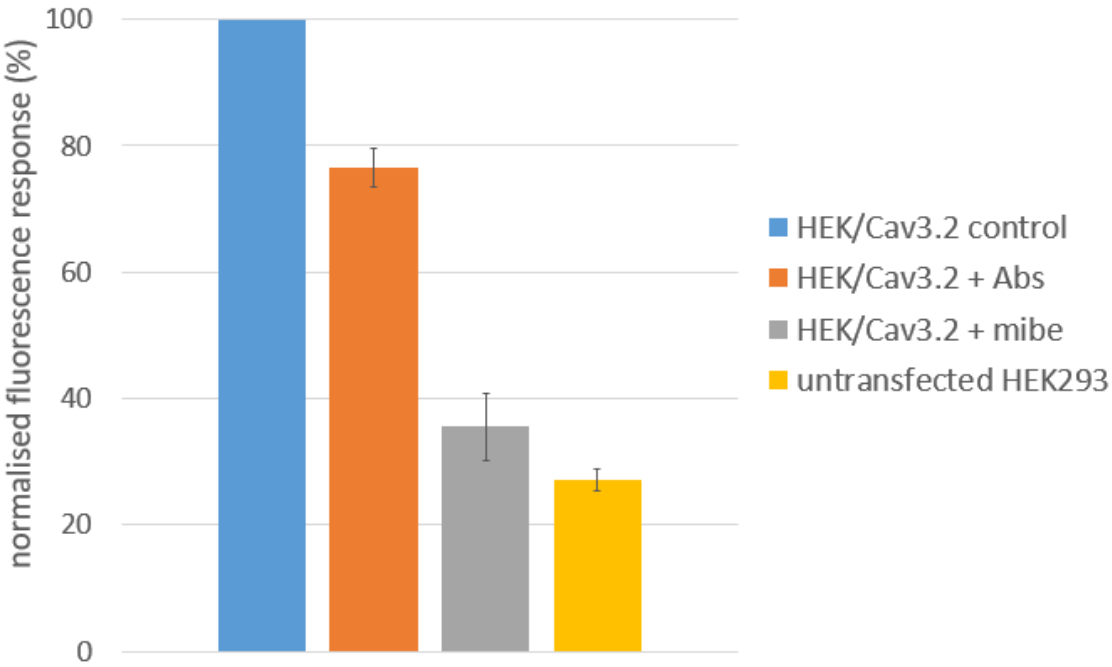


| | HEK/Cav3.2 cells | HEK/Cav3.2 + anti D1:S3/S4 | HEK/Cav3.2 cells + mibefradil | HEK293 cells |
|---|---|---|---|---|
| Average | 100 % | 76.6 % | 35.5 % | 27.1 % |
| SD | | 3.1 % | 5.3 % | 1.7 % |

Figure 33. **Normalised fluorescence response in cells treated with anti-D1:S3/S4 antibodies**

Normalised fluorescence area under the curve values for cells treated with anti-D1:S3/S4 antibody (orange bars), positive (blue bars) and negative (yellow bars) controls, and mibefradil-treated HEK/Cav3.2 cells (grey bars). Four experiment replicates were normalised to positive controls and the data shown represents the average values ± SD.

### *3.1.1.2. Anti-D4:S3/S4 antibody*

The concentration of the purified antibody against the S3/S4 extracellular loop of Cav3.2 in Domain 4 was 238.05 µg/ml. The antibody solution was diluted 1:4 when incubated with cells, giving in final concentration in wells 59.5 µg/ml. The anti-D4:S3/S4 antibody reduced the $Ca^{2+}$ induced fluorescence compared to the fluorescence response evoked in cells not treated with the antibody. The results of four independent experiments are shown in Fig. 34.

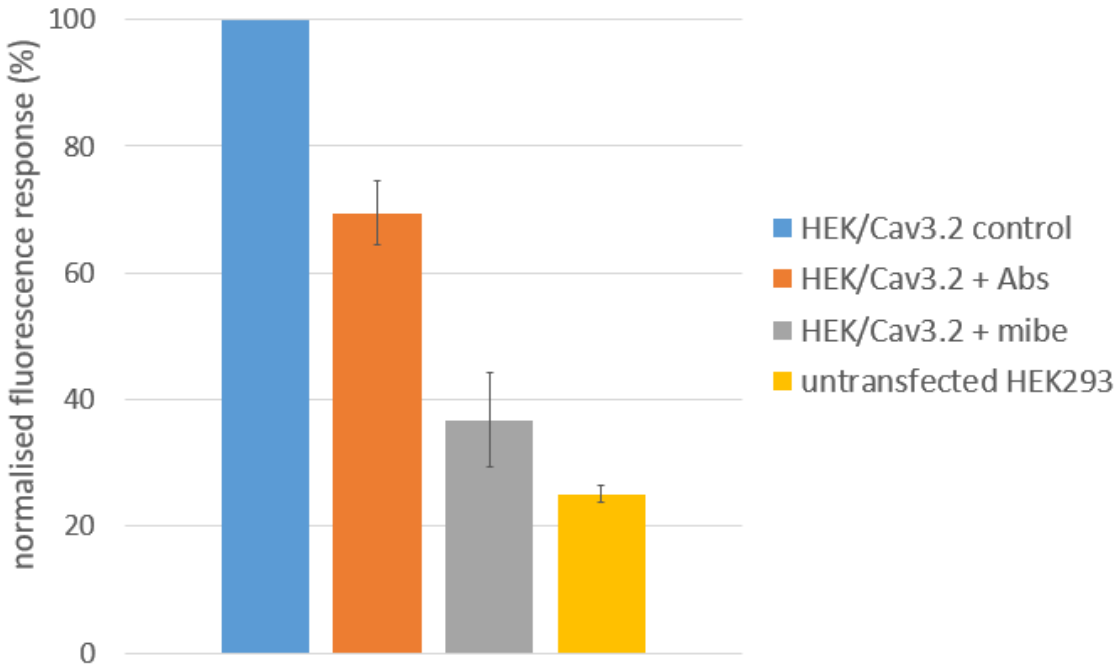


| | HEK/Cav3.2 cells | HEK/Cav3.2 + anti D4:S3/S4 | HEK/Cav3.2 cells + mibefradil | HEK293 cells |
|---|---|---|---|---|
| Average | 100 % | 69.5 % | 36.8 % | 25.1 % |
| SD | | 4.9 % | 7.5 % | 1.3 % |

Figure 34. **Normalised fluorescence response in cells treated with anti-D4:S3/S4 antibodies**

Normalised fluorescence area under the curve values for cells treated with anti-D4:S3/S4 antibody (orange bars), positive (blue bars) and negative (yellow bars) controls, and mibefradil-treated HEK/Cav3.2 cells (grey bars). Four experiment replicates were normalised to positive controls and the data shown represents the average values ± SD.

### *3.1.1.3. Anti-D1:S5/P antibody*

The concentration of the purified antibody against the S5/P extracellular loop of Cav3.2 in Domain 1 was 87.31 µg/ml. The antibody solution was diluted 1:2 when incubated with cells, giving in final concentration in wells 43.7 µg/ml. The anti-D1:S5/P antibody reduced the $Ca^{2+}$ induced fluorescence compared to the fluorescence response evoked in cells not treated with the antibody. The results of four independent experiments are shown in Fig. 35.

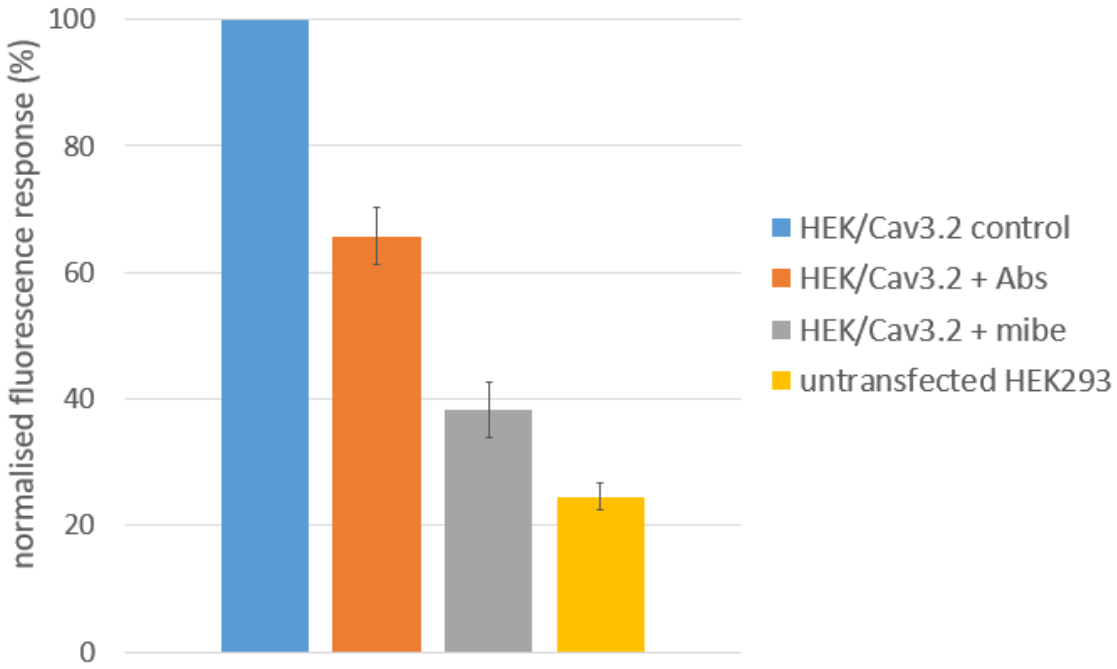


| | HEK/Cav3.2 cells | HEK/Cav3.2 + anti D1:S5/P | HEK/Cav3.2 cells + mibefradil | HEK293 cells |
|---|---|---|---|---|
| Average | 100 % | 65.8 % | 38.3 % | 24.6 % |
| SD | | 4.5 % | 4.4 % | 2.0 % |

Figure 35. **Normalised fluorescence response in cells treated with anti-D1:S5/P antibodies**

Normalised fluorescence area under the curve values for cells treated with anti-D1:S5/P antibody (orange bars), positive (blue bars) and negative (yellow bars) controls, and mibefradil-treated HEK/Cav3.2 cells (grey bars). Four experiment replicates were normalised to positive controls and the data shown represents the average values ± SD.

The results of the average AUC for each of the experiment results were normalised to the positive control (HEK Cav3.2 cells – 100 % response) and the negative control (HEK293 cells not expressing Cav3.2 – 0 %). The percentage response for cells treated with each antibody and the percentage of fluorescence reduction are shown in Table 9. The percentage fluorescence reduction corresponds to the percentage of Cav3.2 channels that are blocked by the action of antibodies. The presence of sodium azide (0.01 % in the antibody solution added to cells) has a mild inhibitory effect on the cell metabolism and thus on the fluorescence response evoked by the addition of $Ca^{2+}$. This effect was calculated using a solution containing 0.01 % sodium azide in 0.1 M Tris/ Glycine pH 7.8. buffer and was estimated to cause approximately 3 % reduction of the fluorescence response compared to positive control, i.e. HEK/Cav3.2 cells without antibodies or mibefradil. Therefore 3 % of the apparent inhibition might have been caused by sodium azide and not the antibodies. Subtracting 3 % from the apparent inhibitory effect of the antibodies gives a more realistic percentage inhibition that can be attributed to the antibodies only.

| | Fluorescence response (%) | % inhibition | SD |
|---|---|---|---|
| HEK Cav3.2 (positive control) | 100 % | | 0 |
| anti-D1:S3/S4 | 76.6 % | 23.4 % (20.4 %) | 3.1 % |
| anti-D1:S5/P | 65.8 % | 34.2 % (31.2 %) | 4.5 % |
| anti-D4:S3/S4 | 69.5 % | 30.5 % (27.5 %) | 4.9 % |
| mibefradil | 36.9 % | 63.1 % | 5.7 % |

Table 9. **Normalised maximum fluorescence response in cells treated with antibodies and mibefradil.**

The table shows the normalised fluorescence response obtained in independent experiments in cells treated with anti-D1:S3/S4, anti-D1:S5/P and anti-D4:S3/S4 antibodies and mibefradil. The reduction in fluorescence response in cells treated with antibodies and mibefradil corresponds to the percentage of Cav3.2 channels that are inhibited by the antibody. The values in brackets represent the values of inhibition achieved after taking into account the sodium azide-mediated metabolic changes that resulted in lower fluorescence response. The antibodies were used at different concentrations, hence a direct comparison of results is not possible.

## 4. Discussion

The aim of the experiments described in this chapter was to test the anti-Cav3.2 antibodies generated earlier in this project for their ability to block Cav3.2 calcium current. Their effect on the channel conductance was measured using previously validated fluorescence based assay described in Chapter 4.

The anti-Cav3.2 antibodies tested using the fluorescence-based assay achieved a significant reduction in recorded fluorescence. The anti-D1:S3/S4 antibodies caused an average 20.4 % inhibition at a concentration of 5.8 µg/ml. The anti-D1:S5/P antibodies caused an average 31.2 % inhibition at a concentration of 43.7 µg/ml. The anti-D4:S3/S4 antibodies caused an average 27.5 % inhibition at a concentration of 59.5 µg/ml. These values take into account the presence of sodium azide in the antibody solution which may slightly reduce the cell metabolism and the $Ca^{2+}$ induced fluorescence. The results obtained in this experiment are promising as current reduction was observed with the use of all the designed antibodies albeit to a different extent. Antibodies inhibiting Cav3.2 channel inhibition are described here for the first time.

## 4.1. Anti-D1:S5/P antibodies

The highest degree of blocking was achieved by the antibodies directed to the pore loop of the channel. Cav3.2 has four different domains and the pore loop sequences in each of these domains are different. Only the extracellular pore loop of Domain 4 was long enough to allow the generation of antibodies against it. Nevertheless, antibodies that only had the ability to bind to one pore loop were still able to affect ion flow through the pore. It is likely that these antibodies exerted their blocking effect through direct pore occlusion and by preventing the ion influx (steric hindrance) without affecting the channel conformational changes. Another possibility is that binding of the antibodies to the pore loop stabilises the channel in a closed state and prevents its opening upon stimulation. It is also possible that the binding of antibodies might exert conformational change and force inactivation (earlier closing) of the channel.

Several research teams have reported that antibodies against pore loop are able to block currents for several ion channels such as potassium channels (*e.g.* Gómez-Varela *et al.*, 2007 and Zhou, Ma and Huang, 1998) and sodium channels (Xu *et al.,* 2005).

The discovery that anti-D1:S5/P antibodies are able to block T-type calcium current in cells expressing Cav3.2 is in line with previously reported findings that antibodies directed to pore loops of L-, P/Q- and N-type calcium channels reduce the calcium current (Barry *et al.,* 1995; Wyatt *et al.,* 1997 and Liao *et al.,* 2008). The blocking effect of antibodies against T-type channel is reported here for the first time. The antibodies against D1:S5/P loop achieved 31.2 % reduction in the channel current at a concentration of 43.7 µg/ml. This concentration is similar to concentrations reported in the literature previously mentioned and the blockage achieved is significant at this concentration. Due to the antibodies being tested at single concentration only, it was not possible to establish the $IC_{50}$ value of these antibodies.

## 4.2. Anti-D1:S3/S4 antibodies

The anti-D1:S3/S4 antibodies were the ones with the lowest concentration obtained during the immunisation of rabbits and subsequent immunopurification. The amount obtained was only 23 µg and the concentration in the column elute was very low at 11.5 µg/ml. The lowest dilution possible was 1:2 to ensure that the cells were incubated with their medium too and not only the antibody solution which might have affected cell metabolism. The final concentration of antibodies in the wells was 5.8 µg/ml. The $Ca^{2+}$ current inhibition was 20.4 %. This was a significant blockage at this low concentration. It may suggest that the D1:S3/S4 loop plays an important role in the channel gating and that immobilisation of this loop by antibody binding causes changes in the channel gating. Similar significant blocking was described by Chioni *et al.* (2005). In this case the nNav1.5 channel current was 50 % inhibited by antibodies against the S3/S4 loop in Domain 1. The concentration of antibodies used was only 5 ng/ml. Nav1.5 and its neonatal version nNav1.5 have similar four-domain structure to Cav3.2. It is likely that the S3/S4 loop in these types of voltage-gated channels may play a gating brake role.

## 4.3. Anti-D4:S3/S4 antibodies

The anti-D4:S3/S4 antibodies were used at highest concentration (59.5 µg/ml) and caused 27.5 % fluorescence inhibition. This is a significant reduction in fluorescence, therefore in $Ca^{2+}$ current, however, the high concentration required to exert this effect suggests that the potency of these antibodies is not as high as the ones described previously. Loop S3/S4 in Domain 4 of Cav3.2 has been investigated previously and it has been reported that tarantula toxin ProTx-I binds specifically to this loop in Cav3.2 (Ohkubo *et al.,* 2010). However, this peptide toxin with characteristic cysteine knot has much higher potency against Cav3.1 – $IC_{50}$ of ProTx-I is 0.2 µM against Cav3.1 and 32 µM against Cav3.2. The finding reported in this chapter that anti-D4:S3/S4 antibodies require a high concentration to reduce $Ca^{2+}$ current and the fact that D4:S3/S4 is not very sensitive to ProTx-I, indicate that this loop alone does not have the ability to significantly alter the channel gating.

# Part III

# General Discussion

## 1. Comparison of polyclonal and monoclonal channel-blocking antibodies

Antibodies against various ion channels have been proved to be effective in blocking the channel conductance. Both polyclonal and monoclonal antibodies blocking channel currents have been reported and their influence on cells has been investigated using mainly electrophysiological methods. The majority of research into the design of antibodies against ion channels has used polyclonal antibodies. Polyclonal antibodies can be raised against a particular peptide (epitope on the channel) or against the whole protein. In the case of antibodies raised against the whole protein the antibodies bind to all accessible epitopes and it is highly unlikely that these antibodies will be able to block the channel current. Moreover, the antibodies produced are mainly against most immunogenic epitopes, which may only be present at a few sites in the protein molecule. These epitopes are not necessarily the ones in close proximity to the channel opening or at sites that may affect the channel gating, such as channel brakes. To date there is no published research documenting the ability of antibodies generated against the whole protein to affect the gating of ion channels. In order to generate antibodies that bind to a specific epitope in a given channel, the antibodies are usually produced using a synthetic linear or circular peptide of the same sequence. This approach is usually successful in generating antibodies that bind to the given epitope in the native conformation. The antibodies generated usually do not bind to the whole peptide sequence but to fragments of this peptide, provided the peptide is long enough (about 5 amino acids) to allow the formation of several epitopes. This results in the generation of a pool of antibodies with variable properties. Some of these antibodies may bind stronger to their corresponding epitope while others may bind with lower affinity but at the right site and therefore influence the channel gating more effectively. There are at least five published examples of polyclonal antibodies generated against a peptide that block ion channels' conductance. The channels blocked by polyclonal antibodies described so far are: Kv1.2 and Kv.3.1 potassium channels (Zhou, Ma and Huang, 1998), TRPC5 transient receptor

potential channel (Xu *et al.,* 2005), Nav1.5 sodium channel (Xu *et al.,* 2005) and its neonatal version nNav1.5 (Chioni *et al.,* 2005).

Monoclonal antibodies have also been used for blocking ion channels. Gómez-Varela *et al.* (2007) described the blocking of human ether à go-go potassium channel (hEag1) with monoclonal antibodies. Monoclonal antibodies require more complex production method than polyclonal antibodies. The process requires the immunization of animals and the subsequent formation of hybridoma of immunised mouse spleen cells and myeloma cells. The hybridoma cells are clonally expanded and suitable clones are selected and propagated. This allows for the production of antibodies that bind to a specific epitope. After clonal expansion of the selected cell lines the production of immunoglobulins reaches a stage at which the amount of antibodies produced is sufficient for research or other use. Monoclonal antibodies against ion channels that have been reported in literature were not more effective than polyclonal antibodies in blocking ion channel currents. However, the monoclonal antibodies are much more useful in identifying the residues that are critical for the channel gating thanks to their defined binding site. The polyclonal antibodies mix contains various antibodies binding with different affinity with their corresponding epitopes. Only some of these epitopes may contain sites crucial for the channel gating, and binding of other antibodies may even prevent binding of the blocking antibodies to their corresponding sites. Therefore the concentration of the polyclonal antibodies probably needs to be higher than the concentration of monoclonal antibodies would be.

The conductance block achieved with the use of antibodies ranges from 40 % to 80 % (Table 10 contains a summary of the published results). Such an effect is generally achieved by the concentration of the antibody in microgram range. The only exception to this was the polyclonal antibody against nNav1.5 that required only 5 ng/ml final concentration to achieve a 50 % block of the channel current. The time of incubation reported also varies, with the shortest time being 5 min and the longest being 20 min.

Interestingly, to my knowledge, no antibodies stimulating channel conductance have been reported. Theoretically, the binding of antibodies could wedge the channel in an open state, thus increasing the current. However, comparing the sizes of the antibodies and the channels provides an answer to this question. The IgG molecule consists of two heavy chains (each one approximately 50 kDa) and two light chains (approx. 25 kDa), therefore the whole molecule weighs about 150 kDa (Janeway *et al.,* 2001). The sizes of ion channels vary, depending on their subunit composition. For example, Cav3.2 molecule is about 260 kDa, with long intracellular N- and C-termini: 11 kDa and 54 kDa. The membrane-embedded part of the molecule is further compacted by the parallel organisation of the transmembrane domains. The weight of an antibody molecule is roughly half of the channel molecule, and the antibody structure is more voluminous therefore the binding of the antibody to the channel most likely covers the whole extracellular face of the channel, thus blocking the pathway of ions.

| Channel | Antibody clonality | [Antibody] | % block achieved | Time of incubation | Reference |
|---|---|---|---|---|---|
| hEag1 | monoclonal | 45 µg/ml | 40 % | 10 min (in HEK293) | Gómez-Varela *et al.* (2007) |
| hEag1 | monoclonal | 45 µg/ml | 45 % | 5 min (in SH-SY5Y) | Gómez-Varela *et al.* (2007) |
| TRPC5 | polyclonal | 60 µg/ml | 50 % | 10 min | Xu *et al.* (2005) |
| Nav1.5–E3 | polyclonal | 15 µg/ml | 60 % | 20 min | Xu *et al.* (2005) |
| nNav1.5 | polyclonal | 5 ng/ml | 50 % | not reported | Chioni *et al*. (2005) |
| Kv1.2 | polyclonal | 250 nM | 70 % | 7-15 min | Zhou, Ma and Huang, (1998) |
| Kv3.1 | polyclonal | 250 nM | 80 % | 7-15 min | Zhou, Ma and Huang, (1998) |

Table 10. **Efficiency of polyclonal and monoclonal antibodies in blocking channel currents**

Several publications report the use of antibodies for blocking ion channel currents. The channel blocked, the required amount of the antibody, the extent of the inhibition and other experimental details are summarised above.

## 2. Comparison of the antibodies' potency

The anti-D1:S3/S4, anti-D4:S3/S4 and anti-D1:S5/P antibodies were tested at different concentrations (5.8 µg/ml; 59.5 µg/ml and 43.7 µg/ml, respectively). Due to the limited amount of antibodies available, it was not possible to repeat experiments at the same concentration of each antibody. Therefore direct comparison of the antibodies' potency is impossible. However, plotting inhibition percentage versus antibody concentration (Fig. 37) gives some indication of the relative potency of the antibodies. Obviously the dose-response curve is not linear, but sigmoidal in shape which makes the comparison difficult. However, from Fig. 37 it can be deduced that anti-D4:S3/S4 antibodies have possibly the lowest potency of all three antibodies. They were used at highest concentration (59.5 µg/ml) and achieved 27.5 % inhibition, which is lower than 31.2 % inhibition achieved by anti-D1:S5/P antibodies used at concentration 27 % lower (concentration 43.7 µg/ml). Apparently the anti-D1:S3/S4 antibodies have the highest potency as the preincubation of cells with a very low concentration of these antibodies (5.8 µg/ml) achieved a significant block at 20.4 %.

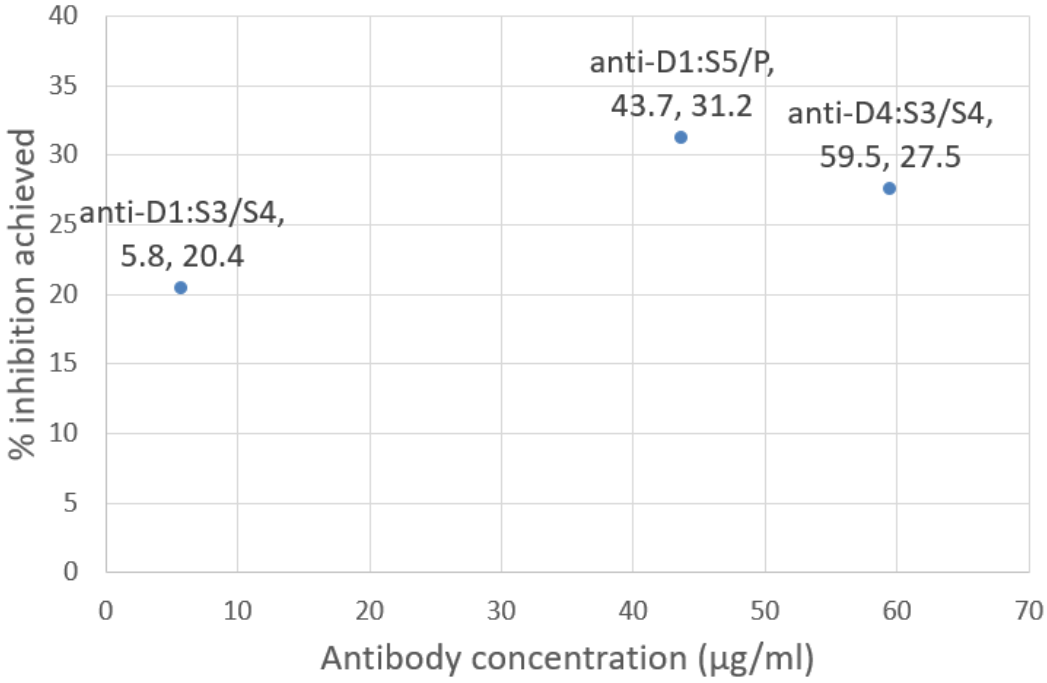


Figure 36. **Antibody concentration and the percentage inhibition achieved**

The plot represents the relationship between antibody concentration and the percentage inhibition achieved. Each antibody was tested at single concentration only (first value in each label) and the percentage inhibition achieved varied (second value).

## 3. Future experiments

The main shortcoming of the experiments described in this chapter was the limited amount of antibodies available. Each peptide was only injected into two rabbits and the antibodies extracted from these two animals. After purification, the amount of antibodies obtained was 23 µg for anti-D1:S3/S4, 384 µg for anti-D1:S5/P antibodies and 1190 µg for anti-D4:S3/S4 antibodies. The amount of antibodies available was especially limited in the case of anti-D1:S3/S4. These antibodies had to be divided for experiments described in this chapter and in the previous chapters such as ELISA and flow cytometry analysis of affinity. This only allowed for initial trial testing at various concentrations and the subsequent repeated testing at a single concentration only. Future experiments in this field will require a production of a higher amount of antibodies. Better availability of antibodies would allow for establishing their $IC_{50}$ value by plotting results of several experiments and finding the antibody concentration that causes half of the maximal inhibition. It would be also interesting to test the antibodies simultaneously and find out if their effect on the $Ca^{2+}$ current is simply additive or possibly synergistic – this could shed new light on channel gating processes. Testing the antibodies against closely related channels such as Cav3.1 and Cav3.3 would allow for the assessment of the antibody selectivity.

The antibodies against extracellular loops of Cav3.2 have been proved to be able to partially block Cav3.2 channel current. This finding may have pathophysiological relevance: the antibodies might be used for the further development of anti-cancer drugs, for example against prostate cancer, in which case the neuroendocrine differentiation of prostate cells causes increased calcium influx into cells and in turn increases the proliferation rate (Gackiere *et al.,* 2008). It would be interesting to check whether the addition of the antibodies into the growth medium of any cell line expressing Cav3.2 causes growth inhibition or possibly increased proliferation rate. Gómez-Varela *et al.* (2007) reports that antibodies against hEag1 showed significant antitumour activity – it

was able to inhibit colony formation in soft agar for a range of cancer-derived cell lines such as breast carcinoma (MDA-MB-435s, NCI-ADR), melanoma (e.g. HT144), ovarian (e.g. OVCAR-3), cervical (HeLa), pancreas, and colon carcinomas. A similar effect may be achieved with the addition of anti-Cav3.2 antibodies to the growth medium of some of these cancer cell lines.

# References


Adams, G.P., Schier, R., McCall, A.M., Simmons, H.H., Horak, E.M., Alpaugh, R.K., Marks, J.D., Weiner, L.M. (2001). High affinity restricts the localization and tumor penetration of single-chain fv antibody molecules. *Cancer Res,* 15(12), pp.4750-4755.

Adams, D. and Levin, M. (2012). Measuring Resting Membrane Potential Using the Fluorescent Voltage Reporters DiBAC4(3) and CC2-DMPE. *Cold Spring Harbor Protocols*, 2012(4), pp.pdb.prot067702-pdb.prot067702.

Aguado, C., García-Madrona, S., Gil-Minguez, M. and Luján, R. (2016). Ontogenic Changes and Differential Localization of T-type Ca2+ Channel Subunits Cav3.1 and Cav3.2 in Mouse Hippocampus and Cerebellum. *Frontiers in Neuroanatomy*, 10(83).

Aidley, D. and Stanfield, P. (1996). *Ion channels*. Cambridge: Cambridge University Press.

Alomone.com. (2016). *Anti-CaV3.2 antibody | #ACC-025 | Alomone labs*. [online] Available at: http://www.alomone.com/p/anti-cav3.2/acc-025/1023 [Accessed 12 May 2016].

Arias-Olguin, I., Vitko, I., Fortuna, M., Baumgart, J., Sokolova, S., Shumilin, I., Van Deusen, A., Soriano-Garcia, M., Gomora, J. and Perez-Reyes, E. (2008). Characterization of the Gating Brake in the I-II Loop of Cav3.2 T-type Ca2+ Channels. *Journal of Biological Chemistry*, 283(13), pp.8136-8144.

Asaga, S., Ueda, M., Jinno, H, Kikuchi, K., Itano, O., Ikeda, T. And Kitajima, M. (2006) Identification of a New Breast Cancer-related Gene by Restriction Landmark Genomic Scanning. *Anticancer Research*, 26(1) pp.35-42

ATCC (2016). *293 [HEK-293] ATCC® CRL-1573™*. [online] Available at: https://www.lgcstandards-atcc.org/products/all/CRL-1573.aspx?geo_country=gb&slp=1#characteristics [Accessed 1 Jun. 2016].

Baldi, L., Muller, N., Picasso, S., Jacquet, R., Girard, P., Thanh, H., Derow, E. and Wurm, F. (2008). Transient Gene Expression in Suspension HEK-293 Cells: Application to Large-Scale Protein Production. *Biotechnol Progress*, 21(1) pp.148-153.

Barry, E., Viglione, M., Kim, Y. and Froehner, S. (1995) Expression and antibody inhibition of P-type calcium channels in human small-cell lung carcinoma cells. *Journal of Neuroscience,* 5(1) pp.274-83.

Belardetti, F., Tringham, E., Eduljee, C., Jiang, X., Dong, H., Hendricson, A., Shimizu, Y., Janke, D., Parker, D., Mezeyova, J., Khawaja, A., Pajouhesh, H., Fraser, R., Arneric, S. and Snutch, T. (2009). A Fluorescence-Based High-Throughput Screening Assay for the Identification of T-Type Calcium Channel Blockers. *ASSAY and Drug Development Technologies*, 7(3), pp.266-280.

Blesneac, I., Chemin, J., Bidaud, I., Huc-Brandt, S., Vandermoere, F. and Lory, P. (2015). Phosphorylation of the Cav3.2 T-type calcium channel directly regulates its gating properties. *Proceedings of the National Academy of Sciences*, 112(44), pp.13705-13710.

Bourinet, E., Alloui, A., Monteil, A., Barrére, C., Couette, B., Poirot, O., Pages, A., McRory, J., Snutch, T., Eschalier, A. and Nargeot, J. (2004). Silencing of the Cav3.2 T-type calcium channel gene in sensory neurons demonstrates its major role in nociception. *The EMBO Journal*, 24(2), pp.315-324.

Burnouf, T. and Radosevich, M. (2001). Affinity chromatography in the industrial purification of plasma proteins for therapeutic use. *Journal of Biochemical and Biophysical Methods*, 49(1-3), pp.575-586.

Byrne, B., Stack, E., Gilmartin, N. and O'Kennedy, R. (2009). Antibody-Based Sensors: Principles, Problems and Potential for Detection of Pathogens and Associated Toxins. *Sensors*, 9(6), pp.4407-4445.

Carafoli, E. and Klee, C. (1999). *Calcium as a cellular regulator*. New York: Oxford University Press.

Carter, P. (2006). Potent antibody therapeutics by design. *Nat Rev Immunol*, 6(5), pp.343-357.

Case, R., Eisner, D., Gurney, A., Jones, O., Muallem, S. and Verkhratsky, A. (2007). Evolution of calcium homeostasis: From birth of the first cell to an omnipresent signalling system. *Cell Calcium*, 42(4-5), pp.345-350.

Catterall, W., Perez-Reyes, E., Snutch, T. P., and Striessnig, J. (2005). International Union of Pharmacology. XLVIII. Nomenclature and Structure-Function Relationships of Voltage-Gated Calcium Channels. *Pharmacological Reviews*, 57(4), pp.411-425.

Catterall, W. (2011). Voltage-Gated Calcium Channels. *Cold Spring Harbor Perspectives in Biology*, 3(8), pp.a003947-a003947.

Chazotte, B. (2011). Labeling Membrane Glycoproteins or Glycolipids with Fluorescent Wheat Germ Agglutinin. *Cold Spring Harbor Protocols*, 2011(5), pp.pdb.prot5623-pdb.prot5623.

Chemin, J., Monteil, A., Briquaire, C., Richard, S., Perez-Reyes, E., Nargeot, J. and Lory, P. (2000). Overexpression of T-type calcium channels in HEK-293 cells increases intracellular calcium without affecting cellular proliferation. *FEBS Letters*, 478(1-2), pp.166-172.

Chen, C. Lamping, K., Nuno, D., Barresi, R., Prouty, S., Lavoie, J., Cribbs, L. and England, S. (2003). Abnormal Coronary Function in Mice Deficient in α1H T-type Ca2+ Channels. *Science*, 302(5649), pp.1416-1418.

Chen, Y., Lu, J., Pan, H., Zhang, Y., Wu, H., Xu, K., Liu, X., Jiang, Y., Bao, X., Yao, Z., Ding, K., Lo, W., Qiang, B., Chan, P., Shen, Y. and Wu, X. (2003). Association between

genetic variation of CACNA1H and childhood absence epilepsy. *Annals of Neurology*, 54(2), pp.239-243.

Chioni, A., Fraser, S., Pani, F., Foran, P., Wilkin, G., Diss, J. and Djamgoz, M. (2005). A novel polyclonal antibody specific for the Nav1.5 voltage-gated Na+ channel 'neonatal' splice form. *Journal of Neuroscience Methods*, 147(2), pp.88-98.

Choi, S., Na, H., Kim, J., Lee, J., Lee, S., Kim, D., Park, J., Chen, C., Campbell, K. and Shin, H. (2007). Attenuated pain responses in mice lacking CaV3.2 T-type channels. *Genes, Brain and Behavior*, 6(5), pp.425-431.

Conroy, P., Hearty, S., Leonard, P. and O'Kennedy, R. (2009). Antibody production, design and use for biosensor-based applications. *Seminars in Cell & Developmental Biology*, 20(1), pp.10-26.

Cribbs, L., Lee, J., Yang, J., Satin, J., Zhang, Y., Daud, A., Barclay, J., Williamson, M., Fox, M., Rees, M. and Perez-Reyes, E. (1998). Cloning and Characterization of α1H From Human Heart, a Member of the T-Type Ca2+ Channel Gene Family. *Circulation Research*, 83(1), pp.103-109.

Daniels, R., Peden, J.F., Lloyd, C., Horsley, S.W., Clark, K., Tufarelli, C., Kearney, L., Buckle, V.J., Doggett, N.A., Flint, J. and Higgs, D.R (2001). Sequence, structure and pathology of the fully annotated terminal 2 Mb of the short arm of human chromosome 16. *Human Molecular Genetics*, 10(4), pp.339-352.

David, L., Garcia, E., Cain, S., Thau, E., Tyson, J. and Snutch, T. (2010). Splice-variant changes of the CaV3.2 T-type calcium channel mediate voltage-dependent facilitation and associate with cardiac hypertrophy and development. *Channels*, 4(5), pp.375-389.

Delves, P., Martin, S., Burton, D. and Roitt, I. (2011). *Roitt's Essential Immunology*. Somerset: Wiley.

Djamgoz, M.B.A., Mycielska, M., Madeja, Z., Fraser, S.P., Korohoda, W. (2001) Directional movement of rat prostate cancer cells in direct-current electric field: involvement of voltage-gated $Na^+$ channel activity. *J Cell Sci.* 114(14), pp. 2697-2705.

Dolphin, A. (2012). Calcium channel auxiliary α2δ and β subunits: trafficking and one step beyond. *Nature Reviews Neuroscience*, 13(9), pp.664-664.

Doyle, D. Morais Cabral, J., Pfuetzner, R., Kuo, A., Gulbis, J., Cohen, S., Chait, B. and MacKinnon, R. (1998). The Structure of the Potassium Channel: Molecular Basis of $K^+$ Conduction and Selectivity. *Science*, 280(5360), pp.69-77.

Ecker, D., Jones, S. and Levine, H. (2015). The therapeutic monoclonal antibody market. *mAbs*, 7(1), pp.9-14.

El-Manzalawy, Y., Dobbs, D. and Honavar, V. (2008). Predicting flexible length linear B-cell epitopes. *Comput Syst Bioinformatics Conf.*, 21(4), pp.243-255.

Elliott, D., Neale, E., Aziz, Q., Dunham, J., Munsey, T., Hunter, M. and Sivaprasadarao, A. (2004). Molecular mechanism of voltage sensor movements in a potassium channel. *EMBO J*, 23(24), pp.4717-4726.

Fernández-Ballester, G., Fernández-Carvajal, A., González-Ros, J. and Ferrer-Montiel, A. (2011). Ionic Channels as Targets for Drug Design: A Review on Computational Methods. *Pharmaceutics*, 3(4), pp.932-953.

Filipek, S. and Modzelewska, A. (2006). Molecular Modelling of Membrane Proteins. In: K. Lundstrom, ed., *Structural Genomics on Membrane Proteins*. Boca Raton: CRC Press, pp.331-348.

Fisher, R. (2005). Tositumomab and Iodine-131 Tositumomab Produces Durable Complete Remissions in a Subset of Heavily Pretreated Patients With Low-Grade and Transformed Non-Hodgkin's Lymphomas. *Journal of Clinical Oncology*, 23(30), pp.7565-7573.

Fraser, S., Diss, J., Chioni, A., Mycielska, M., Pan, H., Yamaci, R., Pani, F., Siwy, Z., Krasowska, M., Grzywna, Z., Brackenbury, W., Theodorou, D., Koyuturk, M., Kaya, H., Battaloglu, E., Tamburo, M., Slade, M., Palmieri, C. and Djamgoz, M. (2005). Voltage-Gated Sodium Channel Expression and Potentiation of Human Breast Cancer Metastasis. *Clinical Cancer Research*, 11(15), pp.5381-5389.

Fulton, J. (2008). *The patch clamp technique applied to real neurons*. [online] Neuronresearch.net. Available at: http://neuronresearch.net/neuron/patchclamp.htm [Accessed 22 Feb. 2017].

Gackière, F., Bidaux, G., Delcourt, P., Van Coppenolle, F., Katsogiannou, M., Dewailly, E., Bavencoffe, A., Van Chuoï-Mariot, M., Mauroy, B., Prevarskaya, N. and Mariot, P. (2008). CaV3.2 T-type Calcium Channels Are Involved in Calcium-dependent Secretion of Neuroendocrine Prostate Cancer Cells. *Journal of Biological Chemistry*, 283(15), pp.10162-10173.

Gomez-Varela, D., Zwick-Wallasch, E., Knotgen, H., Sanchez, A., Hettmann, T., Ossipov, D., Weseloh, R., Contreras-Jurado, C., Rothe, M., Stuhmer, W. and Pardo, L. (2007). Monoclonal Antibody Blockade of the Human Eag1 Potassium Channel Function Exerts Antitumor Activity. *Cancer Research*, 67(15), pp.7343-7349.

Gomora, J., Murbartián, J., Manuel Arias, J., Lee, J. and Perez-Reyes, E. (2002). Cloning and Expression of the Human T-Type Channel Cav3.3: Insights into Prepulse Facilitation. *Biophysical Journal*, 83(1), pp.229-241.

Graham, F., Russell, W., Smiley, J. and Nairn, R. (1977). Characteristics of a Human Cell Line Transformed by DNA from Human Adenovirus Type 5. *Journal of General Virology*, 36(1), pp.59-72.

Guilliams, M., Bruhns, P., Saeys, Y., Hammad, H. and Lambrecht, B. (2014). The function of Fcγ receptors in dendritic cells and macrophages. *Nat Rev Immunol*, 14(2), pp.94-108.

Haverstick, D., Heady, T., Macdonald, T. and Gray, L. (2000). Inhibition of human prostate cancer proliferation in vitro and in a mouse model by a compound synthesized to block Ca2+ entry. *Cancer Res* 60(4), pp.1002-1008.

Heady, T., Gomora, J., Macdonald, T. and Perez-Reyes, E. (2001). Molecular Pharmacology of T-type Ca2+ Channels. *The Japanese Journal of Pharmacology*, 85(4), pp.339-350.

Heron, S., Phillips, H., Mulley, J., Mazarib, A., Neufeld, M., Berkovic, S. and Scheffer, I. (2004). Genetic variation of CACNA1H in idiopathic generalized epilepsy. *Annals of Neurology*, 55(4), pp.595-596.

Hille, B. (1992). *Ionic channels of excitable membranes*. Sunderland, Mass.: Sinauer Associates.

Jagannathan, S., Punt, E., Gu, Y., Arnoult, C., Sakkas, D., Barratt, C. and Publicover, S. (2002). Identification and Localization of T-type Voltage-operated Calcium Channel Subunits in Human Male Germ Cells: EXPRESSION OF MULTIPLE ISOFORMS. *Journal of Biological Chemistry*, 277(10), pp.8449-8456.

Jamur, M. and Oliver, C. (2009). Permeabilization of Cell Membranes. *Immunocytochemical Methods and Protocols*, 588, pp.63-66.

Janeway, C.A., Travers, P., Walport, M. and Shlomchik, M. (2001) *Immunobiology: The Immune System in Health and Disease. 5th edition.* New York: Garland Science.

Kang, H., Park, J., Jeong, S., Kim, J., Moon, H., Perez-Reyes, E. and Lee, J. (2006). A Molecular Determinant of Nickel Inhibition in Cav3.2 T-type Calcium Channels. *Journal of Biological Chemistry*, 281(8), pp.4823-4830.

Kang, H., Vitko, I., Lee, S., Perez-Reyes, E. and Lee, J. (2010). Structural Determinants of the High Affinity Extracellular Zinc Binding Site on Cav3.2 T-type Calcium Channels. *Journal of Biological Chemistry*, 285(5), pp.3271-3281.

Kim, T. and Eberwine, J. (2010). Mammalian cell transfection: the present and the future. *Anal Bioanal Chem*, 397(8), pp.3173-3178.

Klöckner, U., Lee, J., Cribbs, L., Daud, A., Hescheler, J., Pereverzev, A., Perez-Reyes, E. and Schneider, T. (1999). Comparison of the Ca 2 + currents induced by expression of three cloned α1 subunits, α1G, α1H and α1I, of low-voltage-activated T-type Ca 2 + channels. *European Journal of Neuroscience*, 11(12), pp.4171-4178.

Kolaskar, A. and Tongaonkar, P. (1990). A semi-empirical method for prediction of antigenic determinants on protein antigens. *FEBS Letters*, 276(1-2), pp.172-174.

Kricka, L. (1999). Human Anti-Animal Antibody Interferences in Immunological Assays. *Clin Chem*, 45(7), pp.942-956

Kuroda, D., Shirai, H., Jacobson, M.P. and Nakamura, H. (2012). Computer-aided antibody design. *Protein Eng Des Sel,* 25(10), pp.507-21.

Larsson, A., Karlsson, M., Kollberg, H. and Larsson, A. (2004). Chicken IgY: utilizing the evolutionary advantage. *World's Poultry Science Journal*, 60(3), pp.341-348.

Lee, J., Gomora, J., Cribbs, L. and Perez-Reyes, E. (1999). Nickel Block of Three Cloned T-Type Calcium Channels: Low Concentrations Selectively Block α1H. *Biophysical Journal*, 77(6), pp.3034-3042.

Lee, W., Orestes, P., Latham, J., Naik, A., Nelson, M., Vitko, I., Perez-Reyes, E., Jevtovic-Todorovic, V. and Todorovic, S. (2009). Molecular Mechanisms of Lipoic Acid Modulation of T-Type Calcium Channels in Pain Pathway. *Journal of Neuroscience*, 29(30), pp.9500-9509.

Leenaars, P., Hendriksen, C., de Leeuw, W., Carat, F., Delahaut, P., Fischer, R., Halder, M., Hanly, W., Hartinger, J., Hau, J., Lindblad, E., Nicklas, W., Outschoorn, I. and Stewart-Tull, D. (1999) The Production of Polyclonal Antibodies in Laboratory Animals.

The Report and Recommendations of ECVAM Workshop 35. *Alternative to Laboratory Animals*, 27(1) pp.79-102.

Liao, Y., Safa, P., Chen, Y., Sobel, R., Boyden, E. and Tsien, R. (2008). Anti-Ca2+ channel antibody attenuates Ca2+ currents and mimics cerebellar ataxia in vivo. *Proceedings of the National Academy of Sciences*, 105(7), pp.2705-2710.

Los, M., Roodhart, J. and Voest, E. (2007). Target Practice: Lessons from Phase III Trials with Bevacizumab and Vatalanib in the Treatment of Advanced Colorectal Cancer. *The Oncologist*, 12(4), pp.443-450.

Lydyard, P., Whelan, A. and Fanger, M. (2011). *Immunology*. New York: Garland Science.

Makarenko, V., Peng, Y., Yuan, G., Fox, A., Kumar, G., Nanduri, J. and Prabhakar, N. (2015). CaV3.2 T-type Ca2+channels in H2S-mediated hypoxic response of the carotid body. *American Journal of Physiology - Cell Physiology*, 308(2), pp.C146-C154.

Mariot, P., Vanoverberghe, K., Lalevée, N., Rossier, M. and Prevarskaya, N. (2002). Overexpression of an α1H(Cav3.2) T-type Calcium Channel during Neuroendocrine Differentiation of Human Prostate Cancer Cells. *Journal of Biological Chemistry*, 277(13), pp.10824-10833.

Markandeya, Y., Fahey, J., Pluteanu, F., Cribbs, L. and Balijepalli, R. (2011). Caveolin-3 Regulates Protein Kinase A Modulation of the CaV3.2 (α1H) T-type Ca2+Channels. *Journal of Biological Chemistry*, 286(4), pp.2433-2444.

Meissner, P., Pick, H., Kulangara, A., Chatellard, P., Friedrich, K. and Wurm, F. (2001). Transient gene expression: Recombinant protein production with suspension-adapted HEK293-EBNA cells. *Biotechnol. Bioeng.*, 75(2), pp.197-203.

Michels, G., Matthes, J., Handrock, R., Kuchinke, U., Groner, F., Cribbs, L., Pereverzev, A., Schneider, T., Perez-Reyes, E. and Herzig, S. (2002). Single-Channel Pharmacology

of Mibefradil in Human Native T-Type and Recombinant Cav3.2 Calcium Channels. *Molecular Pharmacology*, 61(3), pp.682-694.

Nara, M., Morii, H. and Tanokura, M. (2013). Coordination to divalent cations by calcium-binding proteins studied by FTIR spectroscopy. *Biochimica et Biophysica Acta (BBA) - Biomembranes*, 1828(10), pp.2319-2327.

Nelson, M., Joksovic, P., Su, P., Kang, H., Van Deusen, A., Baumgart, J., David, L., Snutch, T., Barrett, P., Lee, J., Zorumski, C., Perez-Reyes, E. and Todorovic, S. (2007). Molecular Mechanisms of Subtype-Specific Inhibition of Neuronal T-Type Calcium Channels by Ascorbate. *Journal of Neuroscience*, 27(46), pp.12577-12583.

Nelson, A. (2010). Antibody fragments. *mAbs*, 2(1), pp.77-83.

Ober, R. J., Radu, C. G, Ghetie, V. and Ward, E. S. (2001). Differences in promiscuity for antibody-FcRn interactions across species: implications for therapeutic antibodies. *International Immunology*, 13(12), pp.1551-1559.

Ohkubo, T., Yamazaki, J. and Kitamura, K. (2010). Tarantula Toxin ProTx-I Differentiates Between Human T-type Voltage-Gated Ca2+ Channels Cav3.1 and Cav3.2. *J Pharmacol Sci*, 112(4), pp.452-458.

Ono, K. and Iijima, T. (2010). Cardiac T-type Ca2+ channels in the heart. *Journal of Molecular and Cellular Cardiology*, 48(1), pp.65-70.

Orestes, P., Bojadzic, D., Lee, J., Leach, E., Salajegheh, R., DiGruccio, M., Nelson, M. and Todorovic, S. (2010). Free radical signalling underlies inhibition of CaV3.2 T-type calcium channels by nitrous oxide in the pain pathway. *The Journal of Physiology*, 589(1), pp.135-148.

Park, J., Choi, J., Lee, E., Lee, J., Rhim, H., Seo, S., Kim, Y., Doddareddy, M., Pae, A. and Kang, J. (2007). Lead discovery and optimization of T-type calcium channel blockers. *Bioorganic & Medicinal Chemistry*, 15(3), pp.1409-1419.

Perez-Reyes, E. (2003). Molecular Physiology of Low-Voltage-Activated T-type Calcium Channels. *Physiological Reviews*, 83(1), pp.117-161.

Perez-Reyes, E., Van Deusen, A. and Vitko, I. (2008). Molecular Pharmacology of Human Cav3.2 T-Type Ca2+ Channels: Block by Antihypertensives, Antiarrhythmics, and Their Analogs. *Journal of Pharmacology and Experimental Therapeutics*, 328(2), pp.621-627.

Petersen, O., Michalak, M. and Verkhratsky, A. (2005). Calcium signalling: Past, present and future. *Cell Calcium*, 38(3-4), pp.161-169.

Presta, L. (2005). Selection, design, and engineering of therapeutic antibodies. *Journal of Allergy and Clinical Immunology*, 116(4), pp.731-736.

Prigge, M., Rösler, A. and Hegemann, P. (2010). Fast, repetitive light-activation of CaV3.2 using Channelrhodopsin 2. *Channels*, 4(3), pp.241-247.

Purves, D., Augustine, G., Fitzpatrick, D., Katz, L., LaMantia, A., McNamara, J. and Williams, S. (2001). *Neuroscience. 2nd Edition*. Sunderland, Mass.: Sinauer Associates.

Qiagen Bioinformatics (2014). CLC Genomics Workbench User Manual [Online] Available at: http://resources.qiagenbioinformatics.com/manuals/clcgenomicsworkbench/702/User_Manual.pdf pp.303-304 [Accessed 27 May 2017].

Reff, M.E., Hariharan, K. and Braslawsky, G. (2002). Future of monoclonal antibodies in the treatment of hematologic malignancies. *Cancer Control*, 9(2), pp.152-66.

Schmunk, G. and Gargus, J. (2013). Channelopathy pathogenesis in autism spectrum disorders. *Frontiers in Genetics*, 4(222).

Schnell, U., Dijk, F., Sjollema, K. and Giepmans, B. (2012). Immunolabeling artifacts and the need for live-cell imaging. *Nature Methods*, 9(2), pp.152-158.

Senatore, A., Zhorov, B. and Spafford, J. (2012). Cav3 T-type calcium channels. *Wiley Interdisciplinary Reviews: Membrane Transport and Signaling*, 1(4), pp.467-491.

Shaw, G., Morse, S., Ararat, M. and Graham, F. (2002). Preferential transformation of human neuronal cells by human adenoviruses and the origin of HEK 293 cells. *The FASEB Journal,* 16(8), pp.869-71.

Simms, B. and Zamponi, G. (2014). Neuronal Voltage-Gated Calcium Channels: Structure, Function, and Dysfunction. *Neuron*, 82(1), pp.24-45.

Splawski, I., Timothy, K., Sharpe, L., Decher, N., Kumar, P., Bloise, R., Napolitano, C., Schwartz, P., Joseph, R., Condouris, K., Tager-Flusberg, H., Priori, S., Sanguinetti, M. and Keating, M. (2004). CaV1.2 Calcium Channel Dysfunction Causes a Multisystem Disorder Including Arrhythmia and Autism. *Cell*, 119(1), pp.19-31.

Splawski, I., Yoo, D., Stotz, S., Cherry, A., Clapham, D. and Keating, M. (2006). CACNA1HMutations in Autism Spectrum Disorders. *Journal of Biological Chemistry*, 281(31), pp.22085-22091.

Strobeck, M., Okuda, M., Yamaguchi, H., Schwartz, A. and Fukasawa, K. (1999). Morphological Transformation Induced by Activation of the Mitogen-activated Protein Kinase Pathway Requires Suppression of the T-type Ca2+Channel. *Journal of Biological Chemistry*, 274(22), pp.15694-15700.

Taylor, J., Huang, L., Pottle, J., Liu, K., Yang, Y., Zeng, X., Keyser, B., Agrawal, K., Hansen, J. and Li, M. (2008). Selective blockade of T-type Ca2+ channels suppresses human breast cancer cell proliferation. *Cancer Letters*, 267(1), pp.116-124.

Thomas, P. and Smart, T. (2005). HEK293 cell line: A vehicle for the expression of recombinant proteins. *Journal of Pharmacological and Toxicological Methods*, 51(3), pp.187-200.

Tsien R. W. and Wheeler D. B. (1999) Voltage-gated calcium channels. in *Intracellular Calcium,* eds Carafoli E., Klee C. B. (Oxford Univ. Press, New York)

Uebele, V., Nuss, C., Renger, J. and Connolly, T. (2004). Role of voltage-gated calcium channels in potassium-stimulated aldosterone secretion from rat adrenal zona glomerulosa cells. *The Journal of Steroid Biochemistry and Molecular Biology*, 92(3), pp.209-218.

Van Epps, H. (2005). How Heidelberger and Avery sweetened immunology. *The Journal of Experimental Medicine*, 202(10), pp.1306-1306.

Vitko, I., Chen,Y., Arias, J., Shen, Y., Wu, X. and Perez-Reyes, E. (2005). Functional Characterization and Neuronal Modeling of the Effects of Childhood Absence Epilepsy Variants of CACNA1H, a T-Type Calcium Channel. *Journal of Neuroscience*, 25(19), pp.4844-4855.

Williams, M., Washburn, M., Hans, M., Urrutia, A., Brust, P., Prodanovich, P., Harpold, M. and Stauderman, K. (1999). Structure and Functional Characterization of a Novel Human Low-Voltage Activated Calcium Channel. *Journal of Neurochemistry*, 72(2), pp.791-799.

Wolfe, J., Wang, H., Perez-Reyes, E. and Barrett, P. (2002). Stimulation of recombinant Cav3.2, T-type, Ca2+channel currents by CaMKIIγC. *The Journal of Physiology*, 538(2), pp.343-355.

Wurm, F. (2004). Production of recombinant protein therapeutics in cultivated mammalian cells. *Nat Biotechnol*, 22(11), pp.1393-1398.

Wyatt, C., Campbell, V., Brodbeck, J., Brice, N., Page, K., Berrow, N., Brickley, K., Terracciano, C., Naqvi, R., MacLeod, K. and Dolphin, A. (1997). Voltage-dependent binding and calcium channel current inhibition by an anti-α1Dsubunit antibody in rat

dorsal root ganglion neurones and guinea-pig myocytes. *The Journal of Physiology*, 502(2), pp.307-319.

Xie, X., Van Deusen, A., Vitko, I., Babu, D., Davies, L., Huynh, N., Cheng, H., Yang, N., Barrett, P. and Perez-Reyes, E. (2007). Validation of High Throughput Screening Assays Against Three Subtypes of Ca v 3 T-Type Channels Using Molecular and Pharmacologic Approaches. *ASSAY and Drug Development Technologies*, 5(2), pp.191-204.

Xu, S., Zeng, F., Lei, M., Li, J., Gao, B., Xiong, C., Sivaprasadarao, A. and Beech, D. (2005). Generation of functional ion-channel tools by E3 targeting. *Nature Biotechnology*, 23(10), pp.1289-1293.

Xu, S., Sukumar, P., Zeng, F., Li, J., Jairaman, A., English, A., Naylor, J., Ciurtin, C., Majeed, Y., Milligan, C., Bahnasi, Y., Al-Shawaf, E., Porter, K., Jiang, L., Emery, P., Sivaprasadarao, A. and Beech, D. (2008). TRPC channel activation by extracellular thioredoxin. *Nature*, 451(7174), pp.69-72.

Yamane-Ohnuki, N. and Satoh, M. (2009). Production of therapeutic antibodies with controlled fucosylation. *mAbs*, 1(3), pp.230-236.

Yang, M. and Brackenbury, W. (2013). Membrane potential and cancer progression. *Frontiers in Physiology*, 4.

Zamponi, G. (2005). *Voltage-Gated Calcium Channels*. Boston, MA: Eurekah.com and Kluwer Academic / Plenum Publishers.

Zhang, J. Chung, T. and Oldenburg, K. (1999). A Simple Statistical Parameter for Use in Evaluation and Validation of High Throughput Screening Assays. *Journal of Biomolecular Screening*, 4(2), pp.67-73.

Zhong, X., Liu, J., Kyle, J., Hanck, D. and Agnew, W. (2006). A profile of alternative RNA splicing and transcript variation of CACNA1H, a human T-channel gene candidate for idiopathic generalized epilepsies. *Human Molecular Genetics*, 15(9), pp.1497-1512.

Zhou, B., Ma, W. and Huang, X. (1998). Specific Antibodies to the External Vestibule of Voltage-gated Potassium Channels Block Current. *The Journal of General Physiology*, 111(4), pp.555-563.